UNIVERSIDADE FEDERAL DO CEARÁ

CENTRO DE TECNOLOGIA

DEPARTAMENTO DE ENGENHARIA DE TELEINFORMÁTICA

PROGRAMA DE PÓS-GRADUAÇÃO EM ENGENHARIA DE TELEINFORMÁTICA

MESTRADO ACADÊMICO EM ENGENHARIA DE TELEINFORMÁTICA

BRUNO SOKAL

SEMI-BLIND RECEIVERS FOR MULTI-RELAYING MIMO SYSTEMS USING RANK-ONE TENSOR FACTORIZATIONS

FORTALEZA

2017

BRUNO SOKAL

SEMI-BLIND RECEIVERS FOR MULTI-RELAYING MIMO SYSTEMS USING RANK-ONE TENSOR FACTORIZATIONS

Dissertação apresentada ao Curso de Mestrado Acadêmico em Engenharia de Teleinformática do Programa de Pós-Graduação em Engenharia de Teleinformática do Centro de Tecnologia da Universidade Federal do Ceará, como requisito parcial à obtenção do título de mestre em Engenharia de Teleinformática. Área de Concentração: Sinais e Sistemas

Orientador: Prof. Dr. André Lima Férrer de Almeida

FORTALEZA

2017

Dados Internacionais de Catalogação na Publicação
Universidade Federal do Ceará
Biblioteca Universitária
Gerada automaticamente pelo módulo Catalog, mediante os dados fornecidos pelo(a) autor(a)

S1s Sokal, Bruno.
Semi-Blind Receivers for Multi-Relaying MIMO Systems Using Rank-One Tensor Factorizations / Bruno Sokal. – 2017.
85 f. : il. color.

Dissertação (mestrado) – Universidade Federal do Ceará, Centro de Tecnologia, Programa de Pós-Graduação em Engenharia de Teleinformática, Fortaleza, 2017.
Orientação: Prof. Dr. André Lima Férrer de Almeida.

1. MIMO systems. 2. cooperative communications. 3. semi-blind receivers. 4. rank-one tensors. I. Título.

CDD 621.38

BRUNO SOKAL

SEMI-BLIND RECEIVERS FOR MULTI-RELAYING MIMO SYSTEMS USING RANK-ONE TENSOR FACTORIZATIONS

Dissertation presented to the Master Program in Teleinformatics Engineering at the Federal University of Ceará, as part of the requirements for obtaining the Master's Degree in Teleinformatics Engineering. Concentration area: Signal and Systems.

Approved in: 27/07/2017.

EXAMINATION BOARD

Prof. Dr. André Lima Férrer de Almeida (Advisor)
Federal University of Ceará

Prof. Dr. Carlos Alexandre Rolim Fernandes
Federal University of Ceará

Prof. Dr. Walter da Cruz Freitas Junior
Federal University of Ceará

Prof. Dr. João Paulo Carvalho Lustosa da Costa
University of Brasília

ACKNOWLEDGEMENTS

I would like to express my deepest thanks to my mother, who has always encouraged me in the difficult moments of this journey. To my dad, who helped me build one of the contributions of this thesis, the generalization of the Kronecker approximation, and taught me to be more patient, and I would like to thanks to my brothers, Henrique, Junior and Waleska. Special thanks to Camila, for being patient with me and for the support during this period. To Prof. André, whom I also consider as a friend, for inspiring me as a person and as a scientist, and for all the patience he had with me during this journey (I know it must have been a lot). To FUNCAP, for the financial support.

Fortaleza, July 2017.

Bruno Sokal

ABSTRACT

Cooperative communications have shown to be an alternative to combat the impairments of signal propagation in wireless communications, such as path loss and shadowing, creating a virtual array of antennas for the source. In this work, we start with a two-hop MIMO system using a a single relay. By adding a space-time filtering step at the receiver, we propose a rank-one tensor factorization model for the resulting signal. Exploiting this model, two semi-blind receivers for joint symbol and channel estimation are derived: i) an iterative receiver based on the trilinear alternating least squares (Tri-ALS) algorithm and ii) a closed-form receiver based on the truncated higher order SVD (T-HOSVD). For this system, we also propose a space-time coding tensor having a PARAFAC decomposition structure, which gives more flexibility to system design, while allowing an orthogonal coding. In the second part of this work, we present an extension of the rank-one factorization approach to a multi-relaying scenario anda closed-form semi-blind receiver based on coupled SVDs (C-SVD) is derived. The C-SVD receiver efficiently combines all the available cooperative links to enhance channel and symbol estimation performance, while enjoying a parallel implementation.

Keywords: MIMO Systems, Cooperative Communications, Semi-Blind Receivers, Rank-One Tensors.

RESUMO

Comunicações cooperativas têm mostrado ser uma alternativa para combater os efeitos de propagação do sinal em comunicações sem-fio, como, por exemplo, a perda por percurso e sombreamento, criando um array virtual de antenas para a fonte transmissora. Neste trabalho, toma-se como ponto de partida um modelo de sistema MIMO de dois saltos com um único relay. Adicionando um estágio de filtragem no receptor, é proposta uma fatoração de posto unitário para o sinal resultante. A partir deste modelo, dois receptores semi-cegos para estimação conjunta de símbolo e canal são propostos: i) um receptor iterativo baseado no algoritmo trilinear de mínimos quadrados alternados (Tri-ALS) e ii) um receptor de solução fechada baseado na SVD de ordem superior truncada (T-HOSVD). Para este sistema, é também proposto um tensor de codificação espacial-temporal com uma estrutura PARAFAC, o que permite maior flexibilidade de design do sistema, além de uma codificação ortogonal. Na segunda parte deste trabalho, é apresentada uma extensão da fatoração de posto unitário para o cenário multi-relay e um receptor semi-cego de solução fechada baseado em SVDs acopladas (C-SVD) é desenvolvido. O receptor C-SVD combina de modo eficiente todos os *links* cooperativos disponíveis, melhorando o desempenho da estimação de símbolos e de canal, além de oferecer uma implementação paralelizável.

Palavras-chave: Sistemas MIMO, Comunicações Cooperativas, Receptores Semi-Cegos, Tensores de Posto Unitário.

LIST OF FIGURES

LIST OF TABLES

LIST OF ABBREVIATIONS AND ACRONYMS

2LSKP	2 steps Least Square Kronecker Product
ALS	Alternating Least Squares
DS-CDMA	Direct Sequence Code Division Multiple Access
C-SVD	Coupled SVD
CONFAC	Constrained Factor decomposition
E_S/No	Energy per symbol to noise power spectral density ratio
FLOPS	Floating-point Operations Per Second
HOOI	Higher-Order Orthogonal Iteration
HOSVD	Higher-Order Singular Value Decomposition
LS	Least Squares
MIMO	Multiple Inputs Multiple Outputs
MRC	Maximal Ratio Combining
NMSE	Normalized Mean Square Error
NTD(4)	Fourth-Order Nested Tucker Decomposition
NTD(5)	Fifth-Order Nested Tucker Decomposition
PARAFAC	Parallel Factors
QAM	Quadrature Amplitude Modulation
SER	Symbol Error Rate
SIC	Self Interference Cancellation
SNR	Signal-to-Noise Ratio
SVD	Singular Value Decomposition
Tri-ALS	Trilinear Alternating Least Squares
TSTC	Tensor Space-Time Coding
TT	Tensor Train

LIST OF SYMBOLS

$\mathbb{C}$	Field of complex numbers
$(\cdot)^{\mathrm{H}}$	Hermitian operator
$(\cdot)^{\mathrm{T}}$	Transpose operator
$\mathrm{vec}(\cdot)$	Vectorization operator
$\mathrm{unvec}(\cdot)$	Inverse operation to vectorization
$\cdot \circ \cdot$	Outer product
$\cdot \otimes \cdot$	Kronecker product
$\cdot \diamond \cdot$	Khatri-Rao product
$\cdot \times_n \cdot$	n-mode product
$\cdot \bullet_n^m \cdot$	Contraction operator
$\cdot \sqcup_N \cdot$	Concatenation operator
$\|\| \cdot \|\|_F$	Frobenius norm
$\| \cdot \|_2$	Euclidean norm
$\mathscr{O}(\cdot)$	Big-O notation for computational complexity

CONTENTS

1 INTRODUCTION

The use of multiple antennas at the transmitter side and receiver side brought new gains to wireless communications to exploit and new challenges compared with single antenna wireless systems. Among these gains, we highlight spatial diversity and spatial multiplexing gains. The spatial diversity gain comes from the use of multiple antennas to combat the fading in wireless communications. The spatial multiplexing gain comes from the transmission of multiple data streams in rich scattering environments, increasing the system spectral efficiency [1, 2, 3]. However, consider the case of a MIMO wireless system where the source has no line of sight with the destination or, the links between them are too poor. In this scenario, the use of relay stations has shown to be an alternative to combat fading and to increase the capacity and coverage of wireless system [4, 5, 6]. The benefits of relay-assisted wireless communications strongly rely on the accuracy of the CSI for all the links involved in the communication process. Moreover, the use of precoding techniques at the source and/or destination [7, 8] often requires the instantaneous CSI knowledge of all links. An example of a cooperative communication scenario is that of a multi-user system, where each user can be viewed as a relay station that assists the source.

Even thought, those users may have a single antenna only, the system exploits the spatial diversity as a MIMO system, due to the virtual antennas provided by the relay nodes. Some works in this application can be viewed in [9, 10, 11, 12]. In [9], the authors investigate a multi-user cooperative system with relay coding to enhance the performance of 4G systems. In [10] and [11], a multi-user cooperative system with AF protocol at the relay is studied. In[10], the authors focus on the problem in which scenario the relay must cooperate, and in [11], the authors proposed a multi-user detection for uplink DS-CDMA in a multi-relaying scenario taking advantage of the multidimensional nature of the signal, using tensor decompositions for parameter estimation. In [12], the authors investigate the problem of power allocation for a multi-user multi-relaying system with DF protocol in cognitive radio networks using bandwith-power product to reach a optimal spectrum-sharing. In the context of 5G systems, we can cite the recent work [13] where the authors proposed a non-orthogonal multiple access for downlink, where the system is divided in K time slots with $K-1$ users and each user performs a SIC approach to estimate their own data. Since such approach at each receiver demands processing time, in order to turn this operation less complex the authors proposed a modified version of the SIC method. In the past decade, the use of multilinear algebra or

tensor algebra for wireless communications has been growing up, at most after the work of Sidiropoulos [14]. The main interest has been on the use of tensor decompositions to model the received signal as well as to derive receiver algorithms exploiting multiple forms of signal diversity. The two most common tensor decompositions are PARAFAC (Parallel Factor) [15] and Tucker [16] decompositions. Alternative tensor decompositions have been developped recently ([17, 18, 19, 20]). The PARAFAC decomposition is the most popular one, and not only for its conceptual simplicity but also for its uniqueness property [21]. The Tucker decomposition, is note unique in general. However, when the core tensor it is known, the factors are unique under some scalar ambiguity [17]. In the context of MIMO wireless communication, in [19, 20, 22] semi-blind receivers have been proposed to jointly estimate the channel and the symbols using tensors modeling.

In the cooperative scenario, some works that propose receivers based on the use of tensor modelling can be found in [23, 24, 18, 17]. The work [23] develops a tensor-based channel estimation algorithm for two-way MIMO relaying systems using training sequences. In [24], a supervised joint channel estimation algorithm is proposed for one-way three-hop communication systems with two relay layers. In [18], the authors proposed a semi-blind receiver for two-hop MIMO relaying systems using a Nested PARAFAC model. The authors in [17] developed first a generalization of the work [18], so called Nested Tucker decomposition, by using full tensors as space-time coding (random exponential structure), at the source and the relay. They also proposed two semi-blind receivers. The first one is an iterative solution based on the ALS (Alternating Least Squares), while the second is a closed-form solution based on LSKP (Least Squares Kronecker Product) factorization. The ALS receiver exploits the dimensions of the received signal to estimate symbol and channel matrices. However, this algorithm requires extensive matrix products and matrix inversions for each iteration. On the other hand, the Kronecker factorization receiver is suboptimal since it divides the relay-destination channel and symbol estimations into two steps (2LSKP), and the estimation for source-relay channel depends on the accuracy of the previous estimation.

1.1 Relay Channels

Relay channels were introduced by Meulen in 1971 [25], the author investigates the three-terminal system where a user (terminal 1) is assisted by another user (terminal 2) to send

Figure 1 – Three terminal system example

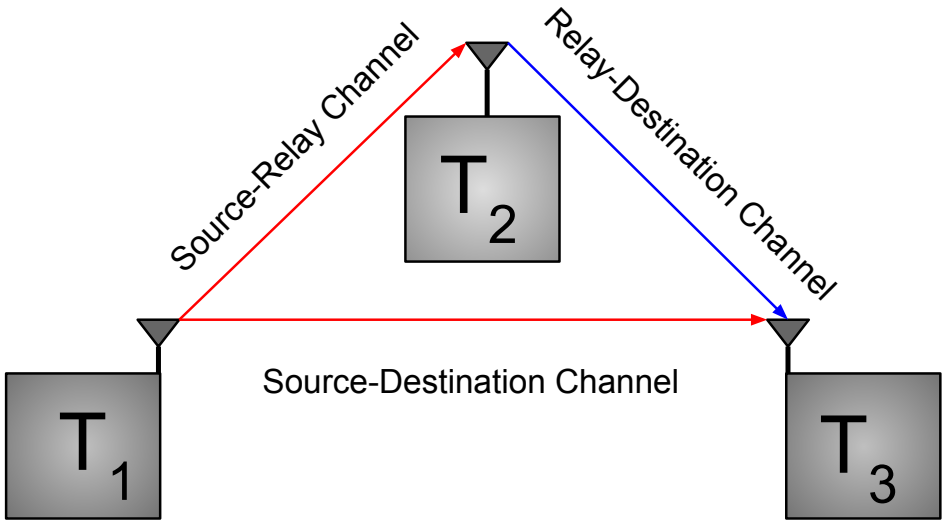

Source: Created by the Author

the data to destination (terminal 3), such cooperation divides the transmission into two phases, in the first, the terminal 1 sends the data to terminal 2 by a source-relay channel and to terminal 3 by a direct link, source-destination channel. Then, in the second phase, the terminal 2 sends to terminal 3 its own data plus the data from terminal 1 in the first phase. The system is illustrated in Figure 1, where the red line represents the transmission in the first phase and the blue in the second phase.

1.1.1 Cooperative Communications

In Figure 2 a three-terminal MIMO system is illustrated. This configuration combines the gains of MIMO systems and cooperative communications which can be summarized as

- **Spatial Diversity**

  As discussed in MIMO wireless advantages, the spatial diversity is related the use of multiple antennas for transmitting and receiving signals. In the case of cooperative communications, this can be achieved by single antenna users, since the relay node can be viewed as a virtual antenna for the source. Such case can be related into multi-user environment where each user (mobile) has a restriction on the number of antennas due to hardware, and in the end, the system takes advantage of the spatial diversity of MIMO systems [6].

Figure 2 – Three terminal MIMO system example

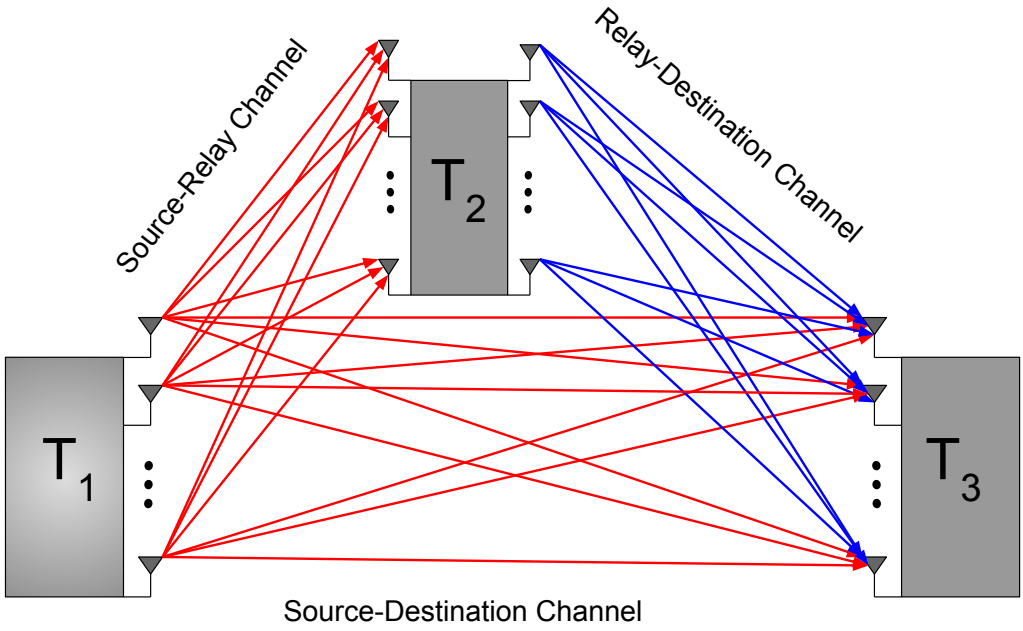

Source: Created by the Author

- **Spatial Multiplexing**

  Considering the system in figure 2 the multiplexing gain is related to the gain of using multiple antennas for transmitting independent data streams (as discussed previously). The difference is that in this cooperative communication, the independent data streams are sent through the relay channels, leading to the next advantage.

- **Coverage Area**

  As seen in Figure 2, the link between terminal 1 and terminal 2 and the link between terminal 2 and terminal 3 are shorter than the link between the terminal 1 and terminal 3, i.e. the path loss is smaller in the relay links than in the direct link, resulting in a less power for terminal 1 to reach terminal 3.

In terms of medium access, the relays usually are characterized as

- **Full-Duplex**

  In the full-duplex configuration, the relay can transmit and receive the signals at the same time.This approach presents a low latency in the system, although cross interference between the transmitted and received signals are introduced and must be accounted for. Some works dealing with full-duplex relays can be found in [26, 27].

- **Half-Duplex**

  In this configuration, the relay receives and transmits at different time slots. However, the latency of the system is increased, which in the case of a two-hop one relay system, the transmission rate has a drop of 50%. This configuration is the most common for relays, and appears in several works [17, 18, 28, 29].

In literature, there are many relay processing protocols that can be found in [4, 30, 31]. Basically, the protocols are divided into fixed relaying schemes and selective relaying schemes [4]. In a simple way, for the fixed relaying schemes the protocol used at the relay node is independent of the quality of the channel. The selective relaying schemes take into account the SNR of the received signal at the relay node. If the SNR exceeds a predefined threshold, the relay can apply the protocol. Else, the relay can remain idle. Next, we present some fixed relaying schemes protocols.

- **Fixed Amplifying and Forward (AF)**

  Also known as a non-regenerative protocol, the relay receives the signal from the source and scales it. This protocol is attractive for systems that consider constant channels, due to simplicity and latency time. The use of the AF protocol makes more sense in the cases where the relay is closer to the destination than the source to compensate the fading. Otherwise, the relay has to use more power which also amplifies the noise in the received signal [6].

- **Fixed Decode and Forward (DF)**

  Also known as a regenerative protocol, the DF consists of decoding the signal at the relay, then possibly applying some coding before forwarding to the destination. This scheme, compared with AF protocol, increases the latency of the system since some signal processing technique must be applied to decode the signal. For such protocol, it is useful that the relay is closer to the source than to the destination to have a better probability to decode the signal correctly than if the relay is closer to the destination [4, 6].

1.2 Contributions

The main contributions of this thesis can be summarized as

1. Minimization of the Frobenius norm of a matrix by the Kronecker product of N matrices.

This process is a generalization of the Kronecker product approximation introduced by Van Loan in [32] that minimizes the Frobenius norm of a matrix by the Kronecker product of two matrices, rearranging the structure to a rank-one matrix. The proposed generalization rearranges the matrix structure into a tensor which can be approximated by the outer products of N vectors, where those vectors are the vectorization of the original matrices involved in the Kronecker product.

2. Orthogonal effective codes designed by the exact Khatri-Rao factorization of a DFT matrix. We show that a DFT of size $K \times K$ can be factorized into the Khatri-Rao product of N matrices, with the constraint that $k_1 k_2 \cdots k_N = K$, where k_n is the number of rows of the *n-th* matrix factor.
3. Two semi-blind receivers for two-hop MIMO cooperative systems are proposed by exploiting a rank-one tensor approximation. The first receiver is iterative (based on ALS), while the second is a closed-form solution (based on the HOSVD).
4. A coupled SVD-based semi-blind (C-SVD) for a multi-relaying MIMO system which provides closed-form estimates of the channels and symbols by coupling multiple SVDs.

1.3 Thesis organization

- **Chapter 2 - Tensor Prerequisites**

  In this chapter, tensor arrays with some definitions and operations are introduced. The useful tensor decompositions for this thesis is presented. Also, an important topic is discussed, the generalization of the Kronecker approximation by Van Loan [32] which is the core part of the signal processing applied in the latest chapters and the DFT factorization by a Khatri-Rao product.

- **Chapter 3 - Two-Hop MIMO Relaying**

  A two-hop MIMO relay system is presented, which is modelled using the decompositions introduced in Chapter 2, resulting into two semi-blind receivers. The first one is iterative while the second is based on a closed-form solution. Both receivers exploit the rank-one tensor formulation of the received signal after a space-time combining.

- **Chapter 4 - Multi-Relaying MIMO System**

  A multi-relaying MIMO system is presented, taking advantage of the two-hop system modelled in Chapter 3 and using the generalized Kronecker approximation of Chapter 2. A closed-form solution to channel and symbol estimation is derived by coupling multiple

rank-one tensors (one for each cooperative link) using the SVD.

- **Chapter 5 - Conclusions**
  In this chapter, we draw the final comments and conclusions of this work, and highlight topics for future work.

1.4 Scientific production

Two papers have been produced as a result of this thesis. The first to a national congress of telecommunications and signal processing (SBrT 2017). The second paper has been submitted to the Journal of Communications and Information Systems, and we are waiting for the response.

1. **Bruno Sokal**, André L. F. de Almeida and Martin Haardt "*Rank-One Tensor Modeling Approach to Joint Channel and Symbol Estimation in Two-Hop MIMO Relaying Systems* published in the XXXV Simpósio Brasileiro de Telecomunicações, São Pedro, Brazil, 2017 ;
2. **Bruno Sokal**, André L. F. de Almeida and Martin Haardt "*Semi-Blind Coupled Receiver to Joint Symbol and Channel Estimation Using Rank-One Tensor Factorizations for MIMO Multi-Relaying System* Journal of Communication and Information Systems, 2017;

2 TENSOR PREREQUISITES

In this chapter, we start with the basis of tensor algebra, some properties and notations. In a second part, some useful decompositions that we make use in this thesis are presented. Finally, the generalized Kronecker approximation and the DFT factorization by a Khatri-Rao product are discussed.

2.1 Tensors

A tensor is an array with order greater than two (scalars have order zero, vectors order one, matrices order two), or simply a multidimensional array.
A tensor $\mathscr{X} \in \mathbb{C}^{I_1 \times I_2 \times \cdots \times I_N}$ is a multidimensional array with order N, with elements $\mathscr{X}_{(i_1,i_2,\cdots,i_n)}$, where $i_n = \{1 \cdots I_N\}$. In the following, some definitions are presented. For a better understanding consider a third-order tensor $\mathscr{X} \in \mathbb{C}^{I \times J \times K}$.

Figure 3 – Illustration of a third-order tensor $\mathscr{X}$

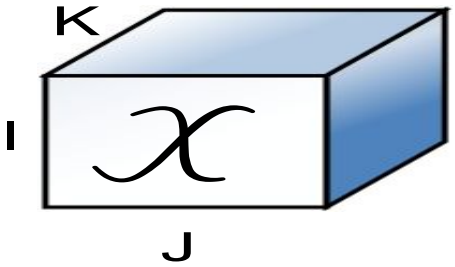

Source: Created by the Author

Definition 1. Fibers

Fibers are vectors formed by fixing the indices of all dimensions with the exception of one. For third-order tensors, there are three types of fibers: Column fibers, denoted by $\mathbf{x}_{.jk}$, where the indices for the J and K dimensions are fixed and the indices of the I dimension is varying, forming a vector of size $I \times 1$; Row fibers are denoted by $\mathbf{x}_{i.k}$, in this case the fixed dimensions are I and K, and the dimension J is varying, resulting in a vector of size $J \times 1$. At last, Tube fibers are denoted by $\mathbf{x}_{ij.}$ creating a vector of size $K \times 1$ by fixing the indices of the I and J dimensions, and varying the indices along the K dimension. Figure 4 illustrates this representation.

Figure 4 – (a) Column fibers; (b) Row fibers; (c) Tube fibers

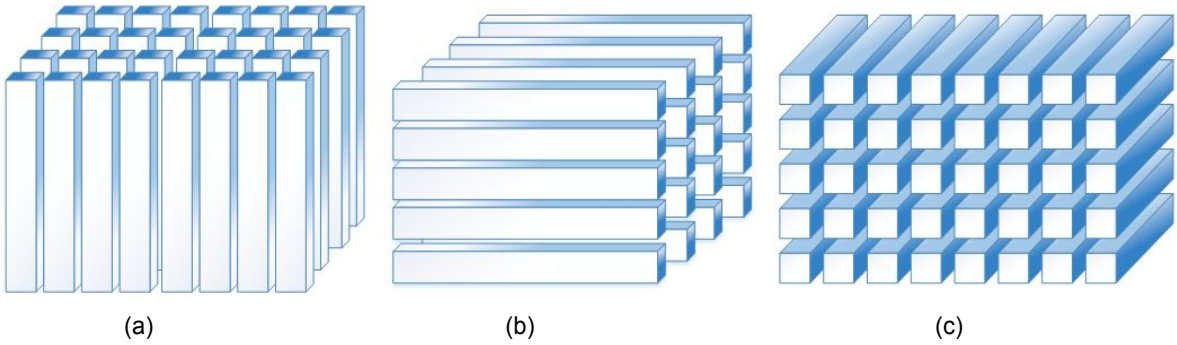

Source: Created by the Author

Figure 5 – (a) Frontal slices; (b) Lateral slices; (c) Horizontal slices

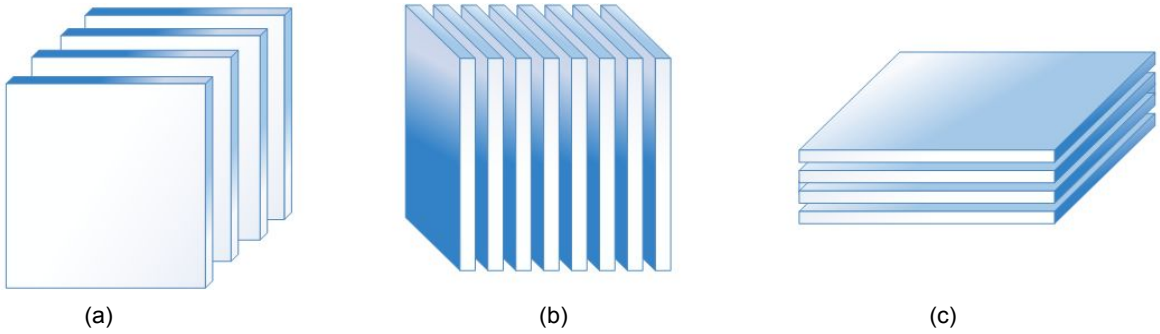

Source: Created by the Author

Definition 2. Slices

Slices are formed by fixing one index and varying the others. For a third-order tensor $\mathscr{X} \in \mathbb{C}^{I \times J \times K}$, slices are matrices and there are three different ways to slice it. Frontal slices are denoted by $\mathbf{X}_{..k}$ and are formed by varying the first and second modes and fixing the index along the third mode resulting in K matrices of size $I \times J$. Lateral slices are denoted by $\mathbf{X}_{.j.}$, in this case the index of the J dimension is fixed while the indices of the first and third modes are varying, at total resulting in J matrices of size $I \times K$. The last one for third-order tensors are the Horizontal slices, denoted by $\mathbf{X}_{i..}$, where now the index of the first mode is fixed and the indices of the second and third modes are now varying, yielding I matrices of size $J \times K$. Figure 5 shows this representation.

Definition 3. n-mode unfolding

One way to matricizes a tensor is to compute the n-mode unfolding. Consider the tensor $\mathscr{X} \in \mathbb{C}^{I \times J \times K}$, the n-mode unfolding of $\mathscr{X}$ is denoted by $\mathbf{X}_{(n)}$ and this operation separates the *n-th* mode fibers and put them along the rows, resulting in the flat n-mode unfolding $\mathbf{X}_{(n)}$, or in the columns forming the tall n-mode unfolding, which is the transposition of the flat one.

Since $\mathscr{X}$ it is a third-order tensor, there are three possible ways to matricize it. Let us denote $\mathbf{X}_{(1)} \in \mathbb{C}^{I \times JK}$, $\mathbf{X}_{(2)} \in \mathbb{C}^{J \times IK}$ and $\mathbf{X}_{(3)} \in \mathbb{C}^{K \times IJ}$ as the flat 1-mode, 2-mode and 3-mode unfolding of $\mathscr{X}$. The elements of the n-mode unfolding $\mathbf{X}_{(1)_{(i,\alpha)}}, \mathbf{X}_{(2)_{(j,\beta)}}$ and $\mathbf{X}_{(3)_{(k,\gamma)}}$ are mapped from $\mathscr{X}$ as

$$\alpha = j + (k-1)J, \tag{2.1}$$

$$\beta = i + (k-1)I, \tag{2.2}$$

$$\gamma = k + (j-1)K, \tag{2.3}$$

with $i = \{1 \cdots I\}$, $j = \{1 \cdots J\}$, $k = \{1 \cdots K\}$, $\alpha = \{1 \cdots JK\}$, $\beta = \{1 \cdots IK\}$ and $\gamma = \{1 \cdots IJ\}$. This mapping is known as the little-endian convention, defined in [33]. For the general case of a *N-th* order tensor $\mathscr{Y} \in \mathbb{C}^{I_1 \times \cdots \times I_N}$, the element of the flat n-mode unfolding $\mathbf{Y}_{(n)_{(in,l)}} \in \mathbb{C}^{I_n \times I_1 \cdots I_{n-1} I_{n+1} \cdots I_N}$ is mapped from $\mathscr{Y}$ as

$$l = i_1 + (i_2 - 1)I_1 + (i_3 - 1)I_1 I_2 + \cdots + (i_N - 1)I_1 \cdots I_{n-1} I_{n+1} \cdots I_{N-1}, \tag{2.4}$$

where $i_n = \{1 \cdots I_n\}$ and $l = \{1 \cdots I_1 \cdots I_{(n-1)} I_{(n+1)} \cdots I_N\}$.

Definition 4. Generalized n-mode unfolding

Instead of separating one mode from the others, as in the n-mode unfolding, the generalized n-mode unfolding matricizes the tensor by combining multiple modes as rows and columns of the resulting unfolding matrix. Defining $j = \{i_1, \cdots, i_n\}$ and $k = \{i_{n+1}, \cdots, i_N\}$ with $i_n = \{1 \cdots I_n\}$, the n-mode generalized unfolding maps the elements of $\mathscr{Y}_{(i_1, \cdots, i_N)}$ into a matrix $\mathbf{Y}_{[j,k]}$ as

$$j = i_1 + (i_2 - 1)I_1 + (i_3 - 1)I_1 I_2 + \cdots + (i_n - 1)I_1 I_2 \cdots I_{n-1} \tag{2.5}$$

$$k = i_{n+1} + (i_{n+2} - 1)I_{n+1} + \cdots + (i_N - 1)I_{n+1} I_{n+2} \cdots I_{N-1} \tag{2.6}$$

Definition 5. n-mode product

Given the third-order tensor $\mathscr{X} \in \mathbb{C}^{I \times J \times K}$ and a matrix $\mathbf{A} \in \mathbb{C}^{R \times I}$, the n-mode product linearly combines the 1-mode fibers with the columns of the matrix $\mathbf{A}$ resulting a tensor $\mathscr{Y}^{R \times J \times K}$. The n-mode product is denoted as

$$\mathscr{Y} = \mathscr{X} \times_1 \mathbf{A}. \tag{2.7}$$

This combination can be also expressed in terms of the n-mode unfolding , i.e.

$$\mathbf{Y}_{(1)} = \mathbf{A}\mathbf{X}_{(1)}. \tag{2.8}$$

The n-mode product has the following property:

$$\mathscr{Y} = \mathscr{X} \times_1 \mathbf{A} \times_1 \mathbf{B} \times_1 \mathbf{C} \tag{2.9}$$

$$= \mathscr{X} \times_1 \mathbf{CBA} \Longleftrightarrow \tag{2.10}$$

$$\mathbf{Y}_{(1)} = \mathbf{CBAX}_{(1)}. \tag{2.11}$$

Definition 6. Contraction

This operation combines two tensors that have a common mode [34]. For example, given two third-order tensors $\mathscr{X}^{I\times J\times K}$ and $\mathscr{Y}^{J\times L\times M}$, where J is a common mode, the contraction between them is defined as

$$\mathscr{G} = \mathscr{X} \bullet_2^1 \mathscr{Y}, \tag{2.12}$$

where $\mathscr{G}^{I\times K\times L\times M}$ is a fourth-order tensor. The upper index in the operator "$\bullet$" refers that the contracted mode is, in this case, involves the first mode of the tensor at the right side and the lower index indicates the mode that will be contracted in the left side tensor. In element-wise, the tensor $\mathscr{G}$ can be written as

$$\mathscr{G}_{(i,k,l,m)} = \sum_{j=1}^{J} \mathscr{X}_{(i,j,k)} \mathscr{Y}_{(j,l,m)} \tag{2.13}$$

Definition 7. Concatenation

Consider the third-order tensor $\mathscr{X}^{I\times J\times K}$ and the following matrices $\mathbf{A}^{(i)}$ of size $I \times J$, with $i = \{1 \cdots R\}$. We can form a tensor $\mathscr{G}^{I\times J\times (K+R)}$ as

$$\mathscr{G} = \mathscr{X} \sqcup_3 \mathbf{A}^{(1)} \sqcup_3 \mathbf{A}^{(1)} \sqcup_3 \cdots \sqcup_3 \mathbf{A}^{(R)}. \tag{2.14}$$

This operation concatenates all the matrices along the third dimension K. In this case, the frontal slices of tensor $\mathscr{G}$ are given by:

$$\mathbf{G}_{\cdot\cdot 1:K} = \mathbf{X}_{\cdot\cdot 1:K} \tag{2.15}$$

$$\mathbf{G}_{\cdot\cdot K+1} = \mathbf{A}^{(1)} \tag{2.16}$$

$$\mathbf{G}_{\cdot\cdot K+r} = \mathbf{A}^{(r)} \tag{2.17}$$

$$\mathbf{G}_{\cdot\cdot K+R} = \mathbf{A}^{(R)}. \tag{2.18}$$

Consider now a fourth-order tensor $\mathscr{Y} \in \mathbb{C}^{I\times J\times K\times L}$ and R third-order tensors $\mathscr{X}^{(r)} \in \mathbb{C}^{I\times K\times L}$, we can concatenate all those R tensors into the second mode of the tensor $\mathscr{Y}$, forming the fourth-order tensor $\mathscr{T} \in \mathbb{C}^{I\times(J+R)\times K\times L}$ as:

$$\mathscr{T} = \mathscr{Y} \sqcup_2 \mathscr{X}^{(1)} \sqcup_2 \cdots \sqcup_2 \mathscr{X}^{(R)} \tag{2.19}$$

The third-order tensors formed by fixing the second mode of $\mathscr{T}$ are given as:

$$\mathscr{T}_{\cdot 1:J\cdot\cdot} = \mathscr{Y} \tag{2.20}$$

$$\mathscr{T}_{\cdot J+1\cdot\cdot} = \mathscr{X}^{(1)} \tag{2.21}$$

$$\mathscr{T}_{\cdot J+r\cdot\cdot} = \mathscr{X}^{(r)} \tag{2.22}$$

$$\mathscr{T}_{\cdot J+R\cdot\cdot} = \mathscr{X}^{(R)} \tag{2.23}$$

Definition 8. Rank-one tensor

A *N-th* order tensor $\mathscr{Y}^{I_1\times\cdots\times I_N}$ is said to have a rank-one if we can write $\mathscr{Y}$ as the outer product of N vectors,

$$\mathscr{Y} = \mathbf{a}^{(1)} \circ \cdots \circ \mathbf{a}^{(N)}, \tag{2.24}$$

where $\mathbf{a}^{(i)}$ is a vector of size $I_i \times 1$, and $i = \{1\cdots N\}$.

Definition 9. Tensor rank

The typical rank of the tensor $\mathscr{X}$ is given by the smallest number of rank-one tensors yield $\mathscr{X}$ as linear combination. If $\mathscr{X}$ has rank R, we have

$$\mathscr{X} = \sum_{r=1}^{R} \mathbf{a}_r \circ \mathbf{b}_r \circ \mathbf{c}_r \tag{2.25}$$

Definition 10. vec(·) operator

Given a matrix $\mathbf{A} \in \mathbb{C}^{I\times J}$

$$\mathbf{A} = \begin{bmatrix} | & \vdots & | \\ \mathbf{a}_1 & \cdots & \mathbf{a}_R \\ | & \vdots & | \end{bmatrix}_{I\times R}, \tag{2.26}$$

the vectorization of $\mathbf{A}$ consists of stacking the columns of $\mathbf{A}$ as:

$$\text{vec}(\mathbf{A}) = \begin{bmatrix} \mathbf{a}_1 \\ \vdots \\ \mathbf{a}_R \end{bmatrix}_{IR\times 1}. \tag{2.27}$$

The unvec$(\cdot)$ operator is the inverse operator of the vec$(\cdot)$.

Definition 11. Kronecker Product

Given a matrix $\mathbf{A}$ of size $I \times J$ and a matrix $\mathbf{B}$ of size $R \times S$, the Kronecker product $\mathbf{C} = \mathbf{A} \otimes \mathbf{B}$ is defined as

$$\mathbf{C} = \begin{bmatrix} a_{11}\mathbf{B} & a_{12}\mathbf{B} & \cdots & a_{1J}\mathbf{B} \\ a_{21}\mathbf{B} & a_{22}\mathbf{B} & \cdots & a_{2J}\mathbf{B} \\ \vdots & \vdots & \ddots & \vdots \\ a_{I1}\mathbf{B} & a_{I2}\mathbf{B} & \cdots & a_{IJ}\mathbf{B} \end{bmatrix}_{RI \times SJ} \tag{2.28}$$

Note that the matrix $\mathbf{C}$ can be viewed as a block matrix with R blocks in the rows, S blocks in the columns and each block is a matrix of size $I \times J$. Let us define some useful properties of this product. For matrices $\mathbf{A}$, $\mathbf{B}$, $\mathbf{C}$ and $\mathbf{D}$ of compatible dimensions, we have:

$$(\mathbf{A} \otimes \mathbf{B})^{\mathrm{T}} = \mathbf{A}^{\mathrm{T}} \otimes \mathbf{B}^{\mathrm{T}} \tag{2.29}$$

$$(\mathbf{A} \otimes \mathbf{B})^{*} = \mathbf{A}^{*} \otimes \mathbf{B}^{*} \tag{2.30}$$

$$(\mathbf{A} \otimes \mathbf{B})^{\dagger} = \mathbf{A}^{\dagger} \otimes \mathbf{B}^{\dagger} \tag{2.31}$$

$$(\mathbf{A} \otimes \mathbf{B})(\mathbf{C} \otimes \mathbf{D}) = \mathbf{AC} \otimes \mathbf{BD} \tag{2.32}$$

$$\mathrm{vec}(\mathbf{ABC}) = (\mathbf{C}^{\mathrm{T}} \otimes \mathbf{A})\mathrm{vec}(\mathbf{B}) \tag{2.33}$$

$$\mathrm{vec}(\mathbf{a}^{(N)} \circ \cdots \circ \mathbf{a}^{(1)}) = \mathbf{a}^{(1)} \otimes \cdots \otimes \mathbf{a}^{(N)} \tag{2.34}$$

Definition 12. Khatri-Rao Product

This product is also known as the column-wise Kronecker product. Given the matrices $\mathbf{X} \in \mathbb{C}^{M \times N}$, $\mathbf{Y} \in \mathbb{C}^{L \times N}$, the Khatri-Rao, defined as $\mathbf{Z} = \mathbf{X} \diamond \mathbf{Y}$, is given by

$$\mathbf{Z} = \begin{bmatrix} \mathbf{x}_1 \otimes \mathbf{y}_1 & \mathbf{x}_2 \otimes \mathbf{y}_2 & \cdots & \mathbf{x}_N \otimes \mathbf{x}_N \end{bmatrix}_{LM \times N} \tag{2.35}$$

where $\mathbf{x}_n$ and $\mathbf{y}_n$ are the *n-th* column of the matrices $\mathbf{X}$ and $\mathbf{Y}$,respectively. For matrices $\mathbf{A}$, $\mathbf{B}$, $\mathbf{C}$ and $\mathbf{D}$ of compatible dimensions, we have:

$$(\mathbf{A} \otimes \mathbf{B})(\mathbf{C} \diamond \mathbf{D}) = \mathbf{AC} \diamond \mathbf{BD} \tag{2.36}$$

$$\mathrm{vec}(\mathbf{A}\mathrm{D}_n(\mathbf{B})\mathbf{C}) = (\mathbf{C}^{\mathrm{T}} \diamond \mathbf{A})\mathbf{b}_n^{\mathrm{T}}, \tag{2.37}$$

where $\mathrm{D}_n(\mathbf{B})$ is a diagonal matrix formed by the *n-th* row of the matrix $\mathbf{B}$, and $\mathbf{b}_n$ is the *n-th* row vector of $\mathbf{B}$.

2.2 Tensor Decompositions

We now present a few tensor decompositions that will be useful in the next chapters, namely the PARAFAC, Tucker and Nested Tucker decompositions. During the past decade, others decompositions were developed with applications in communication systems, such as: CONFAC [19], PARATUCK [20]. More recently, some generalized tensor decompositions have been developed such as the Tensor Train (TT) decomposition [35], Nested PARAFAC [18] and Nested Tucker [17].

2.2.1 PARAFAC Decomposition

Figure 6 – Illustration of a third-order PARAFAC decomposition as the sum of the outer products of three vectors.

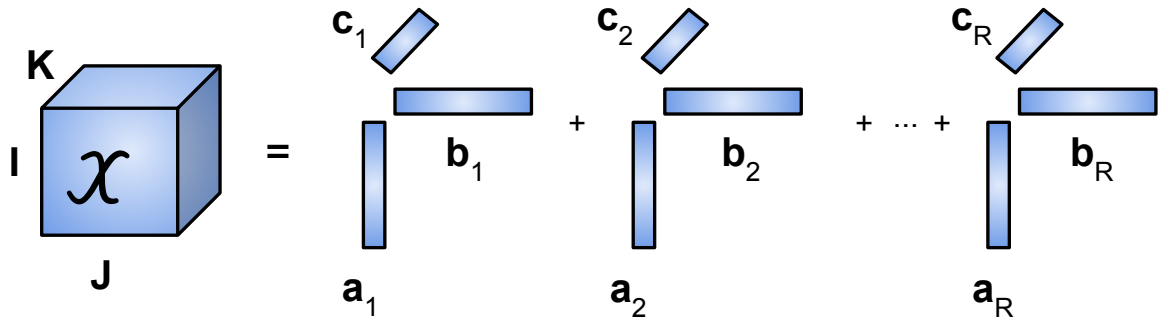

Source: Created by the Author

The Parallel Factors (PARAFAC) decomposition, also known as Canonical Decomposition (CANDECOMP) [36] and Canonical Polyadic (CP) [37], is the most popular tensor decomposition. It factorizes a *N-th* order tensor into a sum of the outer product of N vectors. In order to simplify, Figure 6 shows a PARAFAC decomposition of a third-order tensor $\mathscr{X}^{I\times J\times K}$, with the factors matrices being as

$$\mathbf{A} = \begin{bmatrix} | & | & \cdots & | \\ \mathbf{a}_1 & \mathbf{a}_2 & \cdots & \mathbf{a}_R \\ | & | & \cdots & | \end{bmatrix}_{I\times R} \quad \mathbf{B} = \begin{bmatrix} | & | & \cdots & | \\ \mathbf{b}_1 & \mathbf{b}_2 & \cdots & \mathbf{b}_R \\ | & | & \cdots & | \end{bmatrix}_{J\times R}$$

$$\mathbf{C} = \begin{bmatrix} | & | & \cdots & | \\ \mathbf{c}_1 & \mathbf{c}_2 & \cdots & \mathbf{c}_R \\ | & | & \cdots & | \end{bmatrix}_{K\times R} .$$

So we can write $\mathscr{X}$ using a shorthand notation as

$$\begin{aligned} \mathscr{X} &= \sum_{r=1}^{R} \mathbf{a}_r \circ \mathbf{b}_r \circ \mathbf{c}_r \\ &= [[\mathbf{A}, \mathbf{B}, \mathbf{C}]]. \end{aligned} \tag{2.38}$$

2.2.1.1 PARAFAC Slices

For a third-order PARAFAC tensor, its matrix slices can be represented as a function of its factor matrices. The frontal, horizontal and lateral slices can be respectively written as

$$\mathbf{X}_{..k} = \mathbf{A}\mathrm{D}_k(\mathbf{C})\mathbf{B}^{\mathrm{T}} \tag{2.39}$$

$$\mathbf{X}_{i..} = \mathbf{C}\mathrm{D}_i(\mathbf{A})\mathbf{B}^{\mathrm{T}} \tag{2.40}$$

$$\mathbf{X}_{.j.} = \mathbf{A}\mathrm{D}_j(\mathbf{B})\mathbf{C}^{\mathrm{T}} \tag{2.41}$$

2.2.1.2 n-mode unfolding

Considering now a *N-th* order tensor $\mathscr{X}^{I_1\times\cdots\times I_N}$ of rank R and factor matrices $\mathbf{A}^{(i)}$ of size $I_i \times R$, with $i = \{1\cdots N\}$. The tensor $\mathscr{X}$ can be expressed in terms of the n-mode product notation as

$$\mathscr{X} = \mathscr{I}_R \times_1 \mathbf{A}^{(1)} \times_2 \mathbf{A}^{(2)} \times_3 \cdots \times_N \mathbf{A}^{(N)}, \tag{2.42}$$

where $\mathscr{I}_R$ is the superdiagonal *N-th* order tensor of size $R\times\cdots\times R$ with the entries equal to one, if all indices are the same, and zero else. From Equation (2.42), the flat n-mode unfolding of $\mathscr{X}$ can be written as:

$$\mathbf{X}_{(n)} = \mathbf{A}^{(n)}(\mathbf{A}^{(N)} \diamond \cdots \diamond \mathbf{A}^{(n+1)} \diamond \mathbf{A}^{(n-1)} \diamond \cdots \diamond \mathbf{A}^{(1)})^{\mathrm{T}} \tag{2.43}$$

In the PARAFAC decomposition, the Kronecker operator "$\otimes$" is replaced by the Khatri-Rao operator "$\diamond$" due the core tensor $\mathscr{I}_R$ being an identity tensor.

2.2.1.3 Uniqueness

One of the properties that makes PARAFAC such a popular tensor decomposition is uniqueness. Differing from matrix decompositions, such as SVD, where the pair of singular matrices is unique under the imposition of orthogonality, the uniqueness of the PARAFAC decomposition can be achieved by a far simpler condition. Uniqueness means that in Equation (2.38) the columns of the factor matrices can be arbitrarily permuted and scaled, so that

$$\mathscr{X} = [[\mathbf{A}\mathbf{\Pi}\mathbf{\Delta}_A, \mathbf{B}\mathbf{\Pi}\mathbf{\Delta}_B, \mathbf{C}\mathbf{\Pi}\mathbf{\Delta}_C]], \tag{2.44}$$

where $\mathbf{\Pi}$ is some permutation matrix and $\mathbf{\Delta}_A, \mathbf{\Delta}_B, \mathbf{\Delta}_C$ are diagonal matrices containing the scaling factors, with $\mathbf{\Delta}_A\mathbf{\Delta}_B\mathbf{\Delta}_C = \mathbf{I}_R$, where $\mathbf{I}_R$ is the identity matrix of size $R \times R$.

For third-order tensors, in 1977, Kruskal [21] derived a sufficient condition for uniqueness. This condition relies on the so-called k-rank. If a matrix have a k-rank equal to l, it means that every set of l columns of this matrix is linearly independent. Denoting as $k_{\mathbf{A}}$, $k_{\mathbf{B}}$ and $k_{\mathbf{C}}$ as the k-rank of $\mathbf{A}, \mathbf{B}, \mathbf{C}$ the PARAFAC decomposition is unique if

$$k_{\mathbf{A}} + k_{\mathbf{B}} + k_{\mathbf{C}} \geq 2R + 2. \tag{2.45}$$

In [38], Sidiropoulos and Bro generalized the Kruskal's condition to an *N-th* order tensor. Consider the *N-th* order tensor $\mathscr{X}^{I_1 \times \cdots \times I_N}$ as

$$\mathscr{X} = \mathscr{I}_R \times_1 \mathbf{A}^{(1)} \times_2 \mathbf{A}^{(2)} \times_3 \cdots \times_N \mathbf{A}^{(N)}, \tag{2.46}$$

where $\mathbf{A}^{(n)}$ is a matrix of size $I_n \times R$, with $n = \{1 \cdots N\}$, and R is the tensor rank. The generalization of the Kruskal's condition is given by

$$\sum_{n=1}^{N} k_{\mathbf{A}^{(n)}} \geq 2R + (N-1). \tag{2.47}$$

2.2.1.4 ALS Algorithm

Consider the third-order tensor $\mathscr{X}$ of Equation (2.38). Suppose we want to approximate it by a third-order tensor $\hat{\mathscr{X}} = [[\mathbf{A}, \mathbf{B}, \mathbf{C}]]$, such that

$$\min_{\hat{\mathscr{X}}} ||\mathscr{X} - \hat{\mathscr{X}}||_F. \tag{2.48}$$

Algoritmo 1: ALS

1: Initialize randomly $\hat{\mathbf{B}}_0$ and $\hat{\mathbf{C}}_0$; it $= 0$;
2: it = it + 1;
3: Compute an estimate of $\hat{\mathbf{A}}$
$\hat{\mathbf{A}}_{it} = \mathbf{X}_{(1)}(\hat{\mathbf{C}}_{it-1} \diamond \hat{\mathbf{B}}_{it-1})^{\dagger}$
4: Compute an estimate of $\hat{\mathbf{B}}$
$\hat{\mathbf{B}}_{it} = \mathbf{X}_{(2)}(\hat{\mathbf{C}}_{it-1} \diamond \hat{\mathbf{A}}_{it-1})^{\dagger}$
5: Compute an estimate of $\hat{\mathbf{C}}$
$\hat{\mathbf{C}}_{it} = \mathbf{X}_{(3)}(\hat{\mathbf{B}}_{it-1} \diamond \hat{\mathbf{A}}_{it-1})^{\dagger}$
6: Return to step 2 until convergence.
7: Return $\hat{\mathbf{A}}$, $\hat{\mathbf{B}}$ and $\hat{\mathbf{C}}$.

One solution is to compute the Alternating Least Squares (ALS) algorithm. Since the tensor $\mathscr{X}$ is a third-order PARAFAC tensor, its n-mode unfolding can be written as

$$\mathbf{X}_{(1)} = \mathbf{A}(\mathbf{C} \diamond \mathbf{B})^{\mathrm{T}} \in \mathbb{C}^{I \times JK}, \tag{2.49}$$

$$\mathbf{X}_{(2)} = \mathbf{B}(\mathbf{C} \diamond \mathbf{A})^{\mathrm{T}} \in \mathbb{C}^{J \times IK}, \tag{2.50}$$

$$\mathbf{X}_{(3)} = \mathbf{C}(\mathbf{B} \diamond \mathbf{A})^{\mathrm{T}} \in \mathbb{C}^{K \times IJ}. \tag{2.51}$$

The ALS algorithm is an iterative method that solves a Least Squares (LS) problem for each mode of $\mathscr{X}$, by minimizing the following cost functions

$$\hat{\mathbf{A}} = \underset{\mathbf{A}}{\operatorname{argmin}} ||\mathbf{X}_{(1)} - \mathbf{A}(\hat{\mathbf{C}} \diamond \hat{\mathbf{B}})^{\mathrm{T}}|| \tag{2.52}$$

$$\hat{\mathbf{B}} = \underset{\mathbf{B}}{\operatorname{argmin}} ||\mathbf{X}_{(2)} - \mathbf{B}(\hat{\mathbf{C}} \diamond \hat{\mathbf{A}})^{\mathrm{T}}|| \tag{2.53}$$

$$\hat{\mathbf{C}} = \underset{\mathbf{C}}{\operatorname{argmin}} ||\mathbf{X}_{(3)} - \mathbf{C}(\hat{\mathbf{B}} \diamond \hat{\mathbf{A}})^{\mathrm{T}}||. \tag{2.54}$$

First, the ALS algorithm solves for $\hat{\mathbf{A}}$ using the random initializations of $\hat{\mathbf{B}}$ and $\hat{\mathbf{C}}$, next, it solves for $\mathbf{B}$ using the previously estimated matrix $\hat{\mathbf{A}}$ and the matrix $\hat{\mathbf{C}}$ initialized at the beginning, finally, solves the cost function for $\hat{\mathbf{C}}$ using the matrices $\hat{\mathbf{A}}$ and $\hat{\mathbf{B}}$ computed before, finishing the first iteration. The algorithm continues until the error between two iterations becomes smaller than a predefined threshold or reach the total number of iterations. The random initialization is not optimal and the ALS can be stuck in a local minimum. The authors in [39, 40, 41] proposed some alternatives for initializing the ALS algorithm. The standard ALS algorithm is summarized in Algorithm 1. One usual convergence criterion for the ALS algorithm is

$$||\hat{\mathbf{A}}_{it}(\hat{\mathbf{C}}_{it} \diamond \hat{\mathbf{B}}_{it})^{\mathrm{T}} - \hat{\mathbf{A}}_{it-1}(\hat{\mathbf{C}}_{it-1} \diamond \hat{\mathbf{B}}_{it-1})^{\mathrm{T}}||_F^2 \leq \varepsilon. \tag{2.55}$$

In this thesis we consider $\varepsilon = 10^{-6}$.

2.2.2 *Tucker Decomposition*

Figure 7 – Illustration of a Tucker decomposition.

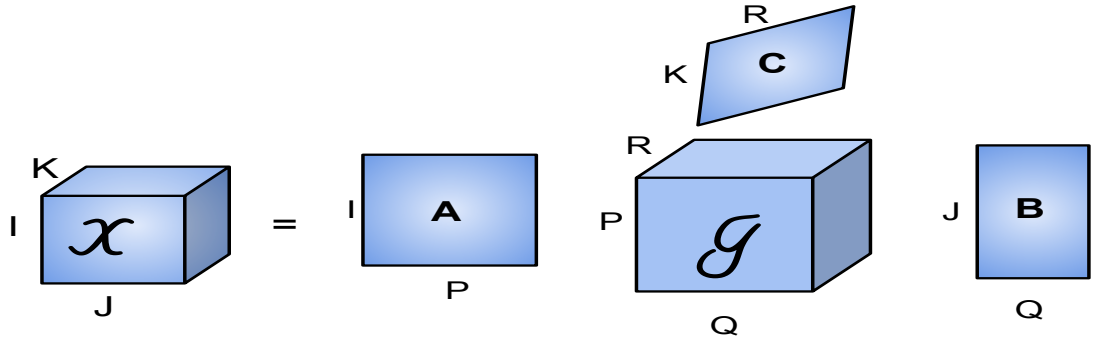

Source: Created by the Author

The Tucker decomposition was introduced by Tucker in 1963 [16]. It decomposes the tensor into a core tensor and factor matrices. The PARAFAC decomposition can be viewed as special case of Tucker decomposition, where the core tensor $\mathscr{I}_R$ is a diagonal tensor. Figure 7 illustrates the Tucker decomposition of a third-order tensor $\mathscr{X}^{I\times J\times K}$ into a core tensor $\mathscr{G}^{P\times Q\times R}$ and the factor matrices $\mathbf{A}\in\mathbb{C}^{I\times P}$, $\mathbf{B}\in\mathbb{C}^{J\times Q}$ and $\mathbf{C}\in\mathbb{C}^{K\times R}$. The tensor $\mathscr{X}$ can be written in n-mode product and scalar forms as

$$\mathscr{X} = \mathscr{G}\times_1\mathbf{A}\times_2\mathbf{B}\times_3\mathbf{C} \tag{2.56}$$

$$\mathscr{X}_{(i,j,k)} = \sum_{p=1}^{P}\sum_{q=1}^{Q}\sum_{r=1}^{R}\mathscr{G}_{(p,q,r)}\mathbf{A}_{(i,p)}\mathbf{B}_{(j,q)}\mathbf{C}_{(k,r)} \tag{2.57}$$

2.2.2.1 *Uniqueness*

In general, the Tucker decomposition is not unique since the core tensor can be transformed by a non-singular matrix and still fit, i.e.

$$\begin{aligned}\mathscr{X} &= \mathscr{G}\times_1\mathbf{U}_1\times_1\mathbf{A}\mathbf{U}_1^{-1}\times_2\mathbf{U}_2\times_2\mathbf{B}\mathbf{U}_2^{-1}\times_3\mathbf{U}_3\times_3\mathbf{C}\mathbf{U}_3^{-1}, &(2.58)\\ &= \mathscr{G}\times_1\mathbf{A}\mathbf{U}_1^{-1}\mathbf{U}_1\times_2\mathbf{B}\mathbf{U}_2^{-1}\mathbf{U}_2\times_3\mathbf{C}\mathbf{U}_3^{-1}\mathbf{U}_3, &(2.59)\\ &= \mathscr{G}\times_1\mathbf{A}\times_2\mathbf{B}\times_3\mathbf{C}. &(2.60)\end{aligned}$$

In [17], the authors showed that if the core tensor is known, the factor matrices are unique under some scaling factors.

Proof. Consider a *N-th* order tensor $\mathscr{X}^{I_1\times\cdots\times I_N}$ with the core tensor $\mathscr{G}^{R_1\times\cdots\times R_N}$ and the factor matrices $\mathbf{A}^{(i)}$ of size $I_i\times R_i$, where $i=\{1\cdots N\}$, and $\mathbf{U}^{(i)}$ of size $R_i\times R_i$ are some non singular

matrices. Computing the 1-mode unfolding of $\mathscr{X}$ we have

$$\mathbf{X}_{(1)} = \mathbf{A}^{(1)}\mathbf{G}_{(1)}(\mathbf{A}^{(N)} \otimes \cdots \otimes \mathbf{A}^{(2)})^{\mathrm{T}} \tag{2.61}$$

Applying Property 2.33 yields

$$\mathrm{vec}(\mathbf{X}_{(1)}) = (\mathbf{A}^{(N)} \otimes \cdots \otimes \mathbf{A}^{(1)})\mathrm{vec}(\mathbf{G}_{(1)}) \tag{2.62}$$

Replacing $\mathbf{A}^{(i)}$ by $\mathbf{A}^{(i)}\mathbf{U}^{(i)}$ we have

$$\begin{aligned}\mathrm{vec}(\mathbf{X}_{(1)}) &= (\mathbf{A}^{(N)}\mathbf{U}^{(N)} \otimes \cdots \otimes \mathbf{A}^{(1)}\mathbf{U}^{(1)})\mathrm{vec}(\mathbf{G}_{(1)}) \\ &= (\mathbf{A}^{(N)} \otimes \cdots \otimes \mathbf{A}^{(1)})(\mathbf{U}^{(N)} \otimes \cdots \otimes \mathbf{U}^{(1)})(\mathbf{G}_{(1)})\end{aligned} \tag{2.63}$$

The equations (2.62) and (2.63) are equal only if the term $\mathbf{U}^{(N)} \otimes \cdots \otimes \mathbf{U}^{(1)}$ is a identity matrix meaning that $\mathbf{U}^{(i)} = \alpha_i \mathbf{I}^{(i)}$ and $\prod_{i=1}^{N} \alpha_i = 1$, with $\mathbf{I}^{(i)}$ is the identity matrix of size $R_i \times R_i$. □

2.2.2.2 Special Tucker Decompositions

Figure 8 – Illustration of a Tucker-(2, 3) decomposition.

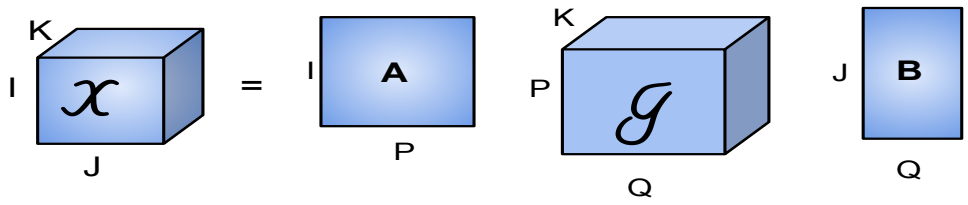

Source: Created by the Author

In [42] the authors introduced the concept of Tucker-(N_1,N), where N denotes the order of the tensor with $N - N_1$ factors matrices equal to the identity matrix. Two decompositions that are used later in this thesis are the Tucker-(2,3) and Tucker-(1,3).

For the Tucker-(2, 3) decomposition, a tensor $\mathscr{X} \in \mathbb{C}^{I \times J \times K}$ is decomposed into a core tensor $\mathscr{G} \in \mathbb{C}^{P \times Q \times K}$ and two factor matrices $\mathbf{A} \in \mathbb{C}^{I \times P}$ and $\mathbf{B} \in \mathbb{C}^{J \times Q}$. Figure 8 illustrates

the decomposition. The tensor $\mathscr{X}$ can be expressed as

$$\mathscr{X} = \mathscr{G} \times_1 \mathbf{A} \times_2 \mathbf{B} \times_3 \mathbf{I}_K \tag{2.64}$$

$$\mathscr{X}_{(i,j,k)} = \sum_{p=1}^{P} \sum_{q=1}^{Q} \mathscr{G}_{p,q,k} \mathbf{A}_{(i,p)} \mathbf{B}_{(j,q)} \tag{2.65}$$

$$\mathbf{X}_{..k} = \mathbf{A}\mathbf{G}_{..k}\mathbf{B}^{\mathrm{T}} \tag{2.66}$$

where $\mathbf{I}_K$ is the identity matrix of size $K \times K$ and $\mathbf{X}_{..k}$ is the *k-th* frontal slice of $\mathscr{X}$.

Figure 9 – Illustration of a Tucker-$(1,3)$ decomposition.

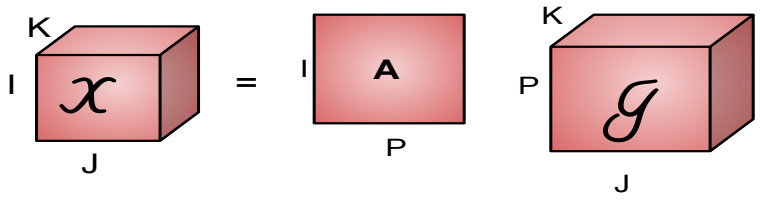

Source: Created by the Author

The Tucker-$(1,3)$ is the case where the tensor $\mathscr{X} \in \mathbb{C}^{I \times J \times K}$ is decomposed into a core tensor $\mathscr{G} \in \mathbb{C}^{P \times J \times K}$ and a factor matrix $\mathbf{A} \in \mathbb{C}^{I \times P}$. Figure 9 shows the decomposition. In this case, the tensor $\mathscr{X}$ is given by

$$\mathscr{X} = \mathscr{G} \times_1 \mathbf{A} \times_2 \mathbf{I}_J \times_3 \mathbf{I}_K \tag{2.67}$$

$$\mathscr{X}_{(i,j,k)} = \sum_{p=1}^{P} \mathbf{A}_{(i,p)} \mathscr{G}_{(p,j,k)} \tag{2.68}$$

$$\mathbf{X}_{..k} = \mathbf{A}\mathbf{G}_{..k} \tag{2.69}$$

2.2.2.3 Higher-Order Singular Value Decomposition (HOSVD) Algorithm

Tucker decomposition is also known as High-Order Singular Value Decomposition [43]. As explained in the uniqueness section, the Tucker decomposition it's not unique, meaning that we can only provide a basis for the true factors. In the case, the HOSVD algorithm computes a basis for each factor matrix by via SVD for each n-mode unfolding of the tensor, selecting the left singular matrix (if it's the flat n-mode unfolding) and truncating into the specific size. Computing the SVD of Equation (2.61) we have

$$\mathbf{X}_{(1)} = \mathbf{U}\mathbf{\Sigma}\mathbf{V}^{\mathrm{H}} = \mathbf{A}^{(1)}\mathbf{G}_{(1)}(\mathbf{A}^{(N)} \otimes \cdots \otimes \mathbf{A}^{(2)})^{\mathrm{T}} \tag{2.70}$$

since $\mathbf{U}$ is an orthogonal matrix that spans the subspace of $\mathbf{A}^{(1)}$ of size $I_1 \times R_1$, and truncating $\mathbf{U}$ to the R_1 columns, will exist a non-singular matrix $\mathbf{T}$, of size $R_1 \times R_1$, such that

$$\mathbf{A} = \mathbf{UT}. \tag{2.71}$$

However, for a rank-one matrix the uniqueness condition is under some scale factor [44]. The HOSVD algorithm is described in Algorithm 2.

Algoritmo 2: HOSVD

1: Compute the SVD for 1-mode of $\mathscr{X}$
   $\mathbf{X}_{(1)} = \mathbf{U}_{(1)}\mathbf{\Sigma}_{(1)}\mathbf{V}_{(1)}^{\mathrm{H}}$
   $\hat{\mathbf{A}} = \mathbf{U}_{(1)}$ Truncated to the first P columns
2: Compute the SVD for 2-mode of $\mathscr{X}$
   $\mathbf{X}_{(2)} = \mathbf{U}_{(2)}\mathbf{\Sigma}_{(2)}\mathbf{V}_{(2)}^{\mathrm{H}}$
   $\hat{\mathbf{B}} = \mathbf{U}_{(2)}$ Truncated to the first Q columns
3: Compute the SVD for 3-mode of $\mathscr{X}$
   $\mathbf{X}_{(3)} = \mathbf{U}_{(3)}\mathbf{\Sigma}_{(3)}\mathbf{V}_{(3)}^{\mathrm{H}}$
   $\hat{\mathbf{C}} = \mathbf{U}_{(3)}$ Truncated to the first R columns
4: Compute the core tensor $\mathscr{G}$ as
   $\mathscr{G} = \mathscr{X} \times_1 \hat{\mathbf{A}}^{\mathrm{H}} \times_2 \hat{\mathbf{B}}^{\mathrm{H}} \times_3 \hat{\mathbf{C}}^{\mathrm{H}}$
5: Return $\mathscr{G}$, $\hat{\mathbf{A}}$, $\hat{\mathbf{B}}$ and $\hat{\mathbf{C}}$.

2.2.3 Nested Tucker Decomposition

Figure 10 – 3-D Illustration of a *N-th* order Nested Tucker decomposition.

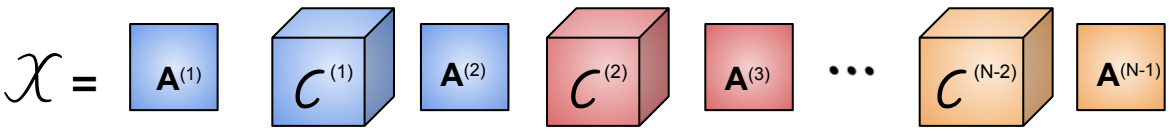

Source: Created by the Author

Nested Tucker decomposition was introduced in [17]. This decomposition is a general case of the Nested PARAFAC decompositions in [18], where the core tensors are full tensors. This decomposition can be viewed as a special case of the TT decomposition developed by Oseledets in 2011 [35]. The difference is that in the TT decomposition, a *N-th* order tensor is decomposed into N third-order core tensors with two matrices in the edges, and the Nested Tucker decomposition is a train of Tuckers-(2,3) and Tuckers-(1,3) in a contraction (or a train

of Tuckers-(1,3) and Tuckers-(2,3)), where those decompositions share a factor matrix. In this thesis, we make use of Nested Tucker decompositions of orders four and five, also referred to as NTD(4) and NTD(5), respectively, to model multi-relaying MIMO systems, as shown in Chapter 4.

Consider the *N-th* order tensor $\mathscr{X}^{I_1\times\cdots\times I_N}$ illustrated in Figure 10, the core tensors $\mathscr{C}^{(n)}$ are of size $R_{2n-1}\times R_{2n}\times I_{n+1}$ with exception of the last core $\mathscr{C}^{(N-2)}$ that is of size $R_{2n-1}\times R_{2n}\times I_N$, and the matrices at the edge $\mathbf{A}^{(1)}$ and $\mathbf{A}^{(N-1)}$ are of size $I_1\times R_1$ and $I_{N-1}\times R_{2N-4}$, while the matrices between the cores $\mathbf{A}^{(n+1)}$ are of size $R_{2n}\times R_{2n+1}$. This will be clear next section where the simple cases are introduced. The tensor $\mathscr{X}$ can be written as

$$\mathscr{X}_{(i_1,i_2,\cdots,i_N)}=\sum_{r_1=1}^{R_1}\sum_{r_2=1}^{R_2}\cdots\sum_{r_{N-1}=1}^{R_{N-1}}\mathbf{A}^{(1)}_{(i_1,r_1)}\mathscr{C}^{(1)}_{(r_1,r_2,i_2)}\cdots\mathscr{C}^{(N-2)}_{(r_{N-2},r_{N-1},i_N)}\mathbf{A}^{(N-1)}_{(i_{N-1},r_{2N-4})} \tag{2.72}$$

2.2.3.1 Fourth-Order Nested Tucker Decompositions (NTD(4))

Figure 11 – 3-D illustration of a 4-*th* order Nested Tucker tensor.

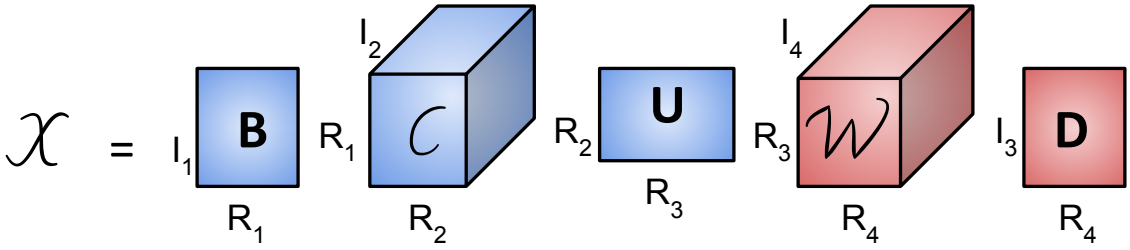

Source: Created by the Author

Also called as NTD(4), it decomposes a fourth-order tensor $\mathscr{X}$ as a contraction between a Tucker-(2,3) and Tucker-(1,3) decompositions. The Nested Tucker decomposition of a fourth-order tensor $\mathscr{X}\in\mathbb{C}^{I_1\times I_2\times I_3\times I_4}$, illustrated in Figure 11, with factor matrices as $\mathbf{B}\in\mathbb{C}^{I_1\times R_1}$, $\mathbf{U}\in\mathbb{C}^{R_2\times R_3}$, $\mathbf{D}\in\mathbb{C}^{I_3\times R_4}$ and core tensors $\mathscr{C}\in\mathbb{C}^{R_1\times R_2\times I_2}$, $\mathscr{W}\in\mathbb{C}^{R_3\times R_4\times I_4}$, is written as

$$\mathscr{X}_{(i_1,i_2,i_3,i_4)}=\sum_{r_1=1}^{R_1}\sum_{r_2=1}^{R_2}\sum_{r_3=1}^{R_3}\sum_{r_4=1}^{R_4}\mathbf{B}_{(i_1,r_1)}\mathscr{C}_{(r_1,r_2,i_2)}\mathbf{U}_{(r_2,r_3)}\mathscr{W}_{(r_3,r_4,i_4)}\mathbf{D}_{(i_3,r_4)} \tag{2.73}$$

Defining the following Tucker-(2,3) and Tucker-(1,3) decompositions:

$$\mathscr{T}^{(1)}=\mathscr{C}\times_1\mathbf{B}\times_2\mathbf{U}^{\mathrm{T}} \qquad \in\mathbb{C}^{I_1\times R_3\times I_2} \tag{2.74}$$

$$\mathscr{T}^{(2)}=\mathscr{W}\times_2\mathbf{D} \qquad \in\mathbb{C}^{R_3\times I_3\times I_4} \tag{2.75}$$

$$\mathscr{T}^{(3)}=\mathscr{C}\times_1\mathbf{B} \qquad \in\mathbb{C}^{I_1\times R_2\times I_2} \tag{2.76}$$

$$\mathscr{T}^{(4)}=\mathscr{W}\times_1\mathbf{U}\times_2\mathbf{D} \qquad \in\mathbb{C}^{R_2\times I_3\times I_4}. \tag{2.77}$$

The tensor $\mathscr{X}$ can be viewed as a contraction involving $\mathscr{T}^{(1)}$ and $\mathscr{T}^{(2)}$ with the common mode as R_3, i.e. a contraction between a Tucker-(2,3) and Tucker-(1,3) tensors. We have:

$$\mathscr{X} = [(\mathscr{C} \times_1 \mathbf{B} \times_2 \mathbf{U}^{\mathrm{T}}) \bullet_2^1 \mathscr{W}] \times_3 \mathbf{D} \tag{2.78}$$

$$= (\mathscr{C} \times_1 \mathbf{B} \times_2 \mathbf{U}^{\mathrm{T}}) \bullet_2^1 (\mathscr{W} \times_2 \mathbf{D}) \tag{2.79}$$

$$= \mathscr{T}^{(1)} \bullet_2^1 \mathscr{T}^{(2)} \tag{2.80}$$

Alternatively, the tensor $\mathscr{X}$ can be viewed as a contraction between tensors $\mathscr{T}^{(3)}$ and $\mathscr{T}^{(4)}$ with the common mode as R_2, i.e. a contraction between Tucker-(1,3) and Tucker-(2,3) tensors, i.e.

$$\mathscr{X} = [(\mathscr{C} \times_1 \mathbf{B}) \bullet_2^1 (\mathscr{W} \times_1 \mathbf{U})] \times_3 \mathbf{D} \tag{2.81}$$

$$= (\mathscr{C} \times_1 \mathbf{B}) \bullet_2^1 (\mathscr{W} \times_1 \mathbf{U} \times_2 \mathbf{D}) \tag{2.82}$$

$$= \mathscr{T}^{(3)} \bullet_2^1 \mathscr{T}^{(4)}. \tag{2.83}$$

In any case, the $(i_2 i_4)$-*th* slice of $\mathscr{X}$ is expressed as

$$\mathbf{X}_{.i_2.i_4} = \mathbf{B}\mathbf{C}_{..i_2}\mathbf{U}\mathbf{W}_{..i_4}\mathbf{D}^{\mathrm{T}} \in \mathbb{C}^{I_1 \times I_3}. \tag{2.84}$$

2.2.3.2 *Fifth-Order Nested Tucker Decomposition (NTD(5))*

Figure 12 – 3-D illustration of a 5-*th* order Nested Tucker tensor.

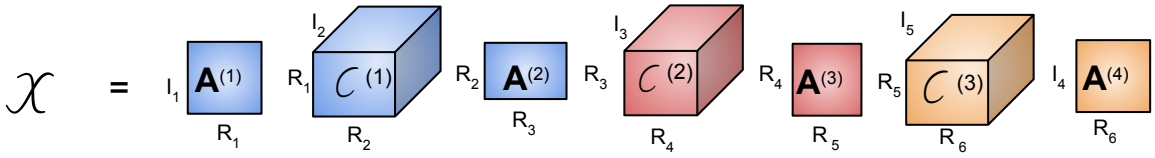

Source: Created by the Author

This particular case is introduced to simplify the understanding of the MIMO relaying system model in Chapter 4. In this case, we can define the following Tucker-(2,3) and Tucker-(1,3)

$$\mathscr{T}^{(1)} = \mathscr{C}^{(1)} \times_1 \mathbf{A}^{(1)} \times_2 \mathbf{A}^{(2)\mathrm{T}} \qquad \in \mathbb{C}^{I_1 \times R_3 \times I_2} \tag{2.85}$$

$$\mathscr{T}^{(2)} = \mathscr{C}^{(2)} \times_2 \mathbf{A}^{(3)\mathrm{T}} \qquad \in \mathbb{C}^{R_3 \times R_5 \times I_3} \tag{2.86}$$

$$\mathscr{T}^{(3)} = \mathscr{C}^{(3)} \times_2 \mathbf{A}^{(4)} \qquad \in \mathbb{C}^{R_5 \times I_4 \times I_5} \tag{2.87}$$

In the NTD(5) case, the tensor $\mathscr{X}$ can be viewed as a train of one Tucker-$(2,3)$ and two Tucker-$(1,3)$ as

$$\mathscr{X} = (\mathscr{T}^{(1)} \bullet_2^1 \mathscr{T}^{(2)}) \bullet_3^1 \mathscr{T}^{(3)}, \tag{2.88}$$

and the $(.i_2 i_3 .i_5)$-*th* slice of $\mathscr{X}$ is given by

$$\mathbf{X}_{.i_2 i_3 .i_5} = \mathbf{A}^{(1)} \mathbf{C}^{(1)}_{..i_2} \mathbf{A}^{(2)} \mathbf{C}^{(2)}_{..i_3} \mathbf{A}^{(3)} \mathbf{C}^{(3)}_{..i_5} \mathbf{A}^{(4)\mathrm{T}} \in \mathbb{C}^{I_1 \times I_4}. \tag{2.89}$$

2.3 Kronecker Product Approximation

In this section, the Kronecker product approximation is presented. First, we introduce the Van Loan case [32] and then we describe our proposed generalization.

2.3.1 From Kronecker Approximation to Rank-one Matrix

Consider the following Kronecker product $\mathbf{X} = \mathbf{B} \otimes \mathbf{C}$, where $\mathbf{X}$ of size $RI \times SJ$, $\mathbf{B}$ of size $I \times J$ and $\mathbf{C}$ of size $R \times S$ and the minimization problem

$$\phi(\mathbf{B}, \mathbf{C}) = ||\mathbf{X} - \mathbf{B} \otimes \mathbf{C}||_F. \tag{2.90}$$

Van Loan in [32] shows that solving (2.90) is the same as solving for a permuted version of $\mathbf{X}$ and then computing a rank-one SVD, as follows

$$\phi(\mathbf{B}, \mathbf{C}) = ||\overline{\mathbf{X}} - \mathrm{vec}(\mathbf{B})\mathrm{vec}(\mathbf{C})^{\mathrm{T}}||_F \tag{2.91}$$

A small example can illustrate this rearrangement. Consider as $J = R = S = 2$ and $I = 3$. The matrix $\mathbf{X}$ can be divided into blocks due to the Kronecker product, as

$$\mathbf{X} = \begin{bmatrix} \mathbf{P}_{(1,1)} & \mathbf{P}_{(1,2)} \\ \mathbf{P}_{(2,1)} & \mathbf{P}_{(2,2)} \\ \mathbf{P}_{(3,1)} & \mathbf{P}_{(3,2)} \end{bmatrix}, \tag{2.92}$$

where each block $\mathbf{P}$ is a matrix of size 2×2. The matrix $\overline{\mathbf{X}}$ is constructed as

$$\overline{\mathbf{X}} = \begin{bmatrix} \mathrm{vec}(\mathbf{P}_{(1,1)})^{\mathrm{T}} \\ \mathrm{vec}(\mathbf{P}_{(2,1)})^{\mathrm{T}} \\ \mathrm{vec}(\mathbf{P}_{(3,1)})^{\mathrm{T}} \\ \mathrm{vec}(\mathbf{P}_{(1,2)})^{\mathrm{T}} \\ \mathrm{vec}(\mathbf{P}_{(2,2)})^{\mathrm{T}} \\ \mathrm{vec}(\mathbf{P}_{(3,2)})^{\mathrm{T}} \end{bmatrix} \tag{2.93}$$

Note that this rearrangement maps the elements of $\mathbf{X}$ into a rank-one matrix $\overline{\mathbf{X}}$ and computing it SVD as

$$\overline{\mathbf{X}} = \mathbf{U}\mathbf{\Sigma}\mathbf{V}^{\mathrm{H}}, \tag{2.94}$$

yields a solution for $\mathbf{B}$ and $\mathbf{C}$ as

$$\hat{\mathbf{B}} = \text{unvec}(\sqrt{\sigma_1}\mathbf{U}_{(:,1)}) \tag{2.95}$$

$$\hat{\mathbf{C}} = \text{unvec}(\sqrt{\sigma_1}\mathbf{V}^*_{(:,1)}). \tag{2.96}$$

Note that the estimated $\hat{\mathbf{B}}$ and $\hat{\mathbf{C}}$ are affected by arbitrary scalar factors that compensate each other, i.e.:

$$\mathbf{B} = \alpha\hat{\mathbf{B}} \tag{2.97}$$

$$\mathbf{C} = \frac{1}{\alpha}\hat{\mathbf{C}} \tag{2.98}$$

2.3.2 From Kronecker Product Approximation to Rank-one Tensor

In [45], the authors already proposed an extension of the Van Loan's Kronecker approximation problem to multiple matrices, by rearranging the cost function into tensor product. Consider the generalized minimization problem as

$$\min_{\mathbf{A}^{(1)}\cdots\mathbf{A}^{(N)}} ||\mathbf{X} - \mathbf{A}^{(1)} \otimes \cdots \otimes \mathbf{A}^{(N)}||_F, \tag{2.99}$$

where $\mathbf{A}^{(i)} \in \mathbb{C}^{p_i \times q_i}$ and $\mathbf{X} \in \mathbb{C}^{p_N \cdots p_1 \times q_N \cdots q_1}$. The authors propose to rearrange the cost function as

$$||\mathscr{M} - \mathscr{S} \times_3 \mathbf{u}^{(3)} \times_4 \mathbf{u}^{(4)} \cdots \times_{N+1} \mathbf{u}^{(N+1)}||_F, \tag{2.100}$$

where $\mathscr{M} \in \mathbb{C}^{p_N \times q_N \times p_1 q_1 \times \cdots \times p_{N-1} q_{N-1}}$, $\mathscr{S} = \mathbf{A}^{(N)} \in \mathbb{C}^{p_N \times q_N \times 1}$ and $\mathbf{u}_3 \cdots \mathbf{u}_{N+1}$ are vectors formed by reshaping the factor matrices $\mathbf{A}^{(1)} \cdots \mathbf{A}^{(N-1)}$. Problem (2.100) can be solved by means of the HOOI (Higher-Order Orthogonal Iterations) algorithm [43].

Our proposed generalization of the Van Loan's Kronecker approximation consists of rearranging the problem into a rank-one tensor where, comparing to [45], the core tensor is a superdiagonal tensor, i.e. assumes a PARAFAC decomposition. Consider the minimization in (2.99), we proposed a permutation in $\mathbf{X}$ such that the minimization problem becomes

$$\min_{\mathbf{a}^{(1)}\cdots\mathbf{a}^{(N)}} ||\overline{\mathbf{x}} - \mathbf{a}^{(1)} \otimes \cdots \otimes \mathbf{a}^{(N)}||_F, \tag{2.101}$$

where $\overline{\mathbf{x}}$ is a vectorization of a permuted version of $\mathbf{X}$ and $\mathbf{a}^{(i)}$ is the vectorization of the $\mathbf{A}^{(i)}$ factor matrix. From Property (2.34), we can rewrite the minimization in (2.102) as

$$\min_{\mathbf{a}^{(N)}\cdots\mathbf{a}^{(1)}} ||\overline{\mathscr{X}} - \mathbf{a}^{(N)} \circ \cdots \circ \mathbf{a}^{(1)}||_F. \tag{2.102}$$

From Definition 8, the tensor $\overline{\mathscr{X}} \in \mathbb{C}^{p_N q_N \times \cdots \times p_1 q_1}$ can be considered as a rank-one tensor. Now, we consider the special case of a Kronecker product involving the Kronecker product of three matrices: $\mathbf{X} = \mathbf{A} \otimes \mathbf{B} \otimes \mathbf{C}$. Consider the following cost function:

$$\phi(\mathbf{A}, \mathbf{B}, \mathbf{C}) = ||\mathbf{X} - \mathbf{A} \otimes \mathbf{B} \otimes \mathbf{C}||_F, \tag{2.103}$$

where $\mathbf{X} \in \mathbb{C}^{I_1 I_2 I_3 \times R_1 R_2 R_3}$, $\mathbf{A} \in \mathbb{C}^{I_3 \times R_3}$, $\mathbf{B} \in \mathbb{C}^{I_2 \times R_2}$ and $\mathbf{C} \in \mathbb{C}^{I_1 \times R_1}$. Minimizing (2.103) is the same as minimizing the following cost function

$$\begin{aligned} \phi(\mathbf{a}, \mathbf{b}, \mathbf{c}) &= ||\overline{\mathbf{x}} - \mathbf{a} \otimes \mathbf{b} \otimes \mathbf{c}||_F \iff \\ &= ||\overline{\mathscr{X}} - \mathbf{c} \circ \mathbf{b} \circ \mathbf{a}||_F \end{aligned} \tag{2.104}$$

where $\mathbf{a} = \text{vec}(\mathbf{A})$, $\mathbf{b} = \text{vec}(\mathbf{B})$, $\mathbf{c} = \text{vec}(\mathbf{C})$, $\overline{\mathbf{x}} = \text{vec}(\overline{\mathbf{X}})$ is a vector of size $I_1 R_1 I_2 R_2 I_3 R_3 \times 1$, and $\overline{\mathscr{X}}$ is a rank-one tensor of size $I_1 R_1 \times I_2 R_2 \times I_3 R_3$.

Due to the Kronecker structure, the matrix $\mathbf{X}$ can be viewed in three different ways: First, as a block matrix of size $I_2 I_3 \times R_2 R_3$ with each element being a matrix of size $I_1 \times R_1$. Second, a block matrix of size $I_3 \times R_3$, where each element is a matrix of size $I_1 I_2 \times R_1 R_2$ formed by the block $\mathbf{B} \otimes \mathbf{C}$, and, finally, the total matrix $\mathbf{X}$. Our goal is to rearrange the elements of $\mathbf{X}$ into a matrix $\overline{\mathbf{X}}$ such that $\overline{\mathbf{x}} = \mathbf{a} \otimes \mathbf{b} \otimes \mathbf{c}$. The matrix $\mathbf{X}$ can be viewed as

$$\mathbf{X} = \begin{bmatrix} \begin{bmatrix} [\mathbf{P}^{(1)}_{(1,1)}] & \cdots & [\mathbf{P}^{(1)}_{(1,R_2)}] \\ \vdots & \ddots & \vdots \\ [\mathbf{P}^{(1)}_{(I_2,1)}] & \cdots & [\mathbf{P}^{(1)}_{(I_2,R_2)}] \end{bmatrix}_{\mathbf{P}^{(2)}_{(1,1)}} & \cdots & \begin{bmatrix} [\mathbf{P}^{(1)}_{(1,1)}] & \cdots & [\mathbf{P}^{(1)}_{(1,R_2)}] \\ \vdots & \ddots & \vdots \\ [\mathbf{P}^{(1)}_{(I_2,1)}] & \cdots & [\mathbf{P}^{(1)}_{(I_2,R_2)}] \end{bmatrix}_{\mathbf{P}^{(2)}_{(1,R_3)}} \\ \vdots & \ddots & \vdots \\ \begin{bmatrix} [\mathbf{P}^{(1)}_{(1,1)}] & \cdots & [\mathbf{P}^{(1)}_{(1,R_2)}] \\ \vdots & \ddots & \vdots \\ [\mathbf{P}^{(1)}_{(I_2,1)}] & \cdots & [\mathbf{P}^{(1)}_{(I_2,R_2)}] \end{bmatrix}_{\mathbf{P}^{(2)}_{(I_3,1)}} & \cdots & \begin{bmatrix} [\mathbf{P}^{(1)}_{(1,1)}] & \cdots & [\mathbf{P}^{(1)}_{(1,R_2)}] \\ \vdots & \ddots & \vdots \\ [\mathbf{P}^{(1)}_{(I_2,1)}] & \cdots & [\mathbf{P}^{(1)}_{(I_2,R_2)}] \end{bmatrix}_{\mathbf{P}^{(2)}_{(I_3,R_3)}} \end{bmatrix}_{\mathbf{P}^{(3)}_{(1,1)}} \tag{2.105}$$

where each block $\mathbf{P}^{(1)}$ is a matrix of size $I_1 \times R_1$, each block $\mathbf{P}^{(2)}$ is a matrix of size $I_1 I_2 \times R_1 R_2$, and the block $\mathbf{P}^{(3)}$ is the total matrix of size $I_1 I_2 I_3 \times R_1 R_2 R_3$. The sub indices only indicates the block position in reference to the big block, e.g. the sub indices of $\mathbf{P}^{(1)}_{(1,1)}$ indicates that is the first block in the bigger block $\mathbf{P}^{(2)}_{(n,m)}$, where $n = \{1 \cdots I_3\}$ and $m = \{1 \cdots R_3\}$. After this block division, we can define a matrix $\overline{\mathbf{X}}^{(n,m)}$ of size $I_1 R_1 \times I_2 R_2$ where each column is the vectorization

of each block $\mathbf{P}^{(1)}$ in the bigger block $\mathbf{P}^{(2)}_{(n,m)}$, following the row sense.

$$\overline{\mathbf{X}}^{(n,m)} = [\text{vec}(\mathbf{P}^{(1)}_{(1,1)}); \text{vec}(\mathbf{P}^{(1)}_{(I_2,1)}); \cdots ; \text{vec}(\mathbf{P}^{(1)}_{(I_2,R_2)})]_{\mathbf{P}^{(2)}_{(n,m)}}.$$

Defining the matrix $\overline{\mathbf{X}}$ of size $I_1R_1I_2R_2 \times I_3R_3$ as the matrix whose column vectors are formed by $\text{vec}(\overline{\mathbf{X}}^{(n,m)})$

$$\overline{\mathbf{X}} = [\text{vec}(\overline{\mathbf{X}}^{(1,1)}); \cdots ; \text{vec}(\overline{\mathbf{X}}^{(I_3,1)}); \cdots ; \text{vec}(\overline{\mathbf{X}}^{(I_3,R_3)})] \tag{2.106}$$

Equation (2.106) represents our rearrangement, i.e. $\text{vec}(\overline{\mathbf{X}}) = \mathbf{a} \otimes \mathbf{b} \otimes \mathbf{c}$, and $\overline{\mathscr{X}}$ is the third-order rank-one tensor of size $I_1R_1 \times I_2R_2 \times I_3R_3$, given by the tensorization of $\overline{\mathbf{x}}$. This tensor can be written as

$$\overline{\mathscr{X}} = \mathbf{c} \circ \mathbf{b} \circ \mathbf{a}. \tag{2.107}$$

In this case, we approximate a matrix by the Kronecker product of three matrices by rearranging it as a third-order rank-one tensor, the matrices can be estimated, for example, by using the ALS algorithm or the HOSVD algorithm and it will be unique with some scaling factor.

Next, a simple example of the rank-one tensor approximation of the Kronecker product of three matrices, $\mathbf{X} = \mathbf{A} \otimes \mathbf{B} \otimes \mathbf{C}$, with the matrices defined as

$$\mathbf{A} = \begin{bmatrix} a_1 & a_3 \\ a_2 & a_4 \end{bmatrix} \qquad \mathbf{B} = \begin{bmatrix} b_1 & b_3 \\ b_2 & b_4 \end{bmatrix} \qquad \mathbf{C} = \begin{bmatrix} c_1 & c_3 \\ c_2 & c_4 \end{bmatrix}. \tag{2.108}$$

Also, we have the vectors $\mathbf{a} = \text{vec}(\mathbf{A})$, $\mathbf{b} = \text{vec}(\mathbf{B})$ and $\mathbf{c} = \text{vec}(\mathbf{C})$,

$$\mathbf{a} = \begin{bmatrix} a_1 \\ a_2 \\ a_3 \\ a_4 \end{bmatrix} \qquad \mathbf{b} = \begin{bmatrix} b_1 \\ b_2 \\ b_3 \\ b_4 \end{bmatrix} \qquad \mathbf{c} = \begin{bmatrix} c_1 \\ c_2 \\ c_3 \\ c_4 \end{bmatrix}. \tag{2.109}$$

Defining $\overline{\mathbf{x}} = \mathbf{a} \otimes \mathbf{b} \otimes \mathbf{c}$, we have:

$$\overline{\mathbf{x}} = \begin{bmatrix} a_1b_1c_1 \\ a_1b_1c_2 \\ a_1b_1c_3 \\ \vdots \\ a_4b_4c_4 \end{bmatrix}_{64\times 1} \tag{2.110}$$

By the proposed block division (2.105), the matrix $\mathbf{X}$ is given as

$$
\mathbf{X} = \left[\begin{array}{cc}
\left[\begin{array}{cc}
\left[\begin{array}{cc} a_1b_1c_1 & a_1b_1c_3 \\ a_1b_1c_2 & a_1b_1c_4 \end{array}\right]_{\mathbf{P}^{(1)}_{(1,1)}} & \left[\begin{array}{cc} a_1b_3c_1 & a_1b_3c_3 \\ a_1b_3c_2 & a_1b_3c_4 \end{array}\right]_{\mathbf{P}^{(1)}_{(1,2)}} \\
\left[\begin{array}{cc} a_1b_2c_1 & a_1b_2c_3 \\ a_1b_2c_2 & a_1b_2c_4 \end{array}\right]_{\mathbf{P}^{(1)}_{(2,1)}} & \left[\begin{array}{cc} a_1b_4c_1 & a_1b_4c_3 \\ a_1b_4c_2 & a_1b_4c_4 \end{array}\right]_{\mathbf{P}^{(1)}_{(2,2)}}
\end{array}\right]_{\mathbf{P}^{(2)}_{(1,1)}} &
\left[\begin{array}{cc}
\left[\begin{array}{cc} a_3b_1c_1 & a_3b_1c_3 \\ a_3b_1c_2 & a_3b_1c_4 \end{array}\right]_{\mathbf{P}^{(1)}_{(1,1)}} & \left[\begin{array}{cc} a_3b_3c_1 & a_3b_3c_3 \\ a_3b_3c_2 & a_3b_3c_4 \end{array}\right]_{\mathbf{P}^{(1)}_{(1,2)}} \\
\left[\begin{array}{cc} a_3b_2c_1 & a_3b_2c_3 \\ a_3b_2c_2 & a_3b_2c_4 \end{array}\right]_{\mathbf{P}^{(1)}_{(2,1)}} & \left[\begin{array}{cc} a_3b_4c_1 & a_3b_4c_3 \\ a_3b_4c_2 & a_3b_4c_4 \end{array}\right]_{\mathbf{P}^{(1)}_{(2,2)}}
\end{array}\right]_{\mathbf{P}^{(2)}_{(1,2)}} \\
\left[\begin{array}{cc}
\left[\begin{array}{cc} a_2b_1c_1 & a_2b_1c_3 \\ a_2b_1c_2 & a_2b_1c_4 \end{array}\right]_{\mathbf{P}^{(1)}_{(1,1)}} & \left[\begin{array}{cc} a_2b_3c_1 & a_2b_3c_3 \\ a_2b_3c_2 & a_2b_3c_4 \end{array}\right]_{\mathbf{P}^{(1)}_{(1,2)}} \\
\left[\begin{array}{cc} a_2b_2c_1 & a_2b_2c_3 \\ a_2b_2c_2 & a_2b_2c_4 \end{array}\right]_{\mathbf{P}^{(1)}_{(2,1)}} & \left[\begin{array}{cc} a_2b_4c_1 & a_2b_4c_3 \\ a_2b_4c_2 & a_2b_4c_4 \end{array}\right]_{\mathbf{P}^{(1)}_{(2,2)}}
\end{array}\right]_{\mathbf{P}^{(2)}_{(2,1)}} &
\left[\begin{array}{cc}
\left[\begin{array}{cc} a_4b_1c_1 & a_4b_1c_3 \\ a_4b_1c_2 & a_4b_1c_4 \end{array}\right]_{\mathbf{P}^{(1)}_{(1,1)}} & \left[\begin{array}{cc} a_4b_3c_1 & a_4b_3c_3 \\ a_4b_3c_2 & a_4b_3c_4 \end{array}\right]_{\mathbf{P}^{(1)}_{(1,2)}} \\
\left[\begin{array}{cc} a_4b_2c_1 & a_4b_2c_3 \\ a_4b_2c_2 & a_4b_2c_4 \end{array}\right]_{\mathbf{P}^{(1)}_{(2,1)}} & \left[\begin{array}{cc} a_4b_4c_1 & a_4b_4c_3 \\ a_4b_4c_2 & a_4b_4c_4 \end{array}\right]_{\mathbf{P}^{(1)}_{(2,2)}}
\end{array}\right]_{\mathbf{P}^{(2)}_{(2,2)}}
\end{array}\right]_{\mathbf{P}^{(3)}_{(1,1)}} \tag{2.111}
$$

As described for the special case of the Kronecker product of three matrices, we start the vectorization in the blue blocks until the first bigger block (red block, $\mathbf{P}^{(2)}_{(1,1)}$) is completed, so we can define the matrix $\overline{\mathbf{X}}^{(1,1)}$ as

$$\overline{\mathbf{D}}^{(1,1)} = [\text{vec}(\mathbf{P}^{(1)}_{(1,1)}); \text{vec}(\mathbf{P}^{(1)}_{(2,1)}); \text{vec}(\mathbf{P}^{(1)}_{(1,2)}); \text{vec}(\mathbf{P}^{(1)}_{(2,2)})]_{\mathbf{P}^{(2)}_{(1,1)}} \tag{2.112}$$

$$= \begin{bmatrix} a_1b_1c_1 & a_1b_2c_1 & a_1b_3c_1 & a_1b_4c_1 \\ a_1b_1c_2 & a_1b_2c_2 & a_1b_3c_2 & a_1b_4c_1 \\ a_1b_1c_3 & a_1b_2c_3 & a_1b_3c_3 & a_1b_4c_1 \\ a_1b_1c_4 & a_1b_2c_4 & a_1b_3c_4 & a_1b_4c_1 \end{bmatrix} \tag{2.113}$$

Note that the vectorization of $\overline{\mathbf{D}}^{(1,1)}$ is equal to the first 16 elements of $\overline{\mathbf{d}}$ in Equation (2.110). Now, we do the same steps in the row sense, i.e. we vectorize the blue blocks of the $\mathbf{P}^{(2)}_{(2,1)}$ red block. So, in the end, our reshaped matrix $\overline{\mathbf{D}}$ is given by

$$\overline{\mathbf{D}} = [\text{vec}(\overline{\mathbf{D}}^{(1,1)}); \text{vec}(\overline{\mathbf{D}}^{(2,1)}); \text{vec}(\overline{\mathbf{D}}^{(1,2)}); \text{vec}(\overline{\mathbf{D}}^{(2,2)})]_{16\times 4}. \tag{2.114}$$

Now, its easy to see that $\overline{\mathbf{d}} = \mathbf{a} \otimes \mathbf{b} \otimes \mathbf{c}$. And finally we define the rank-one tensor $\overline{\mathscr{D}}^{4\times 4\times 4}$ as in Equation (2.107).

2.3.3 From Kronecker-Sum Approximation to Rank-R Tensors

This section is an extension of the problem in Equation (2.99) a rank-R problem of the previous one. Since the Van Loan's case also was extended to a rank-R problem, for our proposed generalization the same logic can be applied. This is equivalent to define the following problem:

$$\min_{\mathbf{A}^{(r)}\otimes\mathbf{B}^{(r)}\otimes\mathbf{C}^{(r)}, r=1,\cdots,R} ||\mathbf{X} - \sum_{r=1}^{R} \mathbf{A}^{(r)} \otimes \mathbf{B}^{(r)} \otimes \mathbf{C}^{(r)}||_F \tag{2.115}$$

Considering the matrices $\mathbf{A}^{(r)}$, $\mathbf{B}^{(r)}$, $\mathbf{C}^{(r)}$ of the same size as in (2.103) and $\mathbf{X}$ of the same size as $\mathbf{D}$. Following the proposed generalization, the minimization in (2.115) can be reformulated as

$$\min_{\mathbf{c}_r\circ\mathbf{b}_r\circ\mathbf{a}_r, r=1,\cdots,R} ||\overline{\mathscr{X}} - \sum_{r=1}^{R} \mathbf{c}_r \circ \mathbf{b}_r \circ \mathbf{a}_r||_F. \tag{2.116}$$

The tensor $\overline{\mathscr{X}}$ is an approximation of a rank-R PARAFAC given by

$$\overline{\mathscr{X}} = \mathscr{I}_R \times_1 \overline{\mathbf{C}} \times_2 \overline{\mathbf{B}} \times_3 \overline{\mathbf{A}}, \tag{2.117}$$

where $\overline{\mathbf{A}} = [\mathbf{a}_1; \mathbf{a}_2; \cdots; \mathbf{a}_R]$ with $\mathbf{a}_r = \text{vec}(\mathbf{A}^{(r)})$, $\overline{\mathbf{B}} = [\mathbf{b}_1; \mathbf{b}_2; \cdots; \mathbf{b}_R]$ with $\mathbf{b}_r = \text{vec}(\mathbf{B}^{(r)})$ and $\overline{\mathbf{C}} = [\mathbf{c}_1; \mathbf{c}_2; \cdots; \mathbf{c}_R]$ with $\mathbf{c}_r = \text{vec}(\mathbf{C}^{(r)})$.

2.4 Khatri-Rao factorization of a DFT matrix

In this section, we show that $\overline{\mathbf{W}} = \mathbf{W}_N \diamond \mathbf{W}_{N-1} \diamond \cdots \diamond \mathbf{W}_1$, where $\overline{\mathbf{W}} \in \mathbb{C}^{K \times K}$ is a DFT matrix and $\mathbf{W}_n \in \mathbb{C}^{K_n \times K}$, with $\prod_{n=1}^{N} K_n = K$.

$$\overline{\mathbf{W}} = \frac{1}{\sqrt{K}} \begin{bmatrix} 1 & 1 & 1 & \cdots & 1 \\ 1 & \omega & \omega^2 & \cdots & \omega^{K-1} \\ 1 & \omega^2 & \omega^4 & \cdots & \omega^{2(K-1)} \\ \vdots & \vdots & \vdots & \ddots & \vdots \\ 1 & \omega^{K-1} & \omega^{2(K-1)} & \cdots & \omega^{(K-1)(K-1)}, \end{bmatrix} \tag{2.118}$$

where $\omega = e^{-2\pi j/K}$. The idea is to factorize each column of $\overline{\mathbf{W}}$ as the Kronecker product of N vectors. Note that for the first column the factorization is straightforward since all the columns is filled with ones, i.e. all the N vectors are vector columns with ones of size $K_n \times 1$. For the $(k+1)$-*th* column of $\overline{\mathbf{W}}$ we have the following relation:

$$\begin{bmatrix} 1 \\ \omega^k \\ \vdots \\ \omega^{k(K-1)} \end{bmatrix} = \begin{bmatrix} 1 \\ \omega^k \\ \vdots \\ \omega^{k(K_N-1)} \end{bmatrix}^{\alpha_N} \otimes \begin{bmatrix} 1 \\ \omega^k \\ \vdots \\ \omega^{k(K_{N-1}-1)} \end{bmatrix}^{\alpha_{N-1}} \otimes \cdots \otimes \begin{bmatrix} 1 \\ \omega^k \\ \vdots \\ \omega^{k(K_1-1)} \end{bmatrix}^{\alpha_1} \tag{2.119}$$

where $\alpha_n = \prod_{i=1}^{n-1} K_i$ with $\alpha_1 = 1$. In this case, we factorize the $(k+1)$-*th* column of the matrix $\overline{\mathbf{W}}$ as the Kronecker product of N vectors, where the *n-th* vector is of size $K_n \times 1$. We can conclude that the matrix $\overline{\mathbf{W}}$ can be factorized as a Khatri-Rao product, since this product is also known as the column-wise Kronecker product.

Let us consider an example. Given a DFT matrix $\overline{\mathbf{W}} \in \mathbb{C}^{8\times 8}$, we want to factorize it as the Khatri-Rao product of three matrices $\mathbf{W}_1 \in \mathbb{C}^{2\times 8}$, $\mathbf{W}_2 \in \mathbb{C}^{2\times 8}$ and $\mathbf{W}_3 \in \mathbb{C}^{2\times 8}$ ($K_1 =$

$K_2 = K_3 = 2$). The matrix $\overline{\mathbf{W}}$ is given by

$$\overline{\mathbf{W}} = \frac{1}{\sqrt{8}} \begin{bmatrix} 1 & 1 & 1 & 1 & 1 & 1 & 1 & 1 \\ 1 & \omega & \omega^2 & \omega^3 & \omega^4 & \omega^5 & \omega^6 & \omega^7 \\ 1 & \omega^2 & \omega^4 & \omega^6 & \omega^8 & \omega^{10} & \omega^{12} & \omega^{14} \\ 1 & \omega^3 & \omega^6 & \omega^9 & \omega^{12} & \omega^{15} & \omega^{18} & \omega^{21} \\ 1 & \omega^4 & \omega^8 & \omega^{12} & \omega^{16} & \omega^{20} & \omega^{24} & \omega^{28} \\ 1 & \omega^5 & \omega^{10} & \omega^{15} & \omega^{20} & \omega^{25} & \omega^{30} & \omega^{35} \\ 1 & \omega^6 & \omega^{12} & \omega^{18} & \omega^{24} & \omega^{30} & \omega^{36} & \omega^{42} \\ 1 & \omega^7 & \omega^{14} & \omega^{21} & \omega^{28} & \omega^{35} & \omega^{42} & \omega^{49} \end{bmatrix} \tag{2.120}$$

As explained, the first column of the $\mathbf{W}_i$ matrix is filled with ones. According to (2.119), the second column of $\overline{\mathbf{W}}$ is given by

$$\begin{bmatrix} 1 \\ \omega \\ \omega^2 \\ \omega^3 \\ \omega^4 \\ \omega^5 \\ \omega^6 \\ \omega^7 \end{bmatrix} = \begin{bmatrix} 1 \\ \omega \end{bmatrix}^{K_2 K_1} \otimes \begin{bmatrix} 1 \\ \omega \end{bmatrix}^{K_1} \otimes \begin{bmatrix} 1 \\ \omega \end{bmatrix} \tag{2.121}$$

The matrices $\mathbf{W}_3$, $\mathbf{W}_2$ and $\mathbf{W}_1$ are given as

$$\mathbf{W}_3 = \frac{1}{\sqrt{2}} \begin{bmatrix} 1 & 1 & 1 & 1 & 1 & 1 & 1 & 1 \\ 1 & \omega^4 & \omega^8 & \omega^{12} & \omega^{16} & \omega^{20} & \omega^{24} & \omega^{28} \end{bmatrix} \tag{2.122}$$

$$\mathbf{W}_2 = \frac{1}{\sqrt{2}} \begin{bmatrix} 1 & 1 & 1 & 1 & 1 & 1 & 1 & 1 \\ 1 & \omega^2 & \omega^4 & \omega^6 & \omega^8 & \omega^{10} & \omega^{12} & \omega^{14} \end{bmatrix} \tag{2.123}$$

$$\mathbf{W}_1 = \frac{1}{\sqrt{2}} \begin{bmatrix} 1 & 1 & 1 & 1 & 1 & 1 & 1 & 1 \\ 1 & \omega & \omega^2 & \omega^3 & \omega^4 & \omega^5 & \omega^6 & \omega^7 \end{bmatrix}. \tag{2.124}$$

At the end, it is easy to see that $\overline{\mathbf{W}} = \mathbf{W}_3 \diamond \mathbf{W}_2 \diamond \mathbf{W}_1$.

In the previous example, we considered the matrix $\overline{\mathbf{W}} \in \mathbb{C}^{8\times 8}$ and we factorize it as the Khatri-Rao product of three matrices with size 2×8. The case where a column of a DFT

matrix it is factorized into the Kronecker product of vectors with two rows, e.g. as in Equation (2.121), we call as the minimum possible factorization, and it is unique in the sense that all vectors are the same (only changing the exponent). However, we have another two possibilities. The first case is to factorize $\overline{\mathbf{W}}$ as the Khatri-Rao product of two matrices $\mathbf{W}_1 \in \mathbb{C}^{4\times 8}$ and $\mathbf{W}_2 \in \mathbb{C}^{2\times 8}$. The second column of $\overline{\mathbf{W}}$ is given by:

$$\begin{bmatrix} 1 \\ \omega \\ \omega^2 \\ \omega^3 \\ \omega^4 \\ \omega^5 \\ \omega^6 \\ \omega^7 \end{bmatrix} = \begin{bmatrix} 1 \\ \omega \end{bmatrix}^4 \otimes \begin{bmatrix} 1 \\ \omega \\ \omega^2 \\ \omega^3 \end{bmatrix}. \tag{2.125}$$

So, in this case we have the two factor matrices are:

$$\mathbf{W}_2 = \frac{1}{\sqrt{2}} \begin{bmatrix} 1 & 1 & 1 & 1 & 1 & 1 & 1 & 1 \\ 1 & \omega^4 & \omega^8 & \omega^{12} & \omega^{16} & \omega^{20} & \omega^{24} & \omega^{28} \end{bmatrix} \tag{2.126}$$

$$\mathbf{W}_1 = \frac{1}{\sqrt{4}} \begin{bmatrix} 1 & 1 & 1 & 1 & 1 & 1 & 1 & 1 \\ 1 & \omega & \omega^2 & \omega^3 & \omega^4 & \omega^5 & \omega^6 & \omega^7 \\ 1 & \omega^2 & \omega^4 & \omega^6 & \omega^8 & \omega^{10} & \omega^{12} & \omega^{14} \\ 1 & \omega^3 & \omega^6 & \omega^9 & \omega^{12} & \omega^{15} & \omega^{18} & \omega^{21} \end{bmatrix}. \tag{2.127}$$

The last possibility is to factorize $\overline{\mathbf{W}}$ as the Khatri-Rao product of two matrices, $\mathbf{W}_1 \in \mathbb{C}^{2\times 8}$ and $\mathbf{W}_2 \in \mathbb{C}^{4\times 8}$. Again, the second column of $\overline{\mathbf{W}}$ is given by:

$$\begin{bmatrix} 1 \\ \omega \\ \omega^2 \\ \omega^3 \\ \omega^4 \\ \omega^5 \\ \omega^6 \\ \omega^7 \end{bmatrix} = \begin{bmatrix} 1 \\ \omega \\ \omega^2 \\ \omega^3 \end{bmatrix}^2 \otimes \begin{bmatrix} 1 \\ \omega \end{bmatrix}. \tag{2.128}$$

In this case, the matrices $\mathbf{W}_1$ and $\mathbf{W}_2$ are given by:

$$\mathbf{W}_2 = \frac{1}{\sqrt{4}} \begin{bmatrix} 1 & 1 & 1 & 1 & 1 & 1 & 1 & 1 \\ 1 & \omega^2 & \omega^4 & \omega^6 & \omega^8 & \omega^{10} & \omega^{12} & \omega^{14} \\ 1 & \omega^4 & \omega^8 & \omega^{12} & \omega^{16} & \omega^{20} & \omega^{24} & \omega^{28} \\ 1 & \omega^6 & \omega^{12} & \omega^{18} & \omega^{24} & \omega^{30} & \omega^{36} & \omega^{42} \end{bmatrix} \tag{2.129}$$

$$\mathbf{W}_1 = \frac{1}{\sqrt{2}} \begin{bmatrix} 1 & 1 & 1 & 1 & 1 & 1 & 1 & 1 \\ 1 & \omega & \omega^2 & \omega^3 & \omega^4 & \omega^5 & \omega^6 & \omega^7 \end{bmatrix}. \tag{2.130}$$

Note that the difference between (2.125) and (2.128) is only a permutation in the order of vector basis leading into a changing of the exponent α_n.

2.5 Summary

In this chapter, some background material on tensor algebra and tensor decompositions have been provided. This material serves as a basis for the next chapters. As a contribution of this thesis, we have elucidated the link between the Kronecker factorization of multiple matrices and a rank-one tensor factorization. This fundamental link will be exploited in the upcoming chapters, in order to connect a Nested Tucker decomposition to a rank-one PARAFAC decomposition.

3 TWO-HOP MIMO RELAYING

In this chapter, we propose two semi-blind receivers for joint channel and symbol estimation in MIMO relay-based communication systems. These receivers are developed for a two-hop system, assuming a tensor coding at the source and relay nodes. The central idea of the proposed approach is on the rank-one tensor modeling of the received signal, which allows the use of efficient estimation algorithms. The first receiver utilizes an iterative solution based on the alternating least squares (ALS) algorithm, while the second provides closed-form estimations of the channel and symbol matrices from a truncated higher-order singular value decomposition (T-HOSVD). The proposed approach has a lower complexity compared to the receiver developed in a previous work, while providing remarkable performance.

3.1 System Model

Figure 13 – System model.

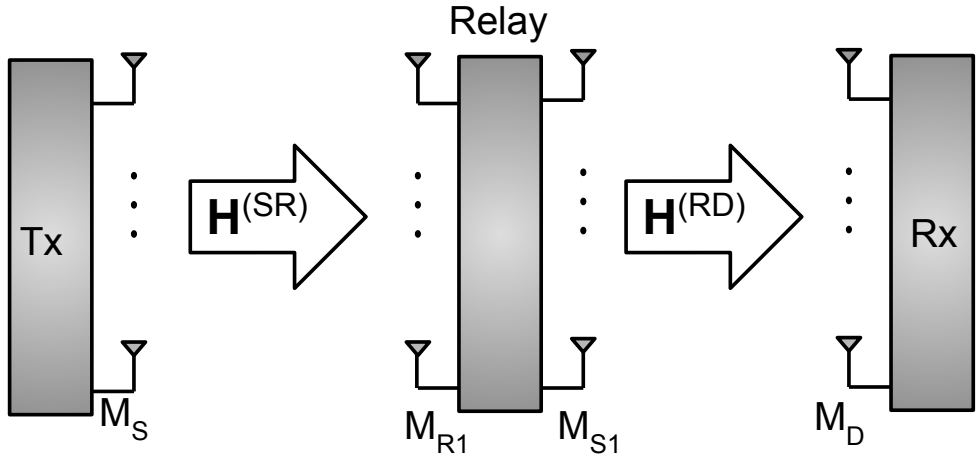

Source: Created by the Author

Consider a one-way two hop MIMO relaying system, where M_S and M_D denote the number of antennas at the source and destination, respectively. We assume that the relay has M_{R_1} receive antennas (operating during the first hop) and M_{S_1} transmit antennas (operating during the second hop). Figure 13 provides an illustration of the system model. The source-relay channel $\mathbf{H}^{(SR)} \in \mathbb{C}^{M_{R_1} \times M_S}$ and the relay-destination $\mathbf{H}^{(RD)} \in \mathbb{C}^{M_D \times M_{S_1}}$ are assumed to undergo flat Rayleigh fading and are constant during the whole transmission period. We consider a

half-duplex relay with AF protocol. At both the source and relay, space-time coding is assumed. Let $\mathbf{S} \in \mathbb{C}^{N \times R}$ denote the symbol matrix containing R data streams with N symbols each. At the source, these R data streams are jointly spread across M_S antennas and P time slots by means of the tensor space-time coding (TSTC) $\mathscr{C} \in \mathbb{C}^{M_S \times R \times P}$. A space-time redundancy is then created since each symbol is repeated P times and loaded into all M_S antennas. The signal received at the relay (in absence of noise) can be written as

$$\mathscr{X}^{(SR)} = \mathscr{C} \times_1 \mathbf{H}^{(SR)} \times_2 \mathbf{S} \in \mathbb{C}^{M_{R_1} \times N \times P}. \tag{3.1}$$

In the second hop, the source stays silent while the relay forwards a space-time coded version of the received signal to the destination. Let $\mathscr{W} \in \mathbb{C}^{M_{S_1} \times M_{R_1} \times J}$ denote the space-time coding tensor used at the relay. The coded signal is given as:

$$\bar{\mathscr{X}}^{(SR)} = \mathscr{W} \bullet_2^1 \mathscr{X}^{(SR)} \in \mathbb{C}^{M_{S_1} \times J \times N \times P} \tag{3.2}$$

In a way similar to the first hop, the role of tensor $\mathscr{W}$ is to jointly spread the received signal across M_{S_1} transmit antennas and J time frames, where each time frame comprises P time slots. At the destination, the noiseless received signal is then given as

$$\mathscr{X}^{(SRD)} = \bar{\mathscr{X}}^{(SR)} \times_1 \mathbf{H}^{(RD)} \in \mathbb{C}^{M_D \times J \times N \times P} \tag{3.3}$$

Define $\bar{\mathscr{H}}^{(RD)}$ as the space-time coded channel linking the M_{S_1} relay antennas to the M_D destination antennas:

$$\bar{\mathscr{H}}^{(RD)} = \mathscr{W} \times_1 \mathbf{H}^{(RD)} \in \mathbb{C}^{M_D \times M_{R_1} \times J} \tag{3.4}$$

Plugging (3.2) into (3.3), and using (3.4), we get:

$$\begin{aligned} \mathscr{X}^{(SRD)} &= (\mathscr{W} \bullet_2^1 \mathscr{X}^{(SR)}) \times_1 \mathbf{H}^{(RD)} \\ &= (\mathscr{W} \times_1 \mathbf{H}^{(RD)}) \bullet_2^1 \mathscr{X}^{(SR)} \\ &= \bar{\mathscr{H}}^{(RD)} \bullet_2^1 \mathscr{X}^{(SR)} \in \mathbb{C}^{M_D \times J \times N \times P} \end{aligned} \tag{3.5}$$

Comparing (3.5) with (2.80) we conclude that the signal received at the destination follows a Nested Tucker model, and the following correspondences can be established:

$$(\mathscr{T}^{(1)}, \mathscr{T}^{(2)}) \Longleftrightarrow (\bar{\mathscr{H}}^{(RD)}, \mathscr{X}^{(SR)}) \tag{3.6}$$

$$(\mathbf{B}, \mathbf{U}, \mathbf{D}) \Longleftrightarrow (\mathbf{H}^{(RD)}, \mathbf{H}^{(SR)}, \mathbf{S}) \tag{3.7}$$

$$(I_1, I_2, I_3, I_4) \Longleftrightarrow (M_D, J, N, P) \tag{3.8}$$

$$(R_1, R_2, R_3, R_4) \Longleftrightarrow (M_{S_1}, M_{R_1}, M_S, R) \tag{3.9}$$

Slicing the received signal tensor $\mathscr{X}^{(SRD)}$ by fixing the second and fourth modes (i.e. p and j) yields the following

$$\mathbf{X}^{(SRD)}_{.j.p.} = \mathbf{H}^{(RD)} \mathbf{W}_{..j} \mathbf{H}^{(SR_1)} \mathbf{C}_{..p} \mathbf{S}^{\mathrm{T}} \in \mathbb{C}^{M_D \times N} \tag{3.10}$$

Let $\mathbf{x}_{jp} \doteq \mathrm{vec}(\mathbf{X}^{(SRD)}_{.j.p})$. Using Property (2.33), we have:

$$\begin{aligned} \mathbf{x}_{jp} &= (\mathbf{S} \otimes \mathbf{H}^{(RD)}) \mathrm{vec}(\mathbf{W}_{..j} \mathbf{H}^{(SR)} \mathbf{C}_{..p}) \\ &= (\mathbf{S} \otimes \mathbf{H}^{(RD)}) (\mathbf{C}^{\mathrm{T}}_{..p} \otimes \mathbf{W}_{..j}) \mathrm{vec}(\mathbf{H}^{(SR)}) \end{aligned} \tag{3.11}$$

Applying again the same property in (3.11) yields

$$\mathbf{x}_{jp} = \left(\mathrm{vec}(\mathbf{H}^{(SR)})^{\mathrm{T}} \otimes \mathbf{S} \otimes \mathbf{H}^{(RD)}\right) \mathrm{vec}(\mathbf{C}^{\mathrm{T}}_{..p} \otimes \mathbf{W}_{..j}). \tag{3.12}$$

Next, using Equation (3.12) the coding tensor will perform a important role in our modelling.

3.1.1 Coding Tensor Structure

Each coding tensor is considered as a tensor with PARAFAC structure, i.e. the source and the Relay 1 coding tensor are given by:

$$\mathscr{C} = \mathscr{I}_{F_1} \times_1 \mathbf{C}_1 \times_2 \mathbf{C}_2 \times_3 \mathbf{C}_3 \in \mathbb{C}^{M_S \times R \times P} \tag{3.13}$$

$$\mathscr{W} = \mathscr{I}_{F_2} \times_1 \mathbf{W}_1 \times_2 \mathbf{W}_2 \times_3 \mathbf{W}_3 \in \mathbb{C}^{M_{S_1} \times M_{R_1} \times J}, \tag{3.14}$$

where $\mathbf{C}_1 \in \mathbb{C}^{M_S \times F_1}$, $\mathbf{C}_2 \in \mathbb{C}^{R \times F_1}$, $\mathbf{C}_3 \in \mathbb{C}^{P \times F_1}$, $\mathbf{W}_1 \in \mathbb{C}^{M_{S_1} \times F_2}$, $\mathbf{W}_2 \in \mathbb{C}^{M_{R_1} \times F_2}$, $\mathbf{W}_3 \in \mathbb{C}^{J \times F_2}$, are the factor matrices of the tensors $\mathscr{C}$ and $\mathscr{W}$ respectively, with F_1 and F_2 being the tensor rank. Using the formula of PARAFAC frontal slices and applying the Properties 2.33, 2.32 and 2.37 at the term $\mathrm{vec}(\mathbf{C}^{\mathrm{T}}_{..p} \otimes \mathbf{W}_{..j})$, we have:

$$\mathrm{vec}(\mathbf{C}^{\mathrm{T}}_{..p} \otimes \mathbf{W}_{..j}) = \mathrm{vec}(\mathbf{C}_2 \mathrm{D}_p(\mathbf{C}_3) \mathbf{C}_1^{\mathrm{T}} \otimes \mathbf{W}_1 \mathrm{D}_j(\mathbf{W}_3) \mathbf{W}_2^{\mathrm{T}}) \tag{3.15}$$

$$= \mathrm{vec}[(\mathbf{C}_2 \otimes \mathbf{W}_1)(\mathrm{D}_p(\mathbf{C}_3) \otimes \mathrm{D}_j(\mathbf{W}_3))(\mathbf{C}_1 \otimes \mathbf{W}_2)^{\mathrm{T}}] \tag{3.16}$$

$$\mathbf{z}_{jp} = [(\mathbf{C}_1 \otimes \mathbf{W}_2) \diamond (\mathbf{C}_2 \otimes \mathbf{W}_1)](\mathbf{C}_{3_p} \otimes \mathbf{W}_{3_j})^{\mathrm{T}} \tag{3.17}$$

Backing to the signal model, the Equation (3.12) can be written as

$$\mathbf{x}_{jp} = (\text{vec}(\mathbf{H}^{(SR)})^{\text{T}} \otimes \mathbf{H}^{(RD)} \otimes \mathbf{S})\mathbf{z}_{jp} \tag{3.18}$$

Defining $\mathbf{X}^{(SRD)}$ as the matrix that contain all the JP vectors collected in Equation (3.18)

$$\mathbf{X}^{(SRD)} = (\text{vec}(\mathbf{H}^{(SR)})^{\text{T}} \otimes \mathbf{H}^{(RD)} \otimes \mathbf{S})\mathbf{Z} \in \mathbb{C}^{M_D N \times JP}, \tag{3.19}$$

where $\mathbf{Z} \in \mathbb{C}^{M_{S_1} R M_{R_1} M_S \times JP}$ is the matrix formed by the collection of the JP vectors $\mathbf{z}_{jp}$, which can be written as

$$\mathbf{Z} = (\mathbf{G}_1 \diamond \mathbf{G}_2)\mathbf{G}_3^{\text{T}}, \tag{3.20}$$

with $\mathbf{G}_1 = \mathbf{C}_1 \otimes \mathbf{W}_2 \in \mathbb{C}^{M_{R_1} M_S \times F_2 F_1}$, $\mathbf{G}_2 = \mathbf{C}_2 \otimes \mathbf{W}_1 \in \mathbb{C}^{M_{S_1} R \times F_2 F_1}$ and $\mathbf{G}_3 = \mathbf{C}_3 \otimes \mathbf{W}_3 \in \mathbb{C}^{JP \times F_2 F_1}$. Note that this Kronecker structure matrix $\mathbf{Z}$ contains the known parameters of the proposed model, i.e. contain the information of the coding tensors from the source and the relay and for that, we propose a orthogonal design for $\mathbf{Z}$. Such design is based on the unitary structure of a DFT matrix where can be factorized by the Khatri-Rao product of N matrices, detailed in Section 2.4.

3.1.2 Noisy model and rank-one tensor formulation

Let $\mathscr{V}^{(SR)} \in \mathbb{C}^{M_{R_1} \times N \times P}$ be the additive noise tensor at the relay. During the second hop, the tensor $\mathscr{V}^{(SR)}$ is filtered by the coding tensor $\mathscr{W}$ and the relay-destination channel $\mathbf{H}^{(RD)}$ as

$$\begin{aligned} \mathscr{V}^{(1)} &= (\mathscr{W} \bullet_2^1 \mathscr{V}^{(SR)}) \times_1 \mathbf{H}^{(RD)} \\ &= (\mathscr{W} \times_1 \mathbf{H}^{(RD)}) \bullet_2^1 \mathscr{V}^{(SR)} \\ &= \bar{\mathscr{H}}^{(RD)} \bullet_2^1 \mathscr{V}^{(SR)} \in \mathbb{C}^{M_D \times J \times N \times P} \end{aligned} \tag{3.21}$$

and considering $\mathscr{V}^{(2)} \in \mathbb{C}^{M_D \times J \times N \times P}$ as the additive noise at the destination, the global noise is given by

$$\mathscr{V}^{(SRD)} = \mathscr{V}^{(1)} + \mathscr{V}^{(2)} \tag{3.22}$$

Plugging the noise term at the Equation (3.19) yields

$$\mathbf{X}^{(SRD)} = \mathbf{Y}\mathbf{Z} + \mathbf{V}^{(SRD)}, \tag{3.23}$$

where $\mathbf{Y} \in \mathbb{C}^{M_{S_1} R M_{R_1} M_S \times JP}$ is the matrix defined as

$$\mathbf{Y} = \text{vec}(\mathbf{H}^{(SR)})^{\mathrm{T}} \otimes \mathbf{S} \otimes \mathbf{H}^{(RD)}, \tag{3.24}$$

and $\mathbf{V}^{(SRD)} \in \mathbb{C}^{M_D N \times JP}$ is the unfolding matrix of the global noise, which is constructed in the same way as $\mathbf{X}^{(SRD)}$.

It is worth drawing a comment on the meaning of matrices $\mathbf{Y}$ and $\mathbf{Z}$. The first involves the Kronecker product of the unknown factors of our system model (i.e. channel matrices and symbol matrix), which we seek to estimate. The latter represents the equivalent space-time coding matrix, accounting for the combined source-relay coding operations. In other words, (3.23) provides an input-output relation. Since the coding tensors $\mathscr{C}$ and $\mathscr{W}$ are known at the receiver, a direct approach to estimate the useful signal matrix $\mathbf{Y}$ in the presence of noise from (3.23) is to use a least squares (LS) criterion, i.e.

$$\widehat{\mathbf{Y}} = \underset{\mathbf{Y}}{\text{argmin}} \|\mathbf{X}^{(SRD)} - \mathbf{Y}\mathbf{Z}\|_F, \tag{3.25}$$

the solution is given by $\widehat{\mathbf{Y}} = \mathbf{X}^{(SRD)}\mathbf{Z}^{\dagger}$. Note that $\widehat{\mathbf{Y}}$ is a linearly transformed version of the received signal obtained by combining (filtering) the columns of the matrix $\mathbf{X}$ containing the space-time samples of the received signal with a zero forcing filter designed from the effective space-time coding matrix $\mathbf{Z}$, and in the orthogonal cases, the matrix $\mathbf{Z}$ can be viewed as a matched filter, i.e. the solution of (3.25) is given by $\widehat{\mathbf{Y}} = \mathbf{X}^{(SRD)}\mathbf{Z}^{\mathrm{H}}$. It is important to notice that the orthogonal design is crucial to our system, since all the useful parameters are in the matrix $\mathbf{Y}$ and the solution of Equation (3.25) will preserve the noise characteristics. Let us have a closer look at the structure of $\widehat{\mathbf{Y}}$. This matrix can be partitioned as follows

$$\widehat{\mathbf{Y}} = \begin{bmatrix} \mathbf{P}_{(1,1)} & \cdots & \mathbf{P}_{(1,RM_{R_1}M_S)} \\ \vdots & \vdots & \vdots \\ \mathbf{P}_{(N,1)} & \cdots & \mathbf{P}_{(N,RM_{R_1}M_S)} \end{bmatrix}, \tag{3.26}$$

i.e., due to the Kronecker structure, the matrix $\widehat{\mathbf{Y}}$ can be viewed as a concatenation of N row blocks and $RM_{R_1}M_S$ column blocks, respectively, where the (i,j)-*th* block $\mathbf{P}_{i,j}$ is of size $M_D \times M_{S_1}$.

Using the Kronecker approximation described in Section 2.3.2, the rank-one tensor can be given

Figure 14 – Rank-one decomposition of the filtered signal tensor.

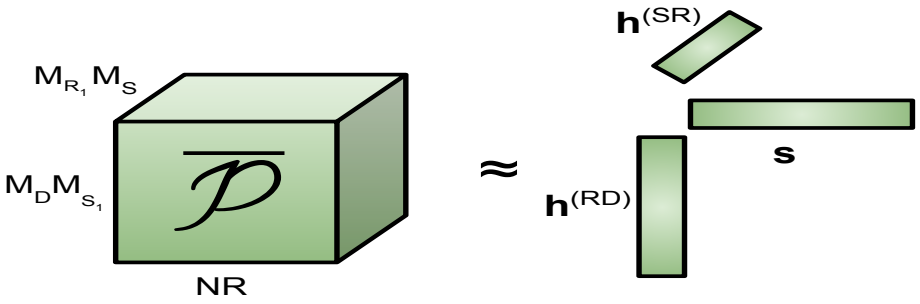

Source: Created by the Author

by

$$\overline{\mathscr{P}} \approx \mathbf{h}^{(RD)} \circ \mathbf{s} \circ \mathbf{h}^{(SR)} \in \mathbb{C}^{M_D M_{S_1} \times NR \times M_{R_1} M_S}, \tag{3.27}$$

with $\mathbf{h}^{(SR)} \in \mathbb{C}^{M_S M_{R_1} \times 1}$, $\mathbf{h}^{(RD)} \in \mathbb{C}^{M_D M_{S_1} \times 1}$, and $\mathbf{s} \in \mathbb{C}^{NR \times 1}$ being the vectorized forms of $\mathbf{S}$, $\mathbf{H}^{(RD)}$ and $\mathbf{H}^{(SR)}$ respectively.

3.1.3 Uniqueness

The uniqueness for Nested Tucker decompositions has been discussed in Section 2.2.2.1. In the three-hop MIMO relaying model, since the coding tensors are known at the receiver, the uniqueness of $\mathbf{S}$ and $\mathbf{H}^{(RD)}$ is guaranteed up to scaling factors. To eliminate this scaling ambiguity, we assume the knowledge of the entries $\mathbf{S}_{(1,1)}$ and $\mathbf{H}^{(RD)}_{(1,1)}$. Solving the Equation (3.25) consists of computing the pseudo-inverse of $\mathbf{Z}$ which must have full row-rank to ensure the uniqueness of the parameters. This implies satisfying the following conditions:

$$P \geq F_1 \geq M_S R \qquad\qquad J \geq F_2 \geq M_{S_1} M_{R_1} \tag{3.28}$$

The proof of these conditions is given in Appendix B.

Since our proposed model was based on the proposed in [17], it is worth to comment the uniqueness conditions of the competitor system. For the ALS Nested Tucker, the authors

derived the following conditions:

$$J \geq \max\left(\frac{M_{S_1}}{M_{R_1}}, \frac{M_{R_1}}{M_{S_1}} \right), \quad P \geq \max\left(\frac{R}{M_S}, \frac{M_S}{R} \right), \tag{3.29}$$

$$N \geq R, \quad PN \geq M_{R_1}, JM_D \geq M_S. \tag{3.30}$$

For the 2LSKP receiver proposed in [17], the uniqueness conditions are similar to our proposed system, i.e. the conditions are given by Equation 3.28, with the difference that the parameters F_1 and F_2 are only addressed to our proposed model, since these parameters are the related to the PARAFAC design imposed in our model, where F_1 and F_2 are the tensor rank of $\mathscr{C}$ and $\mathscr{W}$, respectively. From this conditions, we can conclude that the ALS proposed in [17] has more degrees of freedom. However, as we will see in Section 3.4, this algorithm has the greater computational complexity.

3.2 Semi-Blind Receivers

We present two semi-blind receivers for joint channel and symbol estimation, by capitalizing on the rank-one property of the filtered received signal tensor $\overline{\mathscr{P}}$.

3.2.1 Tri-ALS receiver

The Trilinear (Tri-)ALS algorithm consists of estimating $\mathbf{s}$, $\mathbf{h}^{(RD)}$, and $\mathbf{h}^{(SR)}$ in an alternate way by solving the following three cost functions:

$$\hat{\mathbf{h}}^{(RD)} = \underset{\mathbf{h}^{(RD)}}{\operatorname{argmin}} ||\overline{\mathbf{P}}_{(1)} - \mathbf{h}^{(RD)}(\hat{\mathbf{h}}^{(SR)} \diamond \hat{\mathbf{s}})^{\mathsf{T}}|| \tag{3.31}$$

$$\hat{\mathbf{s}} = \underset{\mathbf{s}}{\operatorname{argmin}} ||\overline{\mathbf{P}}_{(2)} - \mathbf{s}(\hat{\mathbf{h}}^{(SR)} \diamond \hat{\mathbf{h}}^{(RD)})^{\mathsf{T}}|| \tag{3.32}$$

$$\hat{\mathbf{h}}^{(SR)} = \underset{\mathbf{h}^{(SR)}}{\operatorname{argmin}} ||\overline{\mathbf{P}}_{(3)} - \mathbf{h}^{(SR)}(\hat{\mathbf{h}}^{(RD)} \diamond \hat{\mathbf{s}})^{\mathsf{T}}||, \tag{3.33}$$

where $\overline{\mathbf{P}}_{(n=1,2,3)}$, are the n-mode unfoldings of the tensor $\overline{\mathscr{P}}$, constructed according to Equations (2.39) to (2.41) with the following relationship: $(\mathbf{A}, \mathbf{B}, \mathbf{C}) \Longleftrightarrow (\mathbf{h}^{(RD)}, \mathbf{s}, \mathbf{h}^{(SR)})$.
The solutions of Equations (3.31) to (3.33) are given by

$$\hat{\mathbf{h}}^{(RD)} = \frac{\overline{\mathbf{P}}_{(1)}(\hat{\mathbf{h}}^{(SR)} \diamond \hat{\mathbf{s}})^*}{||\hat{\mathbf{h}}^{(SR)}||_2^2 ||\hat{\mathbf{s}}||_2^2} \tag{3.34}$$

$$\hat{\mathbf{s}} = \frac{\overline{\mathbf{P}}_{(2)}(\hat{\mathbf{h}}^{(SR)} \diamond \hat{\mathbf{h}}^{(RD)})^*}{||\hat{\mathbf{h}}^{(SR)}||_2^2 ||\hat{\mathbf{h}}^{(RD)}||_2^2} \tag{3.35}$$

$$\hat{\mathbf{h}}^{(SR)} = \frac{\overline{\mathbf{P}}_{(3)}(\hat{\mathbf{s}} \diamond \hat{\mathbf{h}}^{(RD)})^*}{||\hat{\mathbf{s}}||_2^2 ||\hat{\mathbf{h}}^{(RD)}||_2^2} \tag{3.36}$$

Proof. Considering a full-row rank matrix $\mathbf{A} \in \mathbb{C}^{m\times n}$ full row-rank, its right pseudo-inverse is given by

$$\mathbf{A}^{\dagger} = \mathbf{A}^{\mathrm{H}}(\mathbf{A}\mathbf{A}^{\mathrm{H}})^{-1} \tag{3.37}$$

By replacing $\mathbf{A}$ by $(\hat{\mathbf{h}}^{(SR)} \diamond \hat{\mathbf{s}})^{\mathrm{T}}$ we have

$$[(\hat{\mathbf{h}}^{(SR)} \diamond \hat{\mathbf{s}})^{\mathrm{T}}]^{\dagger} = (\hat{\mathbf{h}}^{(SR)} \diamond \hat{\mathbf{s}})^{*}[(\hat{\mathbf{h}}^{(SR)} \diamond \hat{\mathbf{s}})^{\mathrm{T}}(\hat{\mathbf{h}}^{(SR)} \diamond \hat{\mathbf{s}})^{*}]^{-1} \tag{3.38}$$

Noting that the Khatri-Rao product is the column-wise Kronecker product and since $\hat{\mathbf{h}}^{(SR)}$ and $\hat{\mathbf{s}}$ are only column vectors, we can rewrite Equation (3.38) as

$$[(\hat{\mathbf{h}}^{(SR)} \otimes \hat{\mathbf{s}})^{\mathrm{T}}]^{\dagger} = (\hat{\mathbf{h}}^{(SR)} \otimes \hat{\mathbf{s}})^{*}[(\hat{\mathbf{h}}^{(SR)} \otimes \hat{\mathbf{s}})^{\mathrm{T}}(\hat{\mathbf{h}}^{(SR)} \otimes \hat{\mathbf{s}})^{*}]^{-1}. \tag{3.39}$$

Using Properties (2.31), (2.30) and (2.32) we have

$$\begin{aligned}
[(\hat{\mathbf{h}}^{(SR)} \otimes \hat{\mathbf{s}})^{\mathrm{T}}]^{\dagger} &= (\hat{\mathbf{h}}^{(SR)} \otimes \hat{\mathbf{s}})^{*}[(\hat{\mathbf{h}}^{(SR)} \otimes \hat{\mathbf{s}})^{\mathrm{T}}(\hat{\mathbf{h}}^{(SR)} \otimes \hat{\mathbf{s}})^{*}]^{-1} \\
&= (\hat{\mathbf{h}}^{(SR)} \otimes \hat{\mathbf{s}})^{*}[(\hat{\mathbf{h}}^{(SR)\mathrm{T}}\hat{\mathbf{h}}^{(SR)*} \otimes \hat{\mathbf{s}}^{\mathrm{T}}\hat{\mathbf{s}}^{*}]^{-1} \\
&= \frac{(\hat{\mathbf{h}}^{(SR)} \otimes \hat{\mathbf{s}})^{*}}{||\hat{\mathbf{h}}^{(SR)}||_2^2||\hat{\mathbf{s}}||_2^2}
\end{aligned} \tag{3.40}$$

□

The scaling ambiguity is defined as

$$\mathbf{S} = \alpha_1\hat{\mathbf{S}} \quad \mathbf{H}^{(RD)} = \alpha_2\hat{\mathbf{H}}^{(RD)} \quad \mathbf{H}^{(SR)} = \alpha_3\hat{\mathbf{H}}^{(SR)} \tag{3.41}$$

with,

$$\alpha_1 = \frac{\mathbf{S}_{(1,1)}}{\hat{\mathbf{S}}_{(1,1)}} \quad \alpha_2 = \frac{\mathbf{H}^{(RD)}_{(1,1)}}{\hat{\mathbf{H}}^{(RD)}_{(1,1)}} \quad \alpha_3 = \frac{1}{\alpha_1\alpha_2}$$

The Tri-ALS algorithm is summarized in Algorithm 3.

3.2.2 T-HOSVD receiver

The Truncated (T)-HOSVD algorithm is a closed-form solution based on subspace estimation. It consists of taking the HOSVD on the filtered received signal tensor $\overline{\mathscr{P}}$, which corresponds to calculating the SVD of its matrix unfolding. Since $\overline{\mathscr{P}}$ is a rank-one tensor, the three matrix unfolding can be approximated as rank-one matrices. Therefore, $\mathbf{h}^{(RD)}$, $\mathbf{s}$ and $\mathbf{h}^{(SR)}$ are obtained from the dominant left singular vectors of the unfoldings $\overline{\mathbf{P}}_{(1)} \in \mathbb{C}^{M_D M_{S_1}\times NRM_{R_1}M_S}$,

Algoritmo 3: Tri-ALS

1: Initialize randomly $\hat{\mathbf{h}}_0^{(RD)}$ and $\hat{\mathbf{h}}_0^{(SR)}$; it $= 0$;
2: it = it + 1;
3: Compute an estimate of $\hat{\mathbf{s}}$
$\hat{\mathbf{s}}_{it} = \overline{\mathbf{P}}_{(2)}(\hat{\mathbf{h}}_{it-1}^{(SR)} \diamond \hat{\mathbf{h}}_{it-1}^{(RD)})^* / (||\hat{\mathbf{h}}_{it-1}^{(SR)}||_2^2 ||\hat{\mathbf{h}}_{it-1}^{(RD)}||_2^2)$
4: Compute an estimate of $\hat{\mathbf{h}}^{(RD)}$
$\hat{\mathbf{h}}_{it}^{(RD)} = \overline{\mathbf{P}}_{(1)}(\hat{\mathbf{h}}_{it-1}^{(SR)} \diamond \hat{\mathbf{s}}_{it-1})^* / (||\hat{\mathbf{h}}_{it-1}^{(SR)}||_2^2 ||\hat{\mathbf{s}}_{it-1}||_2^2)$
5: Compute an estimate of $\hat{\mathbf{h}}^{(SR)}$
$\hat{\mathbf{h}}_{it}^{(SR)} = \overline{\mathbf{P}}_{(3)}(\hat{\mathbf{h}}_{it-1}^{(RD)} \diamond \hat{\mathbf{s}}_{it-1})^* / (||\hat{\mathbf{h}}_{it-1}^{(RD)}||_2^2 ||\hat{\mathbf{s}}_{it-1}||_2^2)$
6: Return to step 2 and repeat until convergence;
7: Apply the "unvec" operator to recover $\hat{\mathbf{S}}$, $\hat{\mathbf{H}}^{(RD)}$, $\hat{\mathbf{H}}^{(SR)}$.
8: Remove the scaling ambiguities according to (3.41)

Algoritmo 4: T-HOSVD

1: For $n = 1, 2, 3$:
Compute the SVD of the matrix unfolding $\overline{\mathbf{P}}_{(n)}$;
$\bar{\mathbf{P}}_{(n)} = \mathbf{U}^{(n)} \boldsymbol{\Sigma}^{(n)} \mathbf{V}^{(n)\mathrm{H}}$
2: Select the dominant left singular vector from $\mathbf{U}_{(n)}$:
$\hat{\mathbf{h}}^{(RD)} = \beta_1 \mathbf{U}_{(:,1)}^{(1)}$;
$\hat{\mathbf{s}} \quad\quad = \beta_2 \mathbf{U}_{(:,1)}^{(2)}$;
$\hat{\mathbf{h}}^{(SR)} = \beta_3 \mathbf{U}_{(:,1)}^{(3)}$
3: Apply the "unvec" operator to recover $\hat{\mathbf{S}}$, $\hat{\mathbf{H}}^{(RD)}$, $\hat{\mathbf{H}}^{(SR)}$.
4: Remove the scaling ambiguities according to (3.43)

$\overline{\mathbf{P}}_{(2)} \in \mathbb{C}^{NR \times M_D M_{S_1} M_{R_1} M_S}$, and $\overline{\mathbf{P}}_{(3)} \in \mathbb{C}^{M_{R_1} M_S \times M_D M_{S_1} NR}$.

In case of the HOSVD algorithm, since each n-mode unfolding of $\overline{\mathscr{P}}$ is approximately a rank-one matrix the scaling factors are given as:

$$\mathbf{H}^{(RD)} = \beta_1 \hat{\mathbf{H}}^{(RD)} \quad \mathbf{S} = \beta_2 \hat{\mathbf{S}} \quad \mathbf{H}^{(SR)} = \beta_3 \hat{\mathbf{H}}^{(SR)} \tag{3.42}$$

with,

$$\beta_1 = \frac{\mathbf{H}_{(1,1)}^{(RD)}}{\mathbf{U}_{(1,1)}^{(1)}} \quad \beta_2 = \frac{\mathbf{S}_{(1,1)}}{\mathbf{U}_{(1,1)}^{(2)}} \quad \beta_3 = \frac{\boldsymbol{\Sigma}_{(1,1)}^{(3)} \mathbf{V}_{(1,1)}^{(3)\mathrm{H}}}{\mathbf{S}_{(1,1)} \mathbf{H}_{(1,1)}^{(RD)}} \tag{3.43}$$

where the matrices $\mathbf{U}^{(n)}$, $\boldsymbol{\Sigma}^{(n)}$ and $\mathbf{V}^{(n)}$ are the left singular matrix, singular values matrix and the right singular matrix of $\mathbf{P}_{(n)}$. The T-HOSVD algorithm is described in Algorithm 4.

Table 1 – Computational Complexity for the algorithms

$\mathscr{O}(\cdot)$	Algorithm	
	Tri-ALS	**T-HOSVD**
Multiplication	$\mathscr{O}(12(NRM_DM_{S_1}M_{R_1}M_S))$	
Kronecker	$\mathscr{O}(4(NRM_{R_1}M_S)$ + $\mathscr{O}(4(M_DM_{S_1}M_{R_1}M_S)$ + $\mathscr{O}(4(M_DM_{S_1}NR)$	
SVD		$\mathscr{O}(4(M_DM_{S_1}(NRM_{R_1}M_S)^2 + (M_DM_{S_1})^3)+$ $\mathscr{O}(4(NR(M_DM_{S_1}M_{R_1}M_S)^2 + (NR)^3)+$ $\mathscr{O}(4(M_{R_1}M_S(NRM_DM_{S_1})^2 + (M_{R_1}M_S)^3)$
LS Solution	$\mathscr{O}(4(M_DNM_{S_1}RM_{R_1}M_SJP))$	

3.3 Computational Complexity

Given a matrix $\mathbf{A} \in \mathbb{C}^{m\times n}$ and a matrix $\mathbf{B} \in \mathbb{C}^{n\times p}$ the complexity associated with the multiplication between $\mathbf{A}$ and $\mathbf{B}$ (neglecting the additions) is of order $\mathscr{O}(4(mnp))$. The computation of the Kronecker product $\mathbf{A}\otimes\mathbf{B}$ has a complexity $\mathscr{O}(4mn^2p)$ and the SVD of $\mathbf{A}$, has a complexity $\mathscr{O}(4(mn^2+n^3))$. For the Tri-ALS algorithm, only matrix by vectors multiplications, vectors Kronecker products and some normalizations for each iteration (neglected) are computed, while for the T-HOSVD only three SVD's are required. to be computed. Table 1 shows the number of FLOPS of each algorithm.

3.4 Simulation Results

In this section, we evaluate the performance of the proposed receivers in terms of symbol error rate (SER), normalized mean square error (NMSE) for channel estimation, computational complexity, and convergence, comparing with the receivers proposed in [17]. We consider 64-QAM modulation. The results are averaged over 10^4 Monte Carlo runs, each run corresponding to an independent realization of the channels, symbols, and noise. The channel matrices are assumed to have i.i.d. complex Gaussian entries with zero-mean and unitary variance. The coding tensors $\mathscr{C}$ and $\mathscr{W}$ are normalized as $1/\sqrt{F_1RM_S}$ and $1/\sqrt{F_2M_{S_1}M_{R_1}}$ respectively in order to ensure the same power at the antennas. Note that, with this normalization for $P > RM_S$, $J > M_{R_1}M_{S_1}$ we have $\mathbf{Z}\mathbf{Z}^{\mathrm{H}} = \gamma\mathbf{I}$, where γ can be viewed as the gain obtained by increasing the total redundancy of the system. Also we assume the same noise variance at the relay and destination.

3.4.1 Perfect CSI Channels

In Figure 15 the code gain by varying P and J is illustrated. Note that comparing the cases $P = 4, J = 4$ and $P = 8, J = 4$ with $P = 4, J = 4$ and $P = 4, J = 8$ we can noticed that increasing the value of P is better than increasing J, this was expected since an increase of J also increases the correlation with the noise (Equation (3.21)), which does not evolves the source coding.

3.4.2 Symbol Error Rate

Figure 16 depicts the performance of the Tri-ALS and T-HOSVD receiver in comparison with the two receivers proposed in [17] (namely, ALS Nested Tucker and 2LSKP receivers), using the proposed DFT structure for the source and relay coding tensors. It can be noticed the two proposed receivers reach the same performance as those of [17], while being less complex, as will be shown in the sequel.

3.4.3 Normalized Mean Square Error

The NMSE is given as:

$$\text{NMSE} = \frac{1}{L}\sum_{l=1}^{L}\frac{||\mathbf{H}^{(l)} - \hat{\mathbf{H}}^{(l)}||_F^2}{||\mathbf{H}^{(l)}||_F^2},$$

for both $\mathbf{H}^{(SR)}$ and $\mathbf{H}^{(RD)}$ channels and L is the total number of runs.

Figure 17 and 18 shows the NMSE performance of the estimated channels. We can note that in all cases, the NMSE curves decrease linearly as a function of the E_S/No. In figure 17 the performance of the T-HOSVD receiver is explained by the fact that this receiver computes independents SVD's meaning that each parameter can be computed in parallel, which not occurs for the other receivers, neither the 2LSKP which for the estimation of $\mathbf{H}^{(SR)}$ channel needs the estimation of $\mathbf{H}^{(RD)}$ or $\mathbf{S}$. Now, for the estimation of $\mathbf{H}^{(RD)}$ channel, all receivers has practically the same performance, with a small difference between the subspace methods (T-HOSVD and 2LSKP) and the iterative ones (Tri-ALS and ALS Nested Tucker). To conclude, it was expected that the estimation of $\mathbf{H}^{(RD)}$ would have a better performance than the estimation of $\mathbf{H}^{(SR)}$ due the using of coding at the source and at the relay.

3.4.4 FLOPS

Now, we evaluate the computational complexity of the proposed receivers by measuring the number of floating point operations (FLOPS) required by the different receivers to accomplish joint channel and symbol estimation. To this end, the *lightspeed MATLAB* toolbox [46] was used to count the number of FLOPS. And the relation E_S/No was set in 21dB, i.e. for the iterative algorithms, only three iterations are needed to reach the convergence.

Figure 19 corroborates the benefits of the proposed rank-one tensor based receivers in terms of computational complexity, when compared to the competing receivers. We can note that the Tri-ALS receiver becomes much less complex than its competing Nested Tucker based ALS solution, since the proposed iterative receiver computes three matrix by vector multiplication and normalization for each iteration and three Kronecker product between vectors while the ALS Nested Tucker compute extensive matrix by matrix products for each iteration and also computes inversion and Kronecker between matrices. When it comes to the closed-form receivers, these results show that the T-HOSVD receiver is more attractive than the 2LSKP receiver as the number M_D of antennas grows. Another advantage of T-HOSVD over 2LKSP is related with parallel implementation, since the T-HOSVD consists of three independent SVDs, the estimation of the source-relay, relay-destination and symbol matrices can be carried out in parallel. This is not the case of 2LSKP, which consists of two consecutive SVD's steps, where the result of the second step depends on the output of the first. Figure 20 shows the impact of the proposed DFT-based design for the source and relay coding tensors on the convergence of ALS-based receivers. To this end, we compare the proposed Tri-ALS receiver with the Nested Tucker based ALS receiver. For the latter, we consider the random exponential structure as proposed in [17], and the proposed DFT coding structure. Note that the proposed one yields a reduction on the number of iterations to convergence. For high SNR, the number of iterations reduces approximately from 11 to 3.

Figure 15 – Coding gain of the Zero-Forcing with Perfect CSI knowledge.

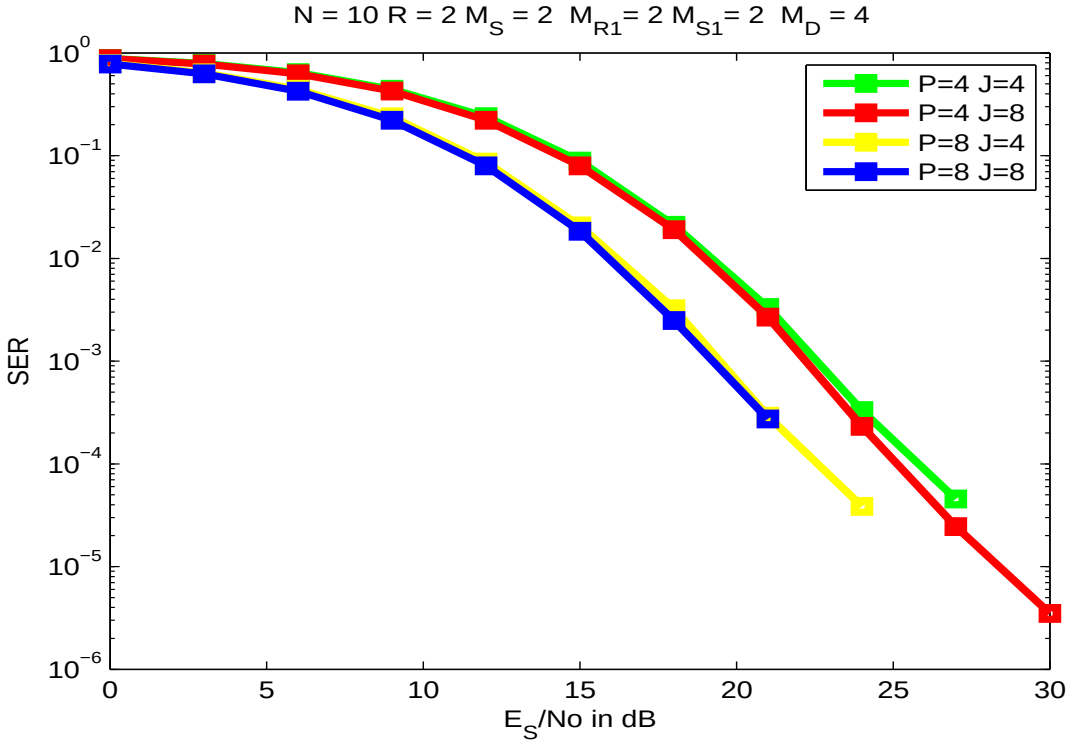

Source: Created by the Author

Figure 16 – Symbol error rate performance vs. E_S/No.

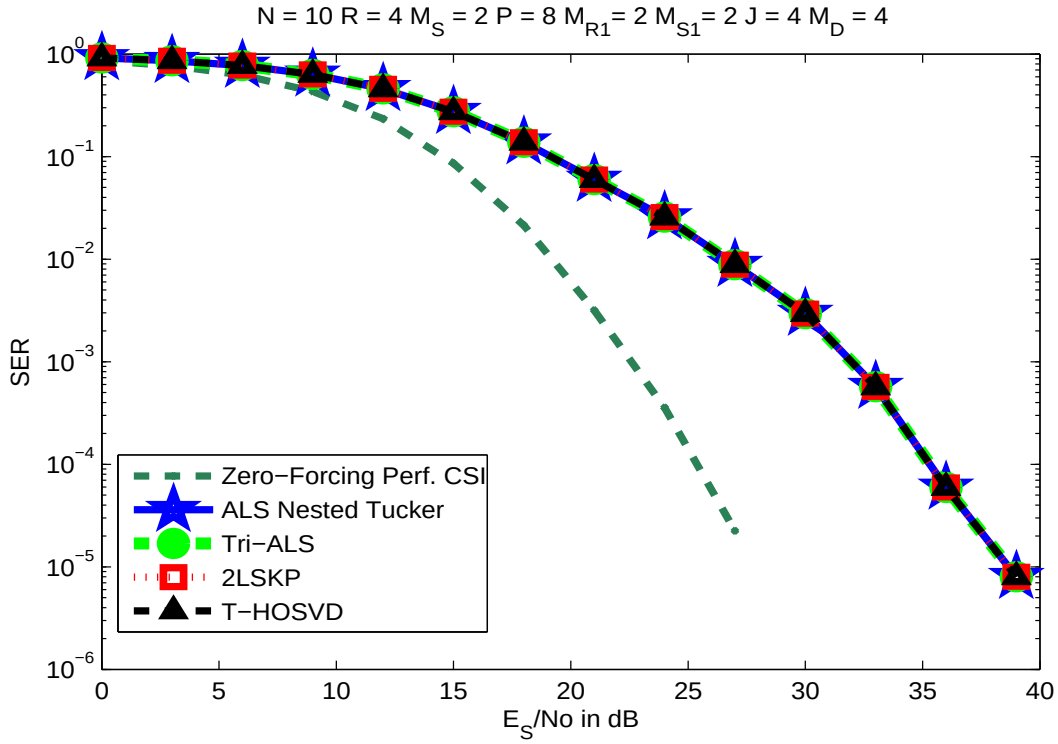

Source: Created by the Author

Figure 17 – NMSE for Source-Relay channel.

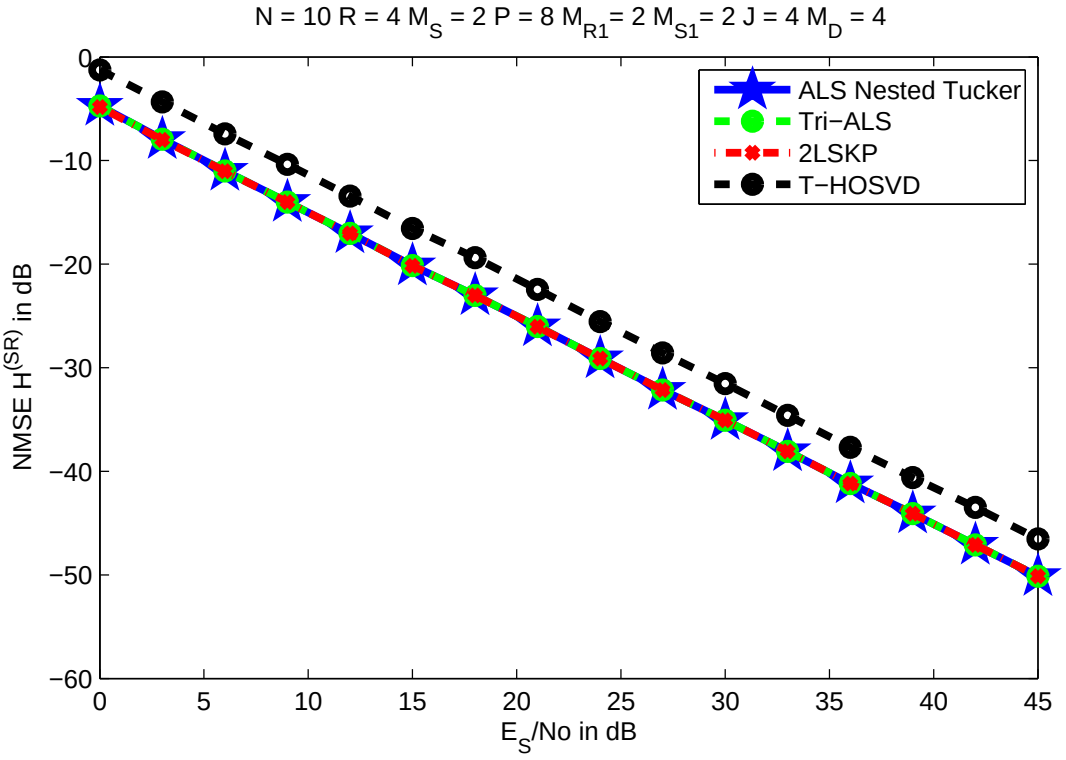

Figure 18 – NMSE for Relay-Destination channel.

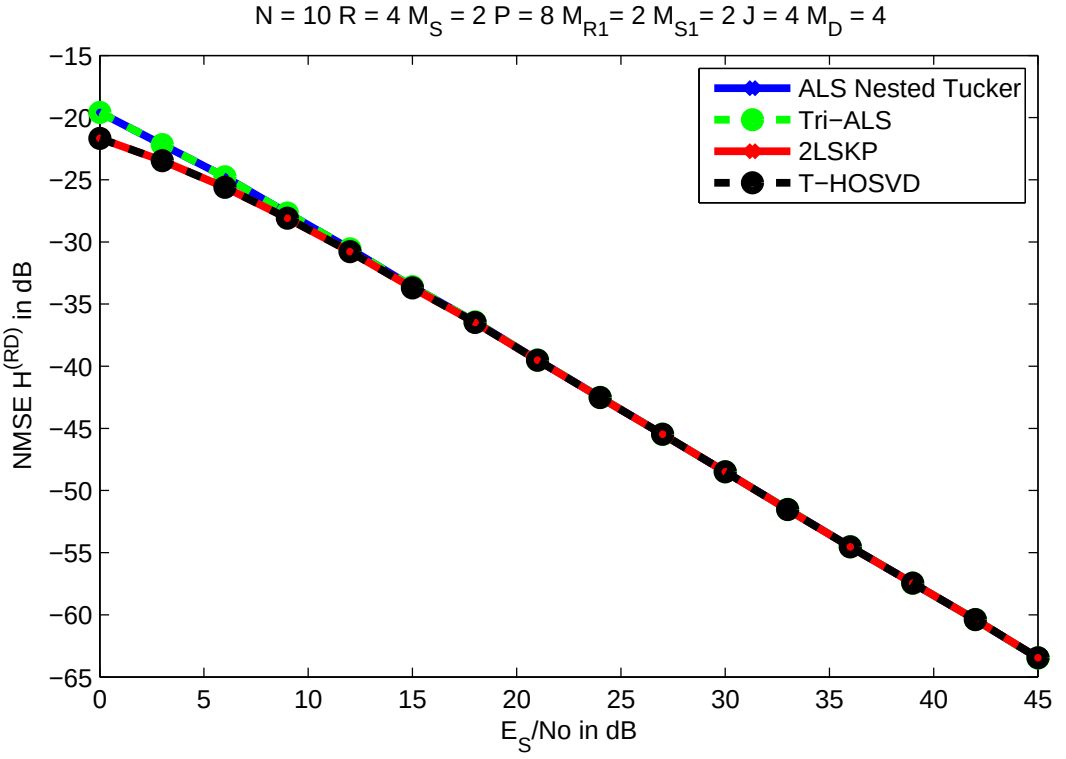

Source: Created by the Author

Figure 19 – Number of FLOPS vs. M_D receiver antennas.

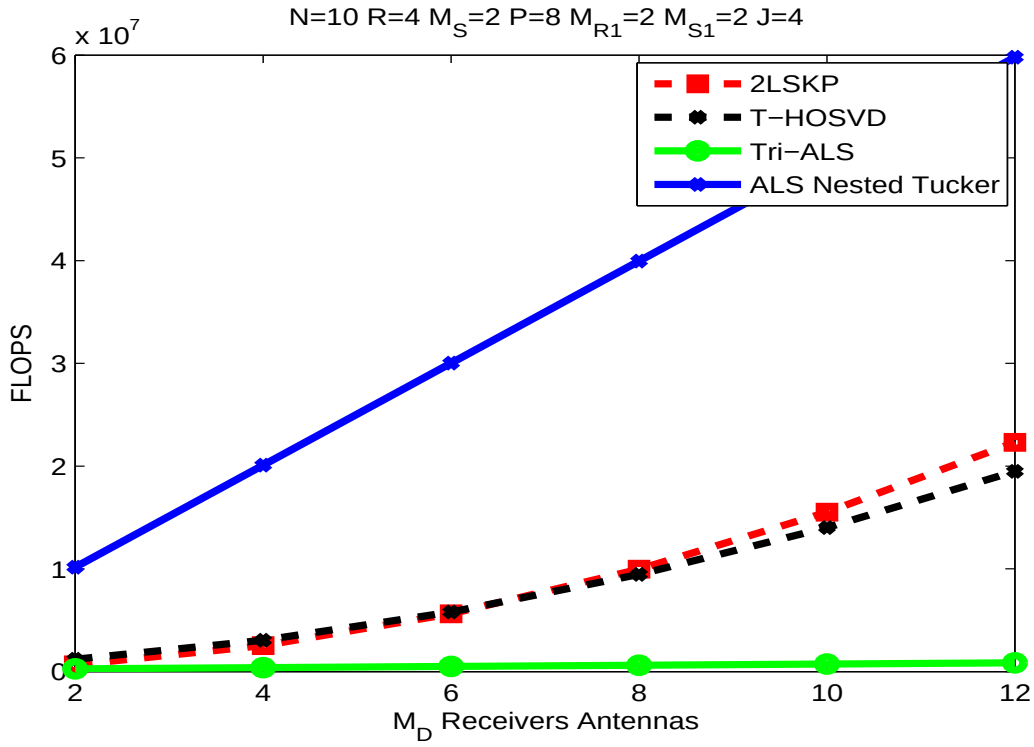

Source: Created by the Author

Figure 20 – Number of iterations for ALS's algorithms to converge.

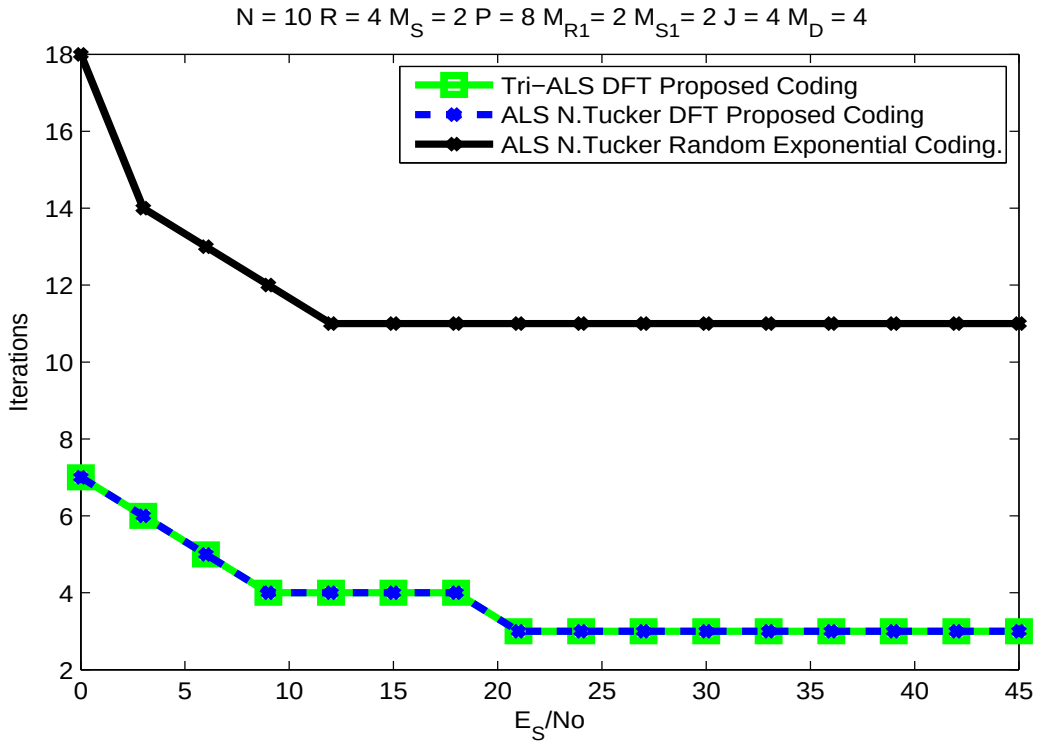

Source: Created by the Author

3.5 Summary

In this chapter the two semi-blind receivers were presented. As shown in the simulations-results, the proposed receiver has the same performance as the receivers proposed in [17]. The Tri-ALS receiver its attractive for high values of E_S/No due to the fewer number of iterations to converge, and the T-HOSVD for the possibility of parallelism. In general, this chapter has demonstrated a satisfactory performance of the proposed modelling based on rank-one tensor approach combined with the orthogonal code design, which resulted in a reduced complexity of the receivers, parallelism (for T-HOSVD receiver), and reduced number of iterations for the iterative receivers to converge.

4 MULTI-RELAYING MIMO SYSTEM

Diversity is one of the key features of MIMO cooperative systems, as discussed in Chapter 1. In order to exploit cooperative diversity, this chapter provides an extension of the rank-one factorization approach to the multi-relaying MIMO scenario, where multiple cooperative MIMO links are combined at the receiver. A coupled-SVD (C-SVD) receiver algorithm, based on a closed-form solution, is developed for joint channel and symbol estimation. In addition to be closed-form, the steps of the C-SVD receiver can be executed in parallel.

4.1 System Model

Figure 21 – MIMO multi-relaying system.

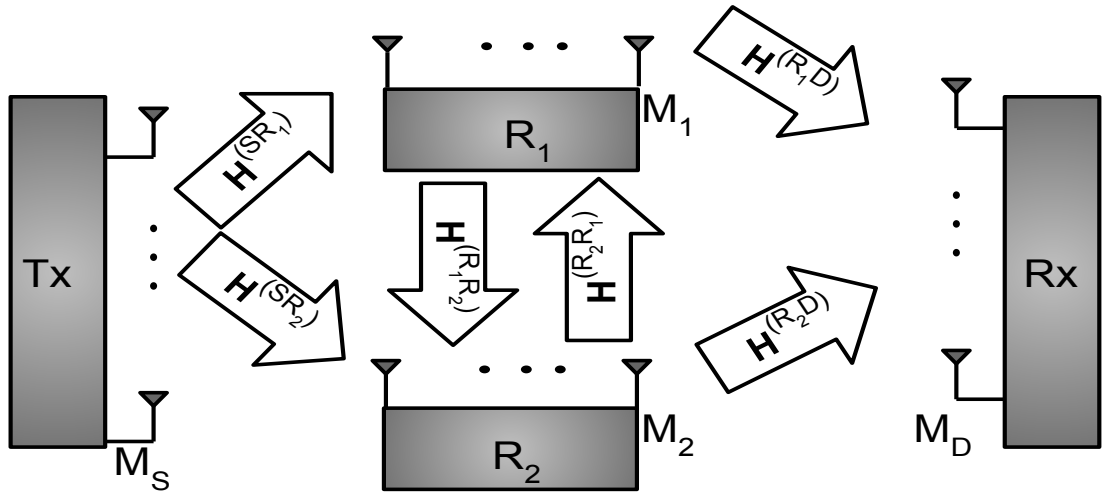

Source: Created by the Author

The scenario consists of a multi-relaying system where the source is assisted by two half-duplex relays using the AF protocol. In this system, M_S denotes the number of transmit antennas from the source, M_1 denotes the total number of antennas at Relay 1, where the number of transmit and receive antennas are denoted by M_{S_1} and M_{R_1} respectively, M_2 is the total number of antennas at the Relay 2 with M_{S_2} being the number of transmit antennas and M_{R_2} the number of receive antennas, and M_D is the number of receive antennas at the destination. Figure 21 illustrates the system configuration.

Phase 1

The source transmits the signal to Relay 1 and Relay 2. The symbol matrix $\mathbf{S} \in \mathbb{C}^{N \times R}$ contains

Figure 22 – First phase of the transmission.

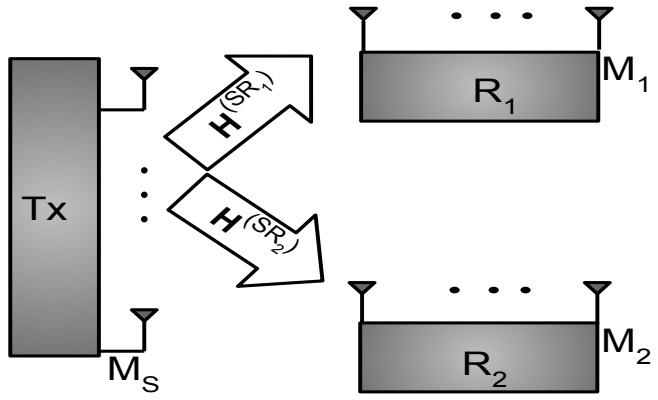

Source: Created by the Author

R data streams of N symbols each. These data streams are encoded at the source by means of a space-time coding tensor $\mathscr{C} \in \mathbb{C}^{M_S \times R \times P}$. Figure 22 shows the system operation in this phase. The transmitted signal tensor $\mathscr{X}^{(S)} \in \mathbb{C}^{M_S \times N \times P}$ is given by the following n-mode product:

$$\mathscr{X}^{(S)} = \mathscr{C} \times_2 \mathbf{S} \tag{4.1}$$

$$\mathbf{X}_{..p}^{(S)} = \mathbf{C}_{..p}\mathbf{S}^{\mathrm{T}}. \tag{4.2}$$

Each symbol is repeated P times over the M_S antennas creating a space-time redundancy. Considering $\mathbf{H}^{(SR_1)} \in \mathbb{C}^{M_{R_1} \times M_S}$ as the channel between the source and the Relay 1, and $\mathbf{H}^{(SR_2)} \in \mathbb{C}^{M_{R_2} \times M_S}$ as the channel between the source and Relay 2, the signal received at Relay 1 is the tensor $\mathscr{X}^{(SR_1)} \in \mathbb{C}^{M_{R_1} \times N \times P}$ and can be written, in n-mode product and slice notation, respectively, as

$$\mathscr{X}^{(SR_1)} = \mathscr{X}^{(S)} \times_1 \mathbf{H}^{(SR_1)} + \mathscr{V}^{(SR_1)} \tag{4.3}$$

$$\mathbf{X}_{..p}^{(SR_1)} = \mathbf{H}^{(SR_1)}\mathbf{C}_{..p}\mathbf{S}^{\mathrm{T}} + \mathbf{V}_{..p}^{(SR_1)} \in \mathbb{C}^{M_{R_1} \times N \times P}, \tag{4.4}$$

where $\mathscr{V}^{(SR_1)} \in \mathbb{C}^{M_{R_1} \times N \times P}$ is the additive noise at Relay 1. The signal received at Relay 2, $\mathscr{X}^{(SR_2)} \in \mathbb{C}^{M_{R_2} \times N \times P}$ is given by

$$\mathscr{X}^{(SR_2)} = \mathscr{X}^{(S)} \times_1 \mathbf{H}^{(SR_2)} + \mathscr{V}^{(SR_2)} \tag{4.5}$$

$$\mathbf{X}_{..p}^{(SR_2)} = \mathbf{H}^{(SR_2)}\mathbf{C}_{..p}\mathbf{S}^{\mathrm{T}} + \mathbf{V}_{..p}^{(SR_2)} \in \mathbb{C}^{M_{R_2} \times N \times P}, \tag{4.6}$$

with $\mathscr{V}^{(SR_2)} \in \mathbb{C}^{M_{R_2} \times N \times P}$ being the additive noise at Relay 2.

Phase 2

The source and Relay 2 stay in silent while Relay 1 transmits the signal $\mathscr{X}^{(SR_1)}$, received in the previous phase, to Relay 2 and destination. The signal is coded at Relay 1 by means of a space-time coding tensor $\mathscr{W} \in \mathbb{C}^{M_{S_1} \times M_{R_1} \times J}$ and sent through the M_{S_1} antennas, as illustrated in Figure 23. Similarly to Phase 1, a space-time redundancy is created, since now the NP symbol periods are repeated J times. Considering $\mathbf{H}^{(R_1R_2)} \in \mathbb{C}^{M_{R_2} \times M_{S_1}}$ as the channel between Relay 1 and Relay 2, and $\mathbf{H}^{(R_1D)} \in \mathbb{C}^{M_D \times M_{S_1}}$ the channel between Relay 1 and destination, the signal received at Relay 2, $\mathscr{X}^{(SR_1R_2)} \in \mathbb{C}^{M_{R_2} \times J \times N \times P}$ is given, in n-mode product and slice notation, respectively, as

Figure 23 – Second phase of the transmission.

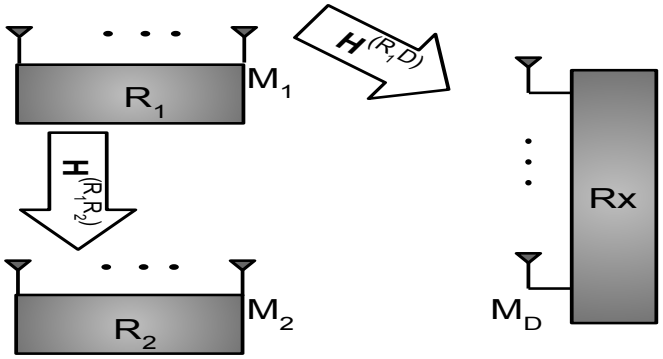

Source: Created by the Author

$$\begin{aligned}
\mathscr{X}^{(SR_1R_2)} &= (\mathscr{W} \bullet_2^1 \mathscr{X}^{(SR_1)}) \times_1 \mathbf{H}^{(R_1R_2)} + \mathscr{V}^{(SR_1R_2)} \\
&= (\mathscr{W} \times_1 \mathbf{H}^{(R_1R_2)}) \bullet_2^1 \mathscr{X}^{(SR_1)} + \mathscr{V}^{(SR_1R_2)} \\
&= \bar{\mathscr{H}}^{(R_1R_2)} \bullet_2^1 \mathscr{X}^{(SR_1)} + \mathscr{V}^{(SR_1R_2)} \in \mathbb{C}^{M_{R_2} \times J \times N \times P} \qquad (4.7) \\
\mathbf{X}_{.j.p}^{(SR_1R_2)} &= \mathbf{H}^{(R_1R_2)} \mathbf{W}_{..j} \mathbf{X}_{..p}^{(SR_1)} + \mathbf{V}_{.j.p}^{(SR_1R_2)} \qquad (4.8)
\end{aligned}$$

where $\mathscr{V}^{(SR_1R_2)} \in \mathbb{C}^{M_{R_2} \times J \times N \times P}$ is the additive noisy tensor at Relay 2 and $\bar{\mathscr{H}}^{(R_1R_2)} \in \mathbb{C}^{M_{R_2} \times M_{R_1} \times J}$ is the effective channel tensor. The signal received at the destination, $\mathscr{X}^{(SR_1D)} \in \mathbb{C}^{M_D \times J \times N \times P}$, can be written as

$$\begin{aligned}
\mathscr{X}^{(SR_1D)} &= \bar{\mathscr{H}}^{(R_1D)} \bullet_2^1 \mathscr{X}^{(SR_1)} + \mathscr{V}^{(SR_1D)} \qquad (4.9) \\
\mathbf{X}_{.j.p}^{(SR_1D)} &= \mathbf{H}^{(R_1D)} \mathbf{W}_{..j} \mathbf{X}_{..p}^{(SR_1)} + \mathbf{V}_{.j.p}^{(SR_1D)} \qquad (4.10)
\end{aligned}$$

with $\mathscr{V}^{(SR_1D)} \in \mathbb{C}^{M_D \times J \times N \times P}$ being the additive noisy tensor at the destination and $\bar{\mathscr{H}}^{(R_1D)} = \mathscr{W} \times_1 \mathbf{H}^{(R_1D)} \in \mathbb{C}^{M_D \times M_{R_1} \times J}$ is the effective channel tensor.

Phase 3

Now, the source and Relay 1 stay silent while Relay 2 transmits the signal received in Phase 1

Figure 24 – Third phase of the transmission.

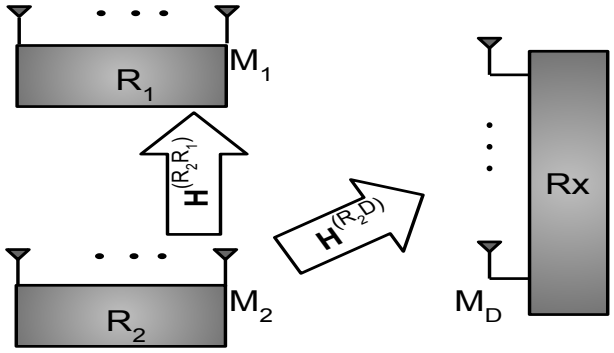

Source: Created by the Author

($\mathscr{X}^{(SR_2)}$) and in Phase 2 ($\mathscr{X}^{(SR_1R_2)}$) to Relay 1 and the destination. This phase is illustrated in Figure 24. For this transmission, the Relay 2 concatenates the signal $\mathscr{X}^{(SR_2)}$ along the second mode of the tensor $\mathscr{X}^{(SR_1R_2)}$ as

$$\overline{\mathscr{X}} = \mathscr{X}^{(SR_1R_2)} \sqcup_2 \mathscr{X}^{(SR_2)} \qquad \in \mathbb{C}^{M_{R_2} \times (J+1) \times N \times P} \tag{4.11}$$

$$\overline{\mathscr{X}}_{\cdot 1:J \cdot \cdot} = \mathscr{X}^{(SR_1R_2)} \qquad \in \mathbb{C}^{M_{R_2} \times J \times N \times P} \tag{4.12}$$

$$\overline{\mathscr{X}}_{\cdot J+1 \cdot \cdot} = \mathscr{X}^{(SR_2)} \qquad \in \mathbb{C}^{M_{R_2} \times 1 \times N \times P}. \tag{4.13}$$

Then, the signal is coded by means of a space-time coding tensor $\mathscr{T} \in \mathbb{C}^{M_{S_2} \times M_{R_2} \times K}$ and sent trough the M_{S_2} antennas. The coding tensor introduces another space-time redundancy to the system, having now, $P(J+1)K$ symbol repetitions (channel uses). Consider $\mathbf{H}^{(R_2R_1)} \in \mathbb{C}^{M_{R_1} \times M_{S_2}}$ as the channel between the Relay 2 and Relay 1, and $\mathbf{H}^{(R_2D)} \in \mathbb{C}^{M_D \times M_{S_2}}$ as the channel between Relay 2 and the destination. The signal received at the destination $\overline{\mathscr{X}}^{(SR_1R_2D)} \in \mathbb{C}^{M_D \times K \times (J+1) \times N \times P}$ is given by:

$$\overline{\mathscr{X}}^{(SR_1R_2D)} = \bar{\mathscr{H}}^{(R_2D)} \bullet_2^1 \overline{\mathscr{X}} + \overline{\mathscr{V}}^{(SR_1R_2D)} \tag{4.14}$$

$$\overline{\mathbf{X}}^{(SR_1R_2D)}_{\cdot k(j+1) \cdot p} = \mathbf{H}^{(R_2D)} \mathbf{T}_{\cdot \cdot k} \overline{\mathbf{X}}_{\cdot (j+1) \cdot p} + \overline{\mathbf{V}}^{(SR_1R_2D)}_{\cdot k(j+1) \cdot p} \tag{4.15}$$

where the $\overline{\mathscr{V}}^{(SR_1R_2D)} \in \mathbb{C}^{M_D \times K \times (J+1) \times N \times P}$ is the additive noisy tensor at the destination, and $\bar{\mathscr{H}}^{(R_2D)} = \mathscr{T} \times_1 \mathbf{H}^{(R_2D)} \in \mathbb{C}^{M_D \times M_{R_2} \times K}$ is the effective channel. The destination extracts the two signals from $\overline{\mathscr{X}}^{(SR_1R_2D)}$ by separating the first J slices of the second mode, forming the signal $\mathscr{X}^{(SR_1R_2D)} \in \mathbb{C}^{M_D \times K \times J \times N \times P}$ and the $(J+1)$-*th* slice to form the signal $\mathscr{X}^{(SR_2D)} \in \mathbb{C}^{M_D \times K \times N \times P}$. In this phase, Relay 1 only considers the signal $\mathscr{X}^{(SR_2)}$, i.e. the slice $(J+1)$-*th* of the tensor $\overline{\mathscr{X}}$, since the tensor $\mathscr{X}^{(SR_1R_2)}$ was sent in the previous phase. So, the received signal at Relay 1, $\mathscr{X}^{(SR_2R_1)} \in \mathbb{C}^{M_{R_1} \times K \times N \times P}$, in Phase 3, is written as:

$$\begin{aligned} \mathscr{X}^{(SR_2R_1)} &= \bar{\mathscr{H}}^{(R_2R_1)} \bullet_2^1 \mathscr{X}^{(SR_2)} + \mathscr{V}^{(SR_2R_1)} \\ \mathbf{X}_{.k.p}^{(SR_2R_1)} &= \mathbf{H}^{(R_2R_1)} \mathbf{T}_{..k} \mathbf{X}_{..p}^{(SR_2)} + \mathbf{V}_{.k.p}^{(SR_2R_1)}, \end{aligned} \tag{4.16}$$

where $\mathscr{V}^{(SR_2R_1)} \in \mathbb{C}^{M_{R_1} \times K \times N \times P}$ is the additive noisy tensor at Relay 1 and $\bar{\mathscr{H}}^{(R_2R_1)} = \mathscr{T} \times_1 \mathbf{H}^{(R_2R_1)} \in \mathbb{C}^{M_{R_1} \times M_{R_2} \times K}$ is the effective channel tensor.

Phase 4

In the last phase, Relay 1 transmits the signal $\mathscr{X}^{(SR_2R_1)} \in \mathbb{C}^{M_{R_1} \times K \times N \times P}$ to the destination, as illustrated in Figure 25. The signal is coded by the space-time coding tensor $\mathscr{W}$, introduced in Phase 2, creating for the signal another redundancy, resulting in PKJ symbol repetitions. The signal $\mathscr{X}^{(SR_2R_1D)} \in \mathbb{C}^{M_D \times J \times K \times N \times P}$ received at the destination can be expressed as

Figure 25 – Fourth phase of the transmission.

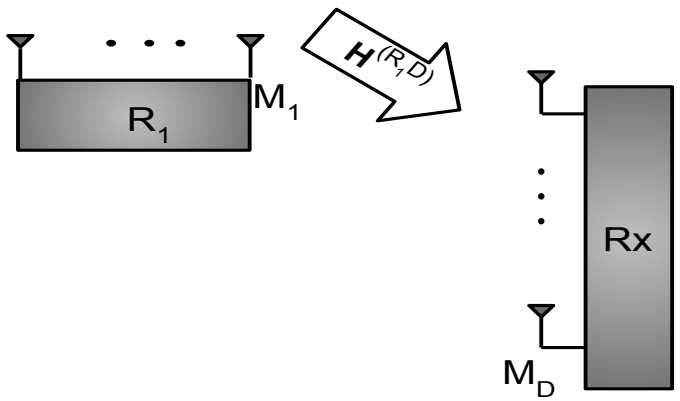

Source: Created by the Author

$$\begin{aligned} \mathscr{X}^{(SR_2R_1D)} &= \mathscr{H}^{R_1D} \bullet_2^1 \mathscr{X}^{(SR_2R_1)} + \mathscr{V}^{(SR_2R_1D)} \\ \mathbf{X}_{.jk.p}^{(SR_2R_1D)} &= \mathbf{H}^{(R_1D)} \mathbf{W}_{..j} \mathbf{X}_{.k.p}^{(SR_2R_1)} + \mathbf{V}_{.jk.p}^{(SR_2R_1D)} \end{aligned} \tag{4.17}$$

The tensor $\mathscr{V}^{(SR_2R_1D)} \in \mathbb{C}^{M_D \times J \times K \times N \times P}$ represents the additive noise at the destination, in Phase 4. Considering that the total redundancy in the system is $NP(J+K+2JK)$ symbols, NPJ from Phase 2, $NPJK+NPK$ from Phase 3 and $NPKJ$ from Phase 4, the rate of the system is given by $\frac{NR-1}{NP(J+K+2JK)}$. The factor $NR-1$ comes from assuming the knowledge of one symbol at the receiver. However, this factor can be neglected by using a differential modulation.

4.1.1 Destination Signals

At the end of transmission, the destination contains four tensors signals, provided by the different phases: $\mathscr{X}^{(SR_1D)}$, $\mathscr{X}^{(SR_2D)}$, $\mathscr{X}^{(SR_1R_2D)}$ and $\mathscr{X}^{(SR_2R_1D)}$. Our idea is to use this diversity to jointly estimate symbol and channel matrices. Before the estimation, we first rearrange all the signals in order to permute their structure to a rank-one approximated tensor. Since $\mathscr{X}^{(SR_1D)}$ has the same structure as $\mathscr{X}^{(SR_2D)}$ and $\mathscr{X}^{(SR_1R_2D)}$ has the same structure as $\mathscr{X}^{(SR_2R_1D)}$, the rank-one approximation will be described only for $\mathscr{X}^{(SR_1D)}$ and $\mathscr{X}^{(SR_1R_2D)}$.

4.1.2 Coding Tensor Structure

As in Chapter 3, we assume a PARAFAC structure for each coding tensor. In this scenario, we have as additional space-time coding tensor from Relay 2,

$$\mathscr{T} = \mathscr{I}_{F_3} \times_1 \mathbf{T}_1 \times_2 \mathbf{T}_2 \times_3 \mathbf{T}_3 \in \mathbb{C}^{M_{S_2} \times M_{R_2} \times K} \tag{4.18}$$

where $\mathbf{T}_1 \in \mathbb{C}^{M_{S_2} \times F_3}$, $\mathbf{T}_2 \in \mathbb{C}^{M_{R_2} \times F_3}$ and $\mathbf{T}_3 \in \mathbb{C}^{K \times F_3}$ are the factor matrices of the tensor $\mathscr{T}$. For the proposed multi-relaying scenario, we have four effective codes. In the $\mathscr{X}^{(SR_1R_2D)}$ processing, there are two matrices used formed by the space-time coding structure, $\mathbf{Z}_J$ and $\mathbf{Z}^{(1)}$. The matrix $\mathbf{Z}_J$ is formed by stacking column-wise the J frontal slices vectorized of the tensor $\mathscr{W}$,

$$\mathbf{Z}_J = [\text{vec}(\mathbf{W}_{..1}); \cdots ; \text{vec}(\mathbf{W}_{..J})] \in \mathbb{C}^{M_{S_1} M_{R_1} \times J}. \tag{4.19}$$

The matrix $\mathbf{Z}^{(1)}$ is equal to the matrix $\mathbf{Z}$ defined in Equation (3.20). Now, for the $\mathscr{X}^{(SR_2R_1D)}$ processing, we have two matrices formed by the space-time coding tensors. The matrix $\mathbf{Z}_K$ is formed by stacking column-wise the K frontal slices of the tensor $\mathscr{T}$. The matrix $\mathbf{Z}^{(2)}$ follows the steps in Equations (3.15) to (3.17) for the term $\text{vec}(\mathbf{C}_{..p}^{\text{T}} \otimes \mathbf{T}_{..k})$. As in Chapter 3, all these matrices have an orthogonal design, as detailed in Appendix A.

4.1.3 $\mathscr{X}^{(SR_1D)}$ Processing

Consider the Equation (4.10), ignoring the noise. By replacing $\mathbf{X}^{(SR_1)}$ in Equation (4.4), we have

$$\begin{aligned}\mathbf{X}^{(SR_1D)}_{.j.p} &= \mathbf{H}^{(R_1D)}\mathbf{W}_{..j}\mathbf{X}^{(SR_1)}_{..p} \\ &= \mathbf{H}^{(R_1D)}\mathbf{W}_{..j}\mathbf{H}^{(SR_1)}\mathbf{C}_{..p}\mathbf{S}^{\mathrm{T}}.\end{aligned} \tag{4.20}$$

Comparing Equation (4.20) with Equation (3.10), it can be noticed that both equations have the same structure, only the parameters are changed, meaning that the same processing applied for Equation (3.10) can be applied to signal $\mathscr{X}^{(SR_1D)}$ and consequentially to signal $\mathscr{X}^{(SR_2D)}$. We can formulate the input-output relation for the signal $\mathscr{X}^{(SR_1D)}$ as

$$\mathbf{X}^{(SR_1D)} = \mathbf{Y}^{(SR_1D)}\mathbf{Z}^{(1)} + \mathbf{V}^{(SR_1D)} \in \mathbb{C}^{M_DN\times JP}, \tag{4.21}$$

where $\mathbf{Y}^{(SR_1D)} \in \mathbb{C}^{M_DN\times M_{S_1}RM_{R_1}M_S}$, $\mathbf{Z}^{(1)} \in \mathbb{C}^{M_{S_1}RM_{R_1}M_S\times JP}$ are defined as:

$$\mathbf{Y}^{(SR_1D)} = \mathrm{vec}\big(\mathbf{H}^{(SR_1)}\big)^{\mathrm{T}} \otimes \mathbf{S} \otimes \mathbf{H}^{(R_1D)} \tag{4.22}$$

$$\mathbf{Z}^{(1)} = (\mathbf{G}_1 \diamond \mathbf{G}_2)\mathbf{G}_3^{\mathrm{T}}. \tag{4.23}$$

Equation (4.21) is a generalized unfolding of the received signal tensor $\mathscr{X}^{(SR_1D)}$ which separates the unknown parameters from the known parameters, which are the coding tensors. Also, $\mathbf{V}^{(SR_1D)} \in \mathbb{C}^{M_DN\times JP}$ is a generalized unfolding of the global noise in this transmission. The first processing at the receiver, since the $\mathbf{Z}^{(1)}$ matrix is known, is to use the LS approach.

$$\hat{\mathbf{Y}}^{(SR_1D)} = \underset{\mathbf{Y}^{(SR_1D)}}{\mathrm{argmin}} \|\mathbf{X}^{(SR_1D)} - \mathbf{Y}^{(SR_1D)}\mathbf{Z}^{(1)}\|_F \tag{4.24}$$

As discussed in Chapter 3, when $\mathbf{Z}^{(1)}$ has an orthogonal design, the solution of Equation (4.24) is $\hat{\mathbf{Y}}^{(SR_1D)} = \mathbf{X}^{(SR_1D)}\mathbf{Z}^{(1)\mathrm{H}}$. Using the generalized Kronecker approximation introduced in Section 2.3.2 for the matrix $\hat{\mathbf{Y}}^{(SR_1D)}$, we can define the approximated third-order rank-one tensor $\mathscr{P}^{(SR_1D)} \in \mathbb{C}^{M_DM_{S_1}\times NR\times M_{R_1}M_S}$.

$$\mathscr{P}^{(SR_1D)} \approx \mathbf{h}^{(R_1D)} \circ \mathbf{s} \circ \mathbf{h}^{(SR_1)}. \tag{4.25}$$

Following the same steps for the signal $\mathscr{X}^{(SR_2D)}$, a similar pre-processing is done with the following correspondences:

$$
\begin{aligned}
(\mathscr{X}^{(SR_1D)}) &\Longleftrightarrow (\mathscr{X}^{(SR_2D)}) \\
(\mathbf{X}^{(SR_1D)}, \mathbf{Y}^{(SR_1D)}) &\Longleftrightarrow (\mathbf{X}^{(SR_2D)}, \mathbf{Y}^{(SR_2D)}) \\
(\mathbf{Z}^{(1)}, \mathbf{V}^{(SR_1D)}) &\Longleftrightarrow (\mathbf{Z}^{(2)}, \mathbf{V}^{(SR_2D)}) \\
(\mathbf{H}^{(SR_1)}, \mathbf{H}^{(R_1D)}) &\Longleftrightarrow (\mathbf{H}^{(SR_2)}, \mathbf{H}^{(R_2D)}) \\
(\mathscr{P}^{(SR_1D)}) &\Longleftrightarrow (\mathscr{P}^{(SR_2D)}).
\end{aligned}
$$

The main difference is that $\mathbf{Z}^{(2)} = (\mathbf{B}_1 \diamond \mathbf{B}_2)\mathbf{B}_3^{\mathrm{T}} \in \mathbb{C}^{M_{S_2} R M_{R_2} M_S \times KP}$, is the matrix formed by collecting the KP vectors of the expression $\mathrm{vec}(\mathbf{C}_{..p}^{\mathrm{T}} \otimes \mathbf{T}_{..k})$, with $\mathbf{B}_1 = (\mathbf{C}_1 \otimes \mathbf{T}_2)$, $\mathbf{B}_2 = (\mathbf{C}_2 \otimes \mathbf{T}_1)$ and $\mathbf{B}_3 = (\mathbf{C}_3 \otimes \mathbf{T}_3)$. The approximated rank-one tensor, obtained from $\mathscr{X}^{(SR_2D)}$ signal, is given by

$$
\mathscr{P}^{(SR_2D)} \approx \mathbf{h}^{(R_2D)} \circ \mathbf{s} \circ \mathbf{h}^{(SR_2)} \in \mathbb{C}^{M_D M_{S_2} \times NR \times M_{R_2} M_S} \tag{4.26}
$$

4.1.4 $\mathscr{X}^{(SR_1R_2D)}$ *Processing*

Following the slice approach used for the $\mathscr{X}^{(SR_1D)}$ using Equations (4.4) and (4.8), ignoring the noise term, we have that:

$$
\begin{aligned}
\mathbf{X}_{.kj.p}^{(SR_1R_2D)} &= \mathbf{H}^{(R_2D)} \mathbf{T}_{..k} \mathbf{X}_{.j.p}^{(SR_1R_2)} \\
&= \mathbf{H}^{(R_2D)} \mathbf{T}_{..k} \mathbf{H}^{(R_1R_2)} \mathbf{W}_{..j} \mathbf{X}^{(SR_1)} \\
&= \mathbf{H}^{(R_2D)} \mathbf{T}_{..k} \mathbf{H}^{(R_1R_2)} \mathbf{W}_{..j} \mathbf{H}^{(SR_1)} \mathbf{C}_{..p} \mathbf{S}^{\mathrm{T}}.
\end{aligned} \tag{4.27}
$$

Note that Equation (4.27) is similar to Equation (2.89), meaning that the signals $\mathscr{X}^{(SR_1R_2D)}$ and $\mathscr{X}^{(SR_2R_1D)}$ follow a fifth-order Nested Tucker decomposition (NTD(5)). Applying Property (2.33) three times, and defining $\mathbf{x}_{kjp} = \mathrm{vec}(\mathbf{X}_{.kj.p}^{(SR_1R_2D)})$ yields

$$
\begin{aligned}
\mathbf{x}_{kjp} &= (\mathbf{S} \otimes \mathbf{H}^{(R_2D)}) \mathrm{vec}(\mathbf{T}_{..k} \mathbf{H}^{(R_1R_2)} \mathbf{W}_{..j} \mathbf{H}^{(SR_1)} \mathbf{C}_{..p}) \\
&= (\mathbf{S} \otimes \mathbf{H}^{(R_2D)}) (\mathbf{C}_{..p}^{\mathrm{T}} \otimes \mathbf{T}_{..k}) \mathrm{vec}(\mathbf{H}^{(R_1R_2)} \mathbf{W}_{..j} \mathbf{H}^{(SR_1)}) \\
&= (\mathbf{S} \otimes \mathbf{H}^{(R_2D)}) (\mathbf{C}_{..p}^{\mathrm{T}} \otimes \mathbf{T}_{..k}) (\mathbf{H}^{(SR_1)\mathrm{T}} \otimes \mathbf{H}^{(R_1R_2)}) \mathrm{vec}(\mathbf{W}_{..j}) \in \mathbb{C}^{M_D N \times 1}.
\end{aligned} \tag{4.28}
$$

Collecting the J frontal slices of $\mathscr{W}$ as in Equation (4.19), we have:

$$
\begin{aligned}
\mathbf{X}_{.k.p} = (\mathbf{S} \otimes \mathbf{H}^{(R_2D)}) (\mathbf{C}_{..p}^{\mathrm{T}} \otimes \mathbf{T}_{..k}) \\
(\mathbf{H}^{(SR_1)\mathrm{T}} \otimes \mathbf{H}^{(R_1R_2)}) \mathbf{Z}_J,
\end{aligned} \tag{4.29}
$$

where $\mathbf{X}_{.k.p} \in \mathbb{C}^{M_D N \times J}$. Multiplying Equation (4.29) at the right-hand side by $\mathbf{Z}_J^{\mathrm{H}}$ (since $\mathbf{Z}_J$ is an orthogonal matrix), we can define the matrix $\overline{\mathbf{X}}_{.k.p} \in \mathbb{C}^{M_D N \times M_{S_1} M_{R_1}}$ as:

$$\overline{\mathbf{X}}_{.k.p} = (\mathbf{S} \otimes \mathbf{H}^{(R_2 D)})(\mathbf{C}_{..p}^{\mathrm{T}} \otimes \mathbf{T}_{..k})(\mathbf{H}^{(SR_1)\mathrm{T}} \otimes \mathbf{H}^{(R_1 R_2)}). \tag{4.30}$$

Applying Property (2.33), with $\overline{\mathbf{x}}_{kp} = \mathrm{vec}(\overline{\mathbf{X}}_{.k.p})$, yields:

$$\overline{\mathbf{x}}_{kp} = (\mathbf{H}^{(SR_1)} \otimes \mathbf{H}^{(R_1 R_2)\mathrm{T}} \otimes \mathbf{S} \otimes \mathbf{H}^{(R_2 D)})\mathrm{vec}(\mathbf{C}_{..p}^{\mathrm{T}} \otimes \mathbf{T}_{..k}) \tag{4.31}$$

Now the KP left vectors are collected to form the matrix $\mathbf{X}^{(SR_1R_2D)} \in \mathbb{C}^{M_D N M_{S_1} M_{R_1} \times KP}$. Note that, collecting the KP vectors of the expression $\mathrm{vec}(\mathbf{C}_{..p}^{\mathrm{T}} \otimes \mathbf{T}_{..k})$ yields the matrix $\mathbf{Z}^{(2)}$.

$$\mathbf{X}^{(SR_1R_2D)} = \mathbf{Y}^{(SR_1R_2D)}\mathbf{Z}^{(2)} + \mathbf{V}^{(SR_1R_2D)}, \tag{4.32}$$

with

$$\mathbf{Y}^{(SR_1R_2D)} = \mathbf{H}^{(SR_1)} \otimes \mathbf{H}^{(R_1R_2)\mathrm{T}} \otimes \mathbf{S} \otimes \mathbf{H}^{(R_2D)} \in \mathbb{C}^{M_D N M_{S_1} M_{R_1} \times M_{S_2} R M_{R_2} M_S} \tag{4.33}$$

$$\mathbf{Z}^{(2)} = (\mathbf{B}_1 \diamond \mathbf{B}_2)\mathbf{B}_3^{\mathrm{T}} \in \mathbb{C}^{M_{S_2} R M_{R_2} M_S \times KP}, \tag{4.34}$$

and $\mathbf{V}^{(SR_1R_2D)} \in \mathbb{C}^{M_D N M_{S_1} M_{R_1} \times KP}$ being the generalized unfolding of the noisy tensor $\mathscr{V}^{(SR_1R_2D)}$. Using the LS criterion, we can formulate

$$\hat{\mathbf{Y}}^{(SR_1R_2D)} = \underset{\mathbf{Y}^{(SR_1R_2D)}}{\mathrm{argmin}} \|\mathbf{X}^{(SR_1R_2D)} - \mathbf{Y}^{(SR_1R_2D)}\mathbf{Z}^{(2)}\|_F. \tag{4.35}$$

Applying the Kronecker approximation of Section 2.3.2, to the matrix $\hat{\mathbf{Y}}^{(SR_1R_2D)}$ we can express the approximated fourth-order rank-one tensor as

$$\mathscr{P}^{(SR_1R_2D)} \approx \mathbf{h}^{(R_2D)} \circ \mathbf{s} \circ \mathbf{h}^{(\overline{R_1R_2})} \circ \mathbf{h}^{(SR_1)}, \tag{4.36}$$

with $\mathscr{P}^{(SR_1R_2D)} \in \mathbb{C}^{M_D M_{S_2} \times NR \times M_{S_1} M_{R_2} \times M_{R_1} M_S}$ and $\mathbf{h}^{(\overline{R_1R_2})} = \mathrm{vec}(\mathbf{H}^{(R_1R_2)\mathrm{T}})$. Similarly to $\mathscr{X}^{(SR_1R_2D)}$, the signal $\mathscr{X}^{(SR_2R_1D)}$ has the same processing, with the difference that the first stack it is in *K-th* mode, so that we have the following correspondences:

$$\begin{gathered}
(\mathscr{X}^{(SR_1R_2D)}) \Longleftrightarrow (\mathscr{X}^{(SR_2R_1D)}) \\
(\mathbf{X}^{(SR_1R_2D)}, \mathbf{Y}^{(SR_1R_2D)}) \Longleftrightarrow (\mathbf{X}^{(SR_2R_1D)}, \mathbf{Y}^{(SR_2R_1D)}) \\
(\mathbf{Z}_J, \mathbf{Z}^{(2)},) \Longleftrightarrow (\mathbf{Z}_K, \mathbf{Z}^{(1)}) \\
(\mathbf{H}^{(SR_1)}, \mathbf{H}^{(R_1R_2)}, \mathbf{H}^{(R_2D)}) \Longleftrightarrow (\mathbf{H}^{(SR_2)}, \mathbf{H}^{(R_2R_1)}, \mathbf{H}^{(R_1D)}) \\
(\mathscr{P}^{(SR_1R_2D)}) \Longleftrightarrow (\mathscr{P}^{(SR_2R_1D)}).
\end{gathered}$$

At the end, the approximated fourth-order rank-one tensor $\mathscr{P}^{(SR_2R_1D)}$ is given by:

$$\mathscr{P}^{(SR_2R_1D)} \approx \mathbf{h}^{(R_1D)} \circ \mathbf{s} \circ \mathbf{h}^{\overline{(R_2R_1)}} \circ \mathbf{h}^{(SR_2)} \in \mathbb{C}^{M_D M_{S_1} \times NR \times M_{R_1} M_{S_2} \times M_{R_2} M_S}. \tag{4.37}$$

4.1.5 Uniqueness

Considering the four signals $\mathscr{X}^{(SR_1)}$, $\mathscr{X}^{(SR_2)}$, $\mathscr{X}^{(SR_1R_2)}$ and $\mathscr{X}^{(SR_2R_1)}$, for each signal an LS estimation is performed, and the conditions to ensure the uniqueness are given by

$$P \geq F_1 \geq M_S R, \tag{4.38}$$

$$J \geq F_2 \geq M_{R_1} M_{S_1}, \tag{4.39}$$

$$K \geq F_3 \geq M_{R_2} M_{S_2}. \tag{4.40}$$

The proof of conditions (4.38) to (4.40) are given in Appendix B.

4.2 C-SVD Receiver

After the pre-processing step at the receiver, the four rank-one approximated tensors are given by

$$\mathscr{P}^{(SR_1D)} \approx \mathbf{h}^{(R_1D)} \circ \mathbf{s} \circ \mathbf{h}^{(SR_1)} \tag{4.41}$$

$$\mathscr{P}^{(SR_2D)} \approx \mathbf{h}^{(R_2D)} \circ \mathbf{s} \circ \mathbf{h}^{(SR_2)} \tag{4.42}$$

$$\mathscr{P}^{(SR_1R_2D)} \approx \mathbf{h}^{(R_2D)} \circ \mathbf{s} \circ \mathbf{h}^{(\overline{R_1R_2})} \circ \mathbf{h}^{(SR_1)} \tag{4.43}$$

$$\mathscr{P}^{(SR_2R_1D)} \approx \mathbf{h}^{(R_1D)} \circ \mathbf{s} \circ \mathbf{h}^{(\overline{R_2R_1})} \circ \mathbf{h}^{(SR_2)}. \tag{4.44}$$

The **C**oupled-**SVD** receiver combines all the four rank-one tensor signals to joint symbol and channel estimation by coupling the n-mode unfolding of those tensors to estimate the parameters via SVDs of rank-one approximated matrices, and those SVDs can be computed in parallel as we show next.

For symbol estimation, in Equation (4.41), we have the vector $\mathbf{s}$ containing the symbols. By coupling the tall 2-mode unfolding of each tensor we have

$$\begin{bmatrix} \mathbf{P}_{(2)}^{(SR_1D)} \\ \mathbf{P}_{(2)}^{(SR_2D)} \\ \mathbf{P}_{(2)}^{(SR_1R_2D)} \\ \mathbf{P}_{(2)}^{(SR_2R_1D)} \end{bmatrix} \approx \begin{bmatrix} (\mathbf{h}^{(SR_1)} \diamond \mathbf{h}^{(R_1D)}) \\ (\mathbf{h}^{(SR_2)} \diamond \mathbf{h}^{(R_2D)}) \\ (\mathbf{h}^{(SR_1)} \diamond \mathbf{h}^{(\overline{R_1R_2})} \diamond \mathbf{h}^{(R_2D)}) \\ (\mathbf{h}^{(SR_2)} \diamond \mathbf{h}^{(\overline{R_2R_1})} \diamond \mathbf{h}^{(R_1D)}) \end{bmatrix} \mathbf{s}^{\mathrm{T}}. \tag{4.45}$$

Equation (4.45) is an approximation to a rank-one matrix of size $M_S M_D[M_{R_1} M_{S_1}(1 + M_{R_2} M_{S_2}) + M_{R_2} M_{S_2}(1 + M_{R_1} M_{S_1})] \times NR$. Computing the SVD of (4.45) as $\mathbf{U}_s \mathbf{\Sigma}_s \mathbf{V}_s^{\mathrm{H}}$, the first right singular vector only provide us a basis, i.e. $\hat{\mathbf{s}} = \alpha_1 \mathbf{V}^*_{s(:,1)}$, where α_1 is a scalar factor that compensates

the orthonormal basis from the SVD. Assuming that we have the knowledge of one symbol, for instance $\mathbf{S}_{(1,1)}$, the scalar factor is found as $\alpha_1 = \mathbf{S}_{(1,1)}/\mathbf{V}^{*}_{s(1,1)}$. At the end, the unvec operator is applied, i.e., $\hat{\mathbf{S}} = \text{unvec}(\hat{\mathbf{s}})$.

For channel estimation, the same approach is applied. Once again, since the SVD only provides a basis for the estimated parameters and to remove the scalar ambiguity, while keeping the parallelism at the receiver, it is necessary to assume the knowledge of at least one link of four channels, which, in this work, are considered as $\mathbf{H}^{(R_1D)}_{(1,1)}$, $\mathbf{H}^{(R_2D)}_{(1,1)}$, $\mathbf{H}^{(R_1R_2)}_{(1,1)}$ and $\mathbf{H}^{(R_2R_1)}_{(1,1)}$.

Coupling the 1-mode unfolding of the tensor $\mathscr{P}^{(SR_1D)}$ and $\mathscr{P}^{(SR_2R_1D)}$, $\mathbf{P}^{(SR_1D)}_{(1)}$ and $\mathbf{P}^{(SR_2R_1D)}_{(1)}$, we have a rank-one approximated matrix of size $M_S NR[M_{R_1}(1+M_{R_2}M_{S_2})] \times M_{S_1}M_D$, given as

$$\begin{bmatrix} \mathbf{P}^{(SR_1D)}_{(1)} \\ \mathbf{P}^{(SR_2R_1D)}_{(1)} \end{bmatrix} \approx \begin{bmatrix} (\mathbf{h}^{(SR_1)} \diamond \mathbf{s}) \\ (\mathbf{h}^{(SR_2)} \diamond \mathbf{h}^{(\overline{R_2R_1})} \diamond \mathbf{s}) \end{bmatrix} \mathbf{h}^{(R_1D)\text{T}} \tag{4.46}$$

Consider the SVD of (4.46) as $\mathbf{U}^{(R_1D)}\mathbf{\Sigma}^{(R_1D)}\mathbf{V}^{(R_1D)\text{H}}$, we have that $\hat{\mathbf{h}}^{(R_1D)} = \alpha_2 \mathbf{V}^{(R_1D)*}_{(:,1)}$, where $\alpha_2 = \mathbf{H}^{(R_1D)}_{(1,1)}/\mathbf{V}^{(R_1D)*}_{(1,1)}$ and $\hat{\mathbf{H}}^{(R_1D)} = \text{unvec}(\hat{\mathbf{h}}^{(R_1D)})$.

For $\hat{\mathbf{h}}^{(R_2D)}$, the $\mathbf{P}^{(SR_2D)}_{(1)}$ and $\mathbf{P}^{(SR_1R_2D)}_{(1)}$, 1-mode unfolding of the tensors $\mathscr{P}^{(SR_2)}$ and $\mathscr{P}^{(SR_1R_2D)}$ respectively, are coupled to form the rank-one approximated matrix of size $M_S NR[M_{R_2}(1+M_{R_1}M_{S_1})] \times M_{S_2}M_D$,

$$\begin{bmatrix} \mathbf{P}^{(SR_2D)}_{(1)} \\ \mathbf{P}^{(SR_1R_2D)}_{(1)} \end{bmatrix} \approx \begin{bmatrix} (\mathbf{h}^{(SR_2)} \diamond \mathbf{s}) \\ (\mathbf{h}^{(SR_1)} \diamond \mathbf{h}^{(\overline{R_1R_2})} \diamond \mathbf{s}) \end{bmatrix} \mathbf{h}^{(R_2D)\text{T}}. \tag{4.47}$$

By computing its SVD as $\mathbf{U}^{(R_2D)}\mathbf{\Sigma}^{(R_2D)}\mathbf{V}^{(R_2D)\text{H}}$, we have that $\hat{\mathbf{H}}^{(R_2D)} = \text{unvec}(\hat{\mathbf{h}}^{(R_2D)})$, where $\hat{\mathbf{h}}^{(R_2D)} = \alpha_3 \mathbf{V}^{(R_2D)*}_{(:,1)}$ and $\alpha_3 = \mathbf{H}^{(R_2D)}_{(1,1)}/\mathbf{V}^{(R_2D)*}_{(1,1)}$.

For the source-Relay 1 channel estimation, the C-SVD receiver couples the 3-mode unfolding of the tensor $\mathscr{P}^{(SR_1D)}$ with the 4-mode unfolding of the tensor $\mathscr{P}^{(SR_1R_2D)}$, forming a rank-one approximated matrix of size $NRM_DM_{S_1}(1+M_{R_2}M_{S_2}) \times M_{R_1}M_S$, given by

$$\begin{bmatrix} \mathbf{P}^{(SR_1D)}_{(3)} \\ \mathbf{P}^{(SR_1R_2D)}_{(4)} \end{bmatrix} \approx \begin{bmatrix} (\mathbf{s} \diamond \mathbf{h}^{(R_1D)}) \\ (\mathbf{h}^{(\overline{R_1R_2})} \diamond \mathbf{s} \diamond \mathbf{h}^{(R_2D)}) \end{bmatrix} \mathbf{h}^{(SR_1)\text{T}}. \tag{4.48}$$

Computing the SVD of (4.48) as $\mathbf{U}^{(SR_1)}\mathbf{\Sigma}^{(SR_1)}\mathbf{V}^{(SR_1)\text{H}}$ the channel is estimated as $\hat{\mathbf{h}}^{(SR_1)} = \alpha_4 \mathbf{V}^{(SR_1)*}_{(:,1)}$. Since, in this case, there is no knowledge of any link of $\mathbf{H}^{(SR_1)}$, the scalar factor is given as $\alpha_4 = \mathbf{U}^{(SR_1)}_{(1,1)}\mathbf{\Sigma}^{(SR_1)}_{(1,1)}/(\mathbf{S}_{(1,1)}\mathbf{H}^{(R_1D)}_{(1,1)})$, and $\hat{\mathbf{H}}^{(SR_1)} = \text{unvec}(\hat{\mathbf{h}}^{(SR_1)})$.

Following the same steps for $\hat{\mathbf{h}}^{(SR_2)}$, the rank-one approximated matrix of size $NRM_DM_{S_2}(1+M_{R_1}M_{S_1})\times M_{R_1}M_S$ is formed by coupling the 3-mode unfolding of $\mathscr{P}^{(SR_2D)}$ with the 4-mode unfolding of $\mathscr{P}^{(SR_2R_1D)}$, $\mathbf{P}_{(3)}^{(SR_2D)}$ and $\mathbf{P}_{(4)}^{(SR_2R_1D)}$, respectively, as

$$\begin{bmatrix} \mathbf{P}_{(3)}^{(SR_2D)} \\ \mathbf{P}_{(4)}^{(SR_2R_1D)} \end{bmatrix} \approx \begin{bmatrix} (\mathbf{s}\diamond\mathbf{h}^{(R_2D)}) \\ (\mathbf{h}^{(\overline{R_2R_1})}\diamond\mathbf{s}\diamond\mathbf{h}^{(R_1D)}) \end{bmatrix} \mathbf{h}^{(SR_2)\mathrm{T}}, \tag{4.49}$$

being $\mathbf{U}^{(SR_2)}\mathbf{\Sigma}^{(SR_2)}\mathbf{V}^{(SR_2)\mathrm{H}}$ the SVD of (4.49), we can estimate the channel as $\hat{\mathbf{H}}^{(SR_2)} = \mathrm{unvec}(\hat{\mathbf{h}}^{(SR_2)})$, where $\hat{\mathbf{h}}^{(SR_2)} = \alpha_5\mathbf{V}_{(:,1)}^{(SR_2)*}$ and the scalar factor as $\alpha_5 = \mathbf{U}_{(1,1)}^{(SR_2)}\mathbf{\Sigma}_{(1,1)}^{(SR_2)}/(\mathbf{S}_{(1,1)}\mathbf{H}_{(1,1)}^{(R_2D)})$.

For the remaining channels ($\mathbf{H}^{(R_1R_2)}$, $\mathbf{H}^{(R_2R_1)}$) we have two different approaches. The first is when the Relay 1 and Relay 2 are transmit with the same number of antennas as they receive ($M_{R_1} = M_{S_1}$ and $M_{R_2} = M_{S_2}$). In this case, we can consider that $\mathbf{H}^{(R_1R_2)} = \mathbf{H}^{(R_2R_1)\mathrm{T}}$, since we assume that the channels are constant during all phases. By coupling the 3-mode unfolding of the tensors $\mathscr{P}^{(SR_1R_2D)}$ and $\mathscr{P}^{(SR_2R_1D)}$, $\mathbf{P}_{(3)}^{(SR_1R_2D)}$ and $\mathbf{P}_{(3)}^{(SR_2R_1D)}$, respectively, we have

$$\begin{bmatrix} \mathbf{P}_{(3)}^{(SR_1R_2D)} \\ \mathbf{\Pi}\mathbf{P}_{(3)}^{(SR_2R_1D)} \end{bmatrix} \approx \begin{bmatrix} (\mathbf{h}^{(SR_1}\diamond\mathbf{s}\diamond\mathbf{h}^{(R_2D)}) \\ \mathbf{\Pi}(\mathbf{h}^{(SR_2}\diamond\mathbf{s}\diamond\mathbf{h}^{(R_1D)}) \end{bmatrix} \mathbf{h}^{(\overline{R_1R_2})\mathrm{T}}, \tag{4.50}$$

where the matrix $\mathbf{\Pi}$ is a permutation matrix that maps the elements from $\mathbf{h}^{(\overline{R_2R_1})}$ to $\mathbf{h}^{(\overline{R_1R_2})}$. The SVD of (4.50) can be given as $\mathbf{U}^{(\overline{R_1R_2})}\mathbf{\Sigma}^{(\overline{R_1R_2})}\mathbf{V}^{(\overline{R_1R_2})\mathrm{H}}$, and following the same steps $\hat{\mathbf{h}}^{(\overline{R_1R_2})} = \alpha_6\mathbf{V}^{(\overline{R_1R_2})*}$, where $\alpha_6 = \mathbf{H}_{(1,1)}^{(R_1R_2)}/\mathbf{V}_{(1,1)}^{(\overline{R_1R_2})*}$. Noting that $\mathbf{h}^{(\overline{R_1R_2})} = \mathrm{vec}(\mathbf{H}^{(R_1R_2)\mathrm{T}})$ and $\mathbf{H}^{(R_1R_2)} = \mathbf{H}^{(R_2R_1)\mathrm{T}}$, we have $\hat{\mathbf{H}}^{(R_1R_2)} = \hat{\mathbf{H}}^{(R_2R_1)\mathrm{T}}$.

In the case where the Relay 1 and Relay 2 transmit with different number of antennas, the channel estimation takes a direct approach from the 3-mode unfolding of the respective tensors, i.e. there is no coupling at the receiver. In the case of $\mathbf{H}^{(R_1R_2)}$, we compute the SVD of the 3-mode unfolding of tensor $\mathscr{P}^{(SR_1R_2D)}$, given by

$$\mathbf{U}^{(\overline{R_1R_2})}\mathbf{\Sigma}^{(\overline{R_1R_2})}\mathbf{V}^{(\overline{R_1R_2})\mathrm{H}} = (\mathbf{h}^{(SR_1)}\diamond\mathbf{s}\diamond\mathbf{h}^{(R_2D)})\mathbf{h}^{(\overline{R_1R_2})\mathrm{T}},$$

and $\hat{\mathbf{h}}^{(\overline{R_1R_2})} = \beta_1\mathbf{V}_{(:,1)}^{(\overline{R_1R_2})*}$ where $\beta_1 = \mathbf{H}_{(1,1)}^{(R_1R_2)\mathrm{T}}/\mathbf{V}_{(1,1)}^{(\overline{R_1R_2})*}$. At the end, applying the unvec operator, we recover the estimated channel matrix as $\hat{\mathbf{H}}^{(R_1R_2)} = \mathrm{unvec}(\hat{\mathbf{h}}^{(\overline{R_1R_2})})^{\mathrm{T}}$.

For $\hat{\mathbf{H}}^{(R_2R_1)}$, the same approach is used, the SVD of the 3-mode unfolding of the tensor $\mathscr{P}^{(SR_2R_1D)}$ is computed as

$$\mathbf{U}^{(\overline{R_2R_1})}\mathbf{\Sigma}^{(\overline{R_2R_1})}\mathbf{V}^{(\overline{R_2R_1})\mathrm{H}} = (\mathbf{h}^{(SR_2)}\diamond\mathbf{s}\diamond\mathbf{h}^{(R_1D)})\mathbf{h}^{(\overline{R_2R_1})\mathrm{T}},$$

we obtain $\hat{\mathbf{h}}^{(\overline{R_2R_1})} = \beta_2\mathbf{V}_{(:,1)}^{(\overline{R_2R_1})*}$, where $\beta_2 = \mathbf{H}_{(1,1)}^{(R_2R_1)\mathrm{T}}/\mathbf{V}_{(1,1)}^{(\overline{R_2R_1})*}$. Finally, applying the unvec operator, we recover the estimated matrix as $\hat{\mathbf{H}}^{(R_2R_1)} = \mathrm{unvec}(\hat{\mathbf{h}}^{(\overline{R_2R_1})})^{\mathrm{T}}$.

4.2.1 Similar Systems

Maintaining the number of relays as two, we have three possible systems. The first is the proposed system, with four phases and four signals that can be coupled in the C-SVD receiver. The second possibility is the proposed system with three phases and, consequentially, only three signals to be coupled at the C-SVD receiver, i.e. the C-SVD receiver contains the signals $\mathscr{X}^{(SR_1D)}$, $\mathscr{X}^{(SR_2D)}$ and $\mathscr{X}^{(SR_1R_2D)}$, or $\mathscr{X}^{(SR_2D)}$, $\mathscr{X}^{(SR_1D)}$ and $\mathscr{X}^{(SR_2R_1D)}$ if, in Phase 2, the Relay 2 transmits instead of Relay 1. For a third variant, we have three phases but only two signals coupled at the C-SVD receiver, $\mathscr{X}^{(SR_1D)}$ and $\mathscr{X}^{(SR_2D)}$, in this case, the relays do not transmit to each other, there is only source to relay and relay to destination transmission. Following this approach, we also compare two other systems, the first is considering three relays, where the destination contains the signals $\mathscr{X}^{(SR_1D)}$, $\mathscr{X}^{(SR_2D)}$ and $\mathscr{X}^{(SR_3D)}$, and the second is the system proposed in Chapter 3, where $\mathscr{X}^{(SR_1D)}$ is the signal received at the destination. Table 2 shows the transmission rate for each system.

The tensors $\mathscr{C}$, $\mathscr{W}$, $\mathscr{T}$ and $\mathscr{L}$ (only in the case of three relays) are normalized by the factor $1/\sqrt{F_1RM_S}$, $1/\sqrt{F_2M_{R_1}M_{S_1}}$, $1/\sqrt{F_3M_{R_2}M_{S_2}}$ and $1/\sqrt{F_4M_{R_3}M_{S_3}}$ respectively, to ensure the antennas have the same power, as in Chapter 3. Noting that, with this normalization for $P > RM_S$, $J > M_{R_1}M_{S_1}$ and $K > M_{R_2}M_{S_2}$ the coding matrices $\mathbf{Z}^{(i)}\mathbf{Z}^{(i)\mathrm{H}} = \beta\mathbf{I}$, where β can be viewed as the gain by increasing the code length. Consider that the space-time coding tensor of Relay 3 is $\mathscr{L} \in \mathbb{C}^{M_{S_3}\times M_{R_3}\times L}$ with factors $\mathbf{L}_1 \in \mathbb{C}^{M_{S_3}\times F_4}$, $\mathbf{L}_2 \in \mathbb{C}^{M_{R_3}\times F_4}$ and $\mathbf{L}_3 \in \mathbb{C}^{L\times F_4}$.

4.3 Simulation Results

In this section, we evaluate the performance of the C-SVD receiver in terms of symbol error rate (SER) and normalized mean square error for the channel estimation. We consider 64-QAM modulation. The results are averaged over 10^4 Monte Carlo runs and each run corresponding to an independent realisation of the channels, symbols, and noise. The channel matrices are assumed to have i.i.d. complex Gaussian entries with zero-mean and unitary variance, the noise variance is assumed to be equal at the relays and destination. First, we present the performance of the Zero-Forcing with perfect CSI for all links. In second, we compare the performance of the proposed system with their variants, mentioned in Section 4.2.1. Finally, we present the normalized mean square error of the channels of the C-SVD receiver, comparing the

Table 2 – Proposed system and its variants

Phases	Relays	Coupled Signals	Rate
4	3	$\mathbf{P}_{(2)}^{SR_1D}$, $\mathbf{P}_{(2)}^{SR_2D}$, $\mathbf{P}_{(2)}^{SR_3D}$	$\frac{NR-1}{NP(J+K+L)}$
3	2	$\mathbf{P}_{(2)}^{SR_1D}$, $\mathbf{P}_{(2)}^{SR_2D}$, $\mathbf{P}_{(2)}^{SR_1R_2D}$ or $\mathbf{P}_{(2)}^{SR_2R_1D}$	$\frac{NR-1}{NP(JK+J+K)}$
3	2	$\mathbf{P}_{(2)}^{SR_1D}$, $\mathbf{P}_{(2)}^{SR_2D}$	$\frac{NR-1}{NP(J+K)}$
4	2	$\mathbf{P}_{(2)}^{SR_1D}$, $\mathbf{P}_{(2)}^{SR_2D}$, $\mathbf{P}_{(2)}^{SR_1R_2D}$, $\mathbf{P}_{(2)}^{SR_2R_1D}$	$\frac{NR-1}{NP(2JK+J+K)}$
2	1	$\mathbf{P}_{(2)}^{SR_1D}$	$\frac{NR-1}{NPJ}$

gain related to the number of signal coupled at the receiver.

4.3.1 Symbol Error Rate

The scenario simulated is the following: $M_S = M_{R_1} = M_{S_1} = M_{R_2} = M_{S_2} = M_{R_3} = M_{S_3} = 2$, $R = 4$, $M_D = 4$, $J = K = L = 4$ $P = 8$, $F_1 = RM_S$, $F_2 = M_{R_1}M_{S_1}$, $F_3 = M_{R_2}M_{S_2}$ and, in the case of three relays, $F_4 = M_{R_3}M_{S_3}$. In the symbol rate analyses, we compare the systems at the maximum rate of each, i.e. $R = P/2$.

Figure 26 shows the code gain for our proposed system with perfect CSI, note that increasing the code length P at the source is more relevant than increasing the code length at the relays (J,K), this is due the fact the increasing J and K also increases the correlation with the noise at the relays, as in Chapter 3.

In Figure 27 an interesting comparison is the performance of the proposed system where we have four phases and four signals coupling (green line) with the three phases system where are only two signals coupling (blue line). Such result for the blue curve can be explained by the fact that in this system the noise is correlated only by one relay, while in our proposed system, two of four signals ($\mathscr{X}^{(SR_1R_2D)}$ and $\mathscr{X}^{(SR_2R_1D)}$) increases even more the correlation with the noise, due to the relay-relay transmission, in this case, the system with three phases and

two signals has the advantage of latency. However, our proposed system is the only one that in the C-SVD receiver all the available links are coupled, resulting in a gain for the channels relay-destination and the relay-relay channels. The system with three relays (yellow curve), have the better performance, as expected, since there the system counts with one more resource and the transmission follows the source-relay relay-destination direction, there is no relay-relay transmission.

4.3.2 Normalized Mean Square Error

Since the scenario can be considered symmetric for the relays (the code-length and the number of antennas are equal), in Figure 28 the NMSE of the links passed by different relays are approximately the same.

The channels of relay-destination have a better performance over relay-relay channels, which have also a better performance over the source-relay channels, as expected. Such results can be explained by the fact the for relay-destination channels the signal has already be encoded by three space-time coding tensors, for relay-relay channels, the signal was encoded by two tensors, and for source-relay channels, the signal was encoded only at the source. Also, for the source-relay channels, there is no knowledge of any link, which causes a degradation in the performance. This also explains, in Figure 29, the approximate performance of $\mathbf{H}^{(R_1R_2)}$ with only one signal (the case where there is no coupling at the receiver) and $\mathbf{H}^{(R_1D)}$ with one signal, since in this case, the signal is modelled from the two-hop system ($\mathscr{X}^{(SR_1D)}$), and for both channels the signal was encoded by two space-time coding tensors. Finally, it can be noticed that there is no gain by coupling the source-relay channel matrix $\mathbf{H}^{(SR_1)}$ at the receiver, this is because for source-relays channels, the signal is encoded only once, however in a scenario where the relays have a different path loss, the coupling approach could be applied for source-relay channel estimation.

Globally, the proposed system exploit all the available links enjoying three space-time coding tensors, which increases the performance for channel estimation. The system with three phases and three signals at the receiver enjoying of three space-time coding tensors, but for one link, i.e. for $\mathscr{X}^{(SR_1R_2D)}$ or $\mathscr{X}^{(SR_2R_1D)}$. The system with three phases but only two signals has the advantage of a reduced latency. However, since there are only two space-time coding tensors, the gap in the performance of relay-destination channels is considerable. It is worth noting that all parameters can be estimated in parallel by computing independents SVDs.

Figure 26 – Perfect CSI performance for different values of P, J and K.

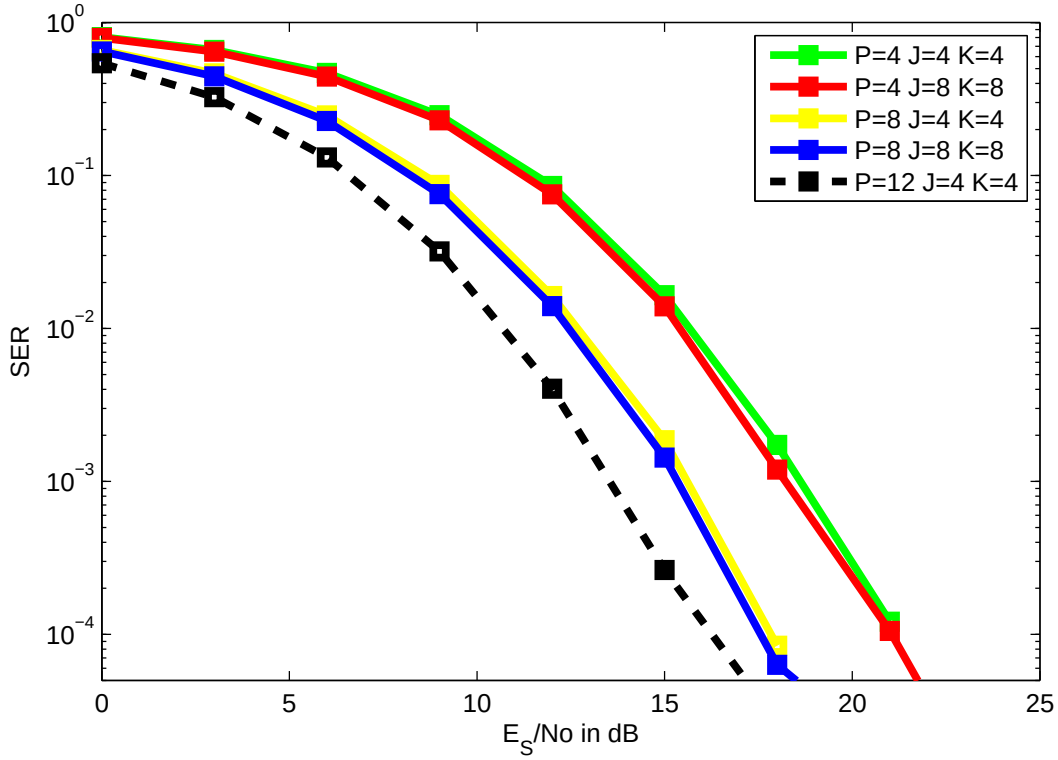

Source: Created by the Author

Figure 27 – Performance of the proposed receiver with different number of phases and signals to couple.

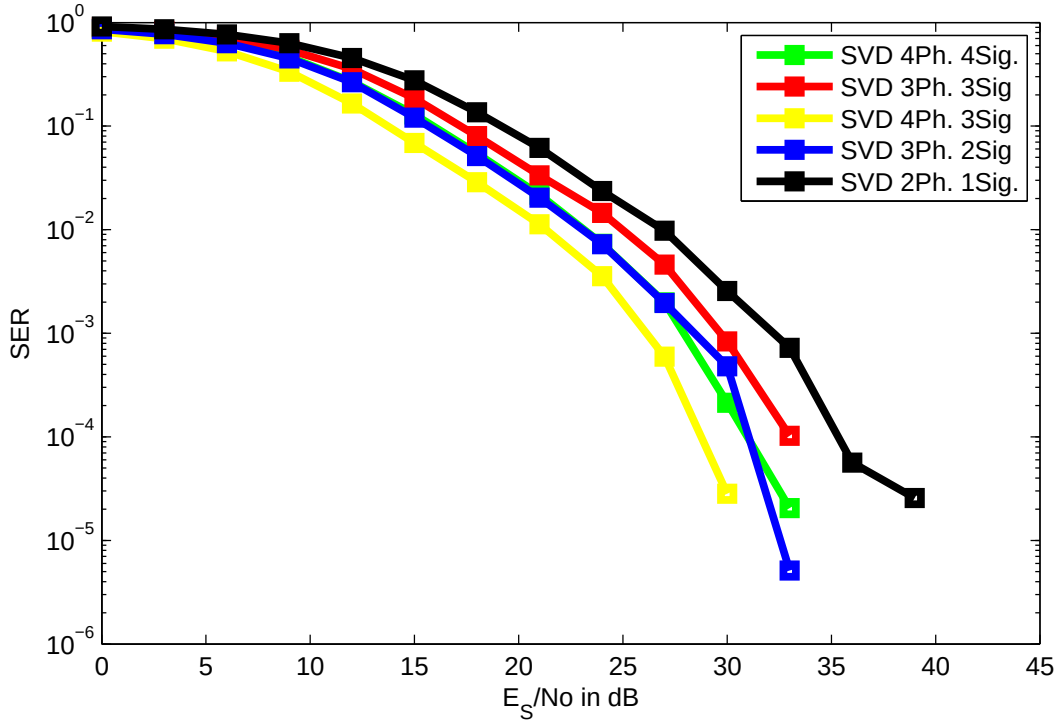

Source: Created by the Author

Figure 28 – Normalized mean square error.

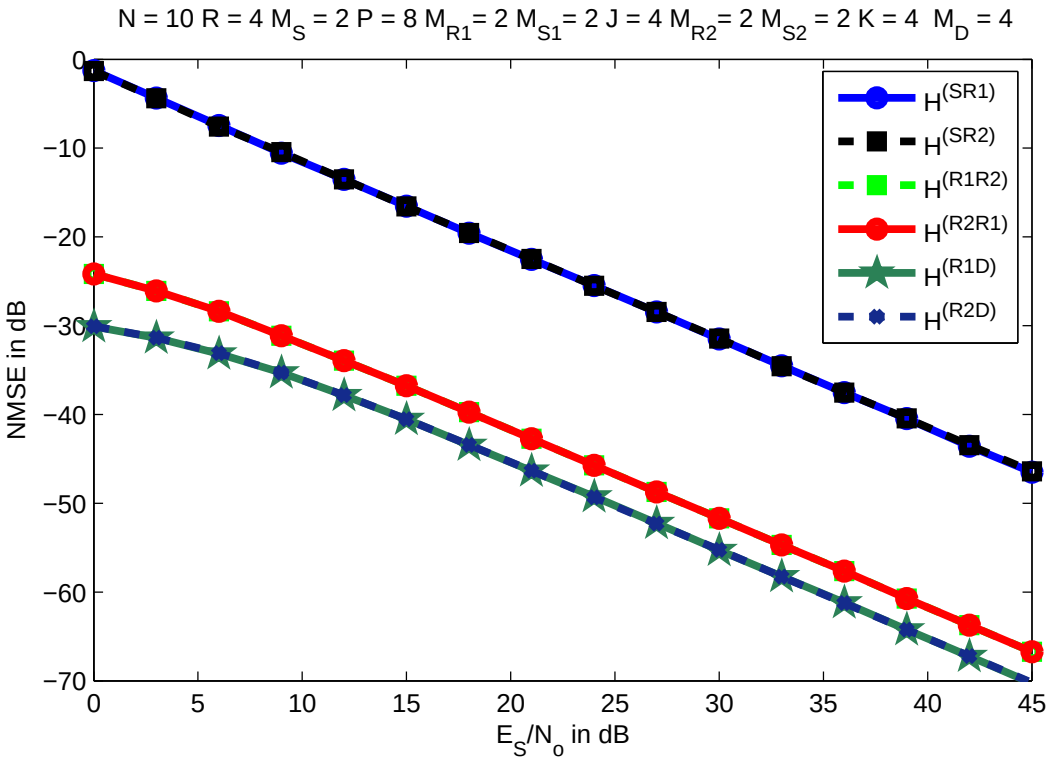

Source: Created by the Author

Figure 29 – NMSE of coupling signals.

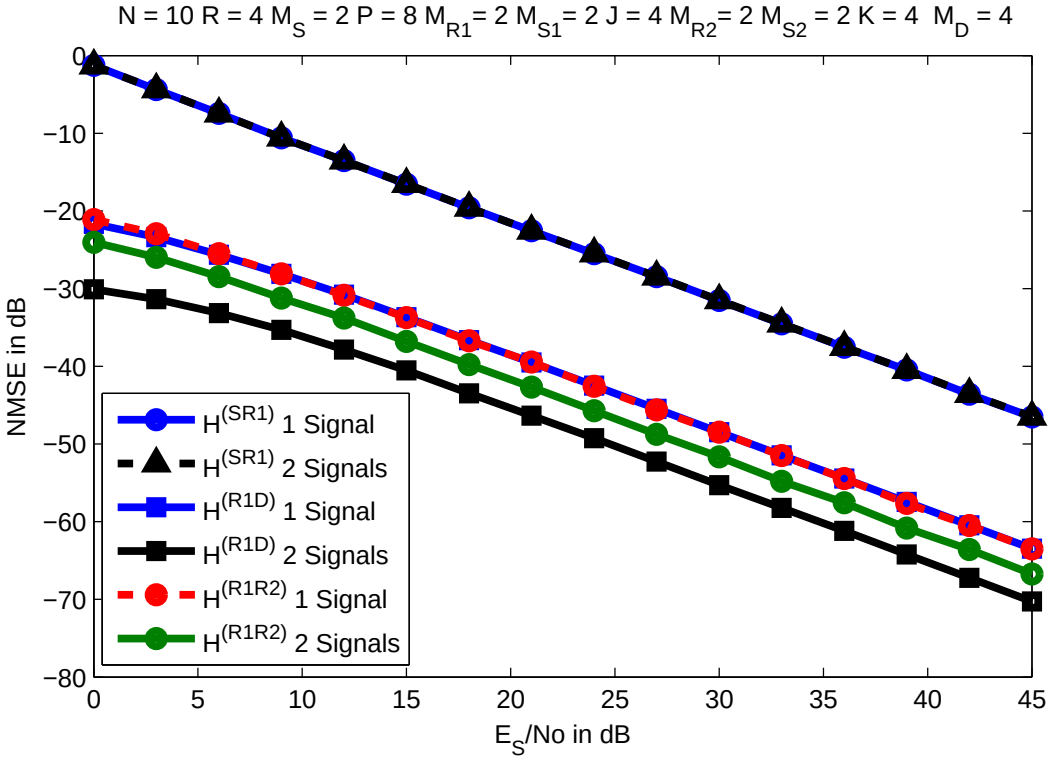

Source: Created by the Author

4.4 Summary

In this chapter, a MIMO multi-relaying system was presented, combining the rank-one tensor approximation with the diversity of cooperative communications, resulting in a semi-blind receiver (C-SVD) capable of estimating the desired parameters via independent SVDs. Moreover, we compared the proposed system with its variants, corroborating the existence of a trade-off between diversity gain and latency.

5 CONCLUSION

In this thesis, we proposed semi-blind receivers for MIMO relay and multi-relaying cooperative systems.

The two-hop MIMO relay, presented in Chapter 3, was based on the Nested Tucker system proposed in [17], and the main differences are: In [17], the authors proposed two semi-blind receivers that have a direct data approach, i.e. using the n-mode unfolding of the received Nested Tucker signal, an iterative receiver (ALS, with high computational complexity) and a two steps closed-form based on receiver (2LSKP), which the estimation of the $\mathbf{H}^{(SR)}$ channel depends on the previous estimation of the symbols ($\mathbf{S}$) or the $\mathbf{H}^{(RD)}$ channel, were proposed. However, our proposed system exploits the knowledge of the space-time coding tensors at the receiver, to form a generalized n-mode unfolding of the Nested Tucker received signal and then design a filter, which is the effective space-time code of the system. The filtered signal is modelled as a rank-one approximated PARAFAC tensor, and from this rank-one tensor, two semi-blind receivers were proposed. The first is a iterative (Tri-ALS) and the second is based on a closed-form solution (T-HOSVD). As shown in Section 3.4, all the receivers achieve the same performance for symbol and channel estimation. However, in terms of computational complexity, our proposed receivers have shown to be more attractive, specially the T-HOSVD receiver which can estimate the desired parameters in parallel. The remarkable performances of our proposed system are due to the orthogonal design of the effective space-times code, leading to the next contribution of our design compared with the desing in [17]. The authors in [17] proposed a random exponential structure for the space-time coding tensors since they only make use of the n-mode unfolding of those tensor in the algorithms. However, in our proposed system, we work with the effective space-time code, which is desirable an orthogonal design for such code since it will preserve the noise properties. From such orthogonal design, we show that a DFT matrix can be factorized into the exact Khatri-Rao product of N matrices, with some conditions in the size. In Chapter 4, a MIMO multi-relaying system is studied by exploiting the rank-one approach discussed in Chapter 3. The proposed scenario takes advantage of the diversity of the cooperative system by combining the multiple copies (in the specific case, four copies) of the transmitted signal from different paths with a coupled receiver (C-SVD). The C-SVD receiver couples the n-mode unfolding of the approximated rank-one tensors into approximated rank-one matrices, enjoying of parallel processing by computing independents SVDs. Also, when we compare the proposed system with its variants, we illustrated a trade-off between latency and performance.

Overall, the rank-one approximation has shown to be an interesting method, due to the system simplification and performance, as shown in Chapters 3 and 4. One drawback of proposed approach is the more restrictive uniqueness conditions for the LS estimator, which limits the transmission rate.

As perspectives for future works, we can highlight the following:

- A deeper study of the tensor contraction operator including the analysis of its properties and its generalization to multiple contractions (i.e. involving several tensors).
- Generalization of the proposed algorithms to multi-user cooperative systems. In this case, we can deduce that the receiver will be based on a rank-R tensor approximation, for R users.
- Adaptation of the proposed algorithms to massive MIMO systems. In [47] the authors proposed a hybrid architecture for massive MIMO where the analogue beamformer is decomposed as the Kronecker product of N vectors, which is basically our proposed rank-one tensor approximation. However, in [47], the authors does not exploit the multidimensional nature.

BIBLIOGRAPHY

1 BIGLIERI, E. et al. *MIMO Wireless Communications*. [S.l.]: Cambridge university press, 2007.

2 OESTGES, C.; CLERCKX, B. *MIMO Wireless Communications: From Real-World Propagation to Space-Time Code Design*. [S.l.]: Academic Press, 2010.

3 HAMPTON, J. R. *Introduction to MIMO Communications*. [S.l.]: Cambridge university press, 2013.

4 LIU, K. J. R. et al. *Cooperative Communications and Networking*. New York, NY, USA: Cambridge University Press, 2009.

5 DOHLER, M.; LI, Y. *Cooperative Communications: Hardware, Channel and PHY*. [S.l.]: John Wiley & Sons, 2010.

6 GIRNYK, M. *Cooperative Communication for Multi-User Cognitive Radio Networks*. Tese (Doutorado) — KTH Royal Institute of Technology, 2012.

7 RONG, Y.; TANG, X.; HUA, Y. A Unified Framework for Optimizing Linear Nonregenerative Multicarrier MIMO Relay Communication Systems. *IEEE Trans. on Signal Process.*, v. 57, p. 4837–4851, Dec. 2009.

8 KONG, T.; HUA, Y. Optimal Channel Estimation and Training Design for MIMO Relays. In: *ASILOMAR-SSC 2010*. Pacific Grove, CA, USA: [s.n.], 2010. p. 663–667.

9 CAO, L.; ZHANG, J.; KANNO, N. Multi-user Cooperative Communications with Relay-coding for Uplink IMT-advanced 4G Systems. In: IEEE. *Global Telecommunications Conference, 2009. GLOBECOM 2009. IEEE*. [S.l.], 2009. p. 1–6.

10 GAO, Y.; CHEN, Y.; LIU, K. R. Cooperation Stimulation for Multiuser Cooperative Communications Using Indirect Reciprocity Game. *IEEE Transactions on Communications*, IEEE, v. 60, n. 12, p. 3650–3661, 2012.

11 ALMEIDA, A. L. F. de; FERNANDES, C. A.; COSTA, D. B. da. Multiuser Detection for Uplink DS-CDMA Amplify-and-Forward Relaying Systems. *IEEE Signal Processing Letters*, IEEE, v. 20, n. 7, p. 697–700, 2013.

12 CHEN, B.; LEI, M.; ZHAO, M. An Optimal Resource Allocation Method for Multi-User Multi-Relay DF Cognitive Radio Networks. *IEEE Communications Letters*, IEEE, v. 20, n. 6, p. 1164–1167, 2016.

13 GENDIA, A.; ELSABROUTY, M.; EMRAN, A. A. Cooperative Multi-Relay Non-orthogonal Multiple Access for Downlink Transmission in 5G Communication Systems. In: IEEE. *Wireless Days, 2017*. [S.l.], 2017. p. 89–94.

14 SIDIROPOULOS, N. D.; GIANNAKIS, G. B.; BRO, R. Blind PARAFAC Receivers for DS-CDMA Systems. *IEEE Transactions on Signal Processing*, IEEE, v. 48, n. 3, p. 810–823, 2000.

15 HARSHMAN, R. A. Foundations of the PARAFAC Procedure: Models and Conditions for an" explanatory" Multi-Modal Factor Analysis. University of California at Los Angeles Los Angeles, CA, 1970.

16 TUCKER, L. R. Some Mathematical Notes on Three-mode Factor Analysis. *Psychometrika*, Springer, v. 31, n. 3, p. 279–311, 1966.

17 FAVIER, G.; FERNANDES, C. A. R.; ALMEIDA, A. L. F. de. Nested Tucker Tensor Decomposition with Application to MIMO Relay Systems Using Tensor Space–Time Coding (TSTC). *Signal Processing*, Elsevier, v. 128, p. 318–331, 2016.

18 XIMENES, L. R.; FAVIER, G.; ALMEIDA, A. L. F. de. Semi-Blind Receivers for Non-Regenerative Cooperative MIMO Communications Based on Nested PARAFAC Modeling. *IEEE Transactions on Signal Processing*, IEEE, v. 63, n. 18, p. 4985–4998, 2015.

19 ALMEIDA, A. L. F. de; FAVIER, G.; MOTA, J. C. M. A Constrained Factor Decomposition with Application to MIMO Antenna Systems. *IEEE Transactions on Signal Processing*, IEEE, v. 56, n. 6, p. 2429–2442, 2008.

20 FAVIER, G. et al. Tensor Space-Time (TST) coding for {MIMO} Wireless Communication Systems . *Signal Processing*, v. 92, n. 4, p. 1079 – 1092, 2012.

21 KRUSKAL, J. B. Three-way Arrays: Rank and Uniqueness of Trilinear Decompositions, with Application to Arithmetic Complexity and Statistics. *Linear algebra and its applications*, Elsevier, v. 18, n. 2, p. 95–138, 1977.

22 ALMEIDA, A. L. F. de; FAVIER, G. Double Khatri–Rao Space-Time-Frequency Coding Using Semi-Blind PARAFAC Based Receiver. *IEEE Signal Processing Letters*, IEEE, v. 20, n. 5, p. 471–474, 2013.

23 ROEMER, F.; HAARDT, M. Tensor-Based Channel Estimation and Iterative Refinements for Two-Way Relaying with Multiple Antennas and Spatial Reuse. *IEEE Transactions on Signal Processing*, v. 58, n. 11, p. 5720–5735, nov. 2010.

24 CAVALCANTE, I. V.; ALMEIDA, A. L. F. de; HAARDT, M. Tensor-based Approach to Channel Estimation in Amplify-and-Forward MIMO Relaying Systems. In: IEEE. *Sensor Array and Multichannel Signal Processing Workshop (SAM), 2014 IEEE 8th*. [S.l.], 2014. p. 445–448.

25 MEULEN, E. C. V. der. Three-Terminal Communication Channels. *Advances in Applied Probability*, Applied Probability Trust, v. 3, p. 120–154, 1971.

26 SOFOTASIOS, M. K. F. P. C.; MUHAIDAT, S. Relay Selection Based Full-Duplex Cooperative Systems under Adaptive Transmission. *IEEE Wireless Communications Letters*, IEEE, 2017.

27 CHEN, G. et al. Full-Duplex Wireless-Powered Relay in Two Way Cooperative Networks. *IEEE Access*, IEEE, v. 5, p. 1548–1558, 2017.

28 FANG, Z.; HUA, Y.; KOSHY, J. C. Joint Source and Relay Optimization for a Non-regenerative MIMO Relay. In: IEEE. *Sensor Array and Multichannel Processing, 2006. Fourth IEEE Workshop on*. [S.l.], 2006. p. 239–243.

29 RANKOV, B.; WITTNEBEN, A. Spectral efficient protocols for half-duplex fading relay channels. *IEEE Journal on Selected Areas in Communications*, IEEE, v. 25, n. 2, 2007.

30 LANEMAN, J. N.; TSE, D. N. C.; WORNELL, G. W. Cooperative Diversity in Wireless Networks: Efficient Protocols and Outage Behavior. *IEEE Transactions on Information Theory*, v. 50, n. 12, p. 3062–3080, Dec 2004. ISSN 0018-9448.

31 UPADHYAY, P. K.; PRAKRIYA, S. Bidirectional cooperative relaying. In: *Radio Communications*. [S.l.]: InTech, 2010. cap. 15.

32 LOAN, C. V.; PITSIANIS, N. *Approximation with Kronecker Products*. [S.l.], 1992.

33 DOLGOV, S. V.; SAVOSTYANOV, D. V. Alternating Minimal Energy Methods for Linear Systems in Higher Dimensions. *SIAM Journal on Scientific Computing*, SIAM, v. 36, n. 5, p. A2248–A2271, 2014.

34 CICHOCKI, A. Tensor Networks for Big Data Analytics and Large-scale Optimization Problems. *arXiv preprint arXiv:1407.3124*, 2014.

35 OSELEDETS, I. V. Tensor-Train Decomposition. *SIAM Journal on Scientific Computing*, SIAM, v. 33, n. 5, p. 2295–2317, 2011.

36 CARROLL, J. D.; CHANG, J.-J. Analysis of Individual Differences in Multidimensional Scaling via an N-way Generalization of "Eckart-Young" Decomposition. *Psychometrika*, Springer, v. 35, n. 3, p. 283–319, 1970.

37 HITCHCOCK, F. L. The Expression of a Tensor or a Polyadic as a Sum of Products. *J. Math. Phys*, v. 6, n. 1, p. 164–189, 1927.

38 SIDIROPOULOS, N. D.; BRO, R. On the Uniqueness of Multilinear Decomposition of N-way Arrays. *Journal of Chemometrics*, John Wiley & Sons, Ltd., v. 14, n. 3, p. 229–239, 2000. ISSN 1099-128X. Disponível em: <http://dx.doi.org/10.1002/1099-128X(200005/06)14:3<229::AID-CEM587>3.0.CO;2-N>.

39 SHARAN, V.; VALIANT, G. Orthogonalized ALS: A Theoretically Principled Tensor Decomposition Algorithm for Practical Use. *arXiv preprint arXiv:1703.01804*, 2017.

40 RAJIH, M.; COMON, P.; HARSHMAN, R. A. Enhanced Line Search: A Novel Method to Accelerate PARAFAC. *SIAM journal on matrix analysis and applications*, SIAM, v. 30, n. 3, p. 1128–1147, 2008.

41 NAVASCA, C.; LATHAUWER, L. D.; KINDERMANN, S. Swamp Reducing Technique for Tensor Decomposition. In: IEEE. *Signal Processing Conference, 2008 16th European*. [S.l.], 2008. p. 1–5.

42 FAVIER, G.; ALMEIDA, A. L. F. de. Overview of Constrained PARAFAC Models. *EURASIP Journal on Advances in Signal Processing*, Springer, v. 2014, n. 1, p. 142, 2014.

43 KOLDA, T. G.; BADER, B. W. Tensor Decompositions and Applications. *SIAM review*, SIAM, v. 51, n. 3, p. 455–500, 2009.

44 ALMEIDA, A. L. F. de. *Tensor Modeling and Signal Processing for Wireless Communication Systems*. Tese (Doutorado) — Université de Nice Sophia Antipolis, 2007.

45 WU, K. K. et al. Kronecker Product Approximation with Multiple Factor Matrices via the Tensor Product Algorithm. In: IEEE. *Systems, Man, and Cybernetics (SMC), 2016 IEEE International Conference on*. [S.l.], 2016. p. 004277–004282.

46 MINKA, T. The lighspeed MATLAB toolbox, efficient operations for MATLAB programming. *Microsoft Corp.*, v. 2.2, 2007.

47 ZHU, G. et al. Hybrid Beamforming via the Kronecker Decomposition for the Millimeter-Wave Massive MIMO Systems. *arXiv preprint arXiv:1704.03611*, 2017.

APPENDIX A – CODING ORTHOGONALITY DESIGN

As previous defined, the factor matrices of the coding tensors are, $\mathbf{C}_1 \in \mathbb{C}^{M_S \times F_1}$, $\mathbf{C}_2 \in \mathbb{C}^{R \times F_1}$, $\mathbf{C}_3 \in \mathbb{C}^{P \times F_1}$, $\mathbf{W}_1 \in \mathbb{C}^{M_{S_1} \times F_2}$, $\mathbf{W}_2 \in \mathbb{C}^{M_{R_1} \times F_2}$, $\mathbf{W}_3 \in \mathbb{C}^{J \times F_2}$, $\mathbf{T}_1 \in \mathbb{C}^{M_{S_2} \times F_3}$, $\mathbf{T}_2 \in \mathbb{C}^{M_{R_2} \times F_3}$ and $\mathbf{T}_3 \in \mathbb{C}^{K \times F_3}$. Given the structure of matrix $\mathbf{Z}^{(1)}$, or $\mathbf{Z}^{(2)}$, we design the parameter such that $\mathbf{Z}^{(1)}\mathbf{Z}^{(1)\mathrm{H}} = \mathbf{I}$ or $\mathbf{Z}^{(2)}\mathbf{Z}^{(2)\mathrm{H}} = \mathbf{I}$. Taking the example of $\mathbf{Z}^{(1)}$ given by equation (3.20), by applying some permutation, we define the matrix $\mathbf{Z}_P^{(1)} \in \mathbb{C}^{M_{R_1} M_{S_1} R M_S \times JP}$ as

$$\begin{aligned}\mathbf{Z}_P^{(1)} &= \mathbf{Z}^{(1)}\mathbf{\Pi} \\ &= [(\mathbf{C}_1 \otimes \mathbf{W}_2) \diamond (\mathbf{C}_2 \otimes \mathbf{W}_1)](\mathbf{C}_3 \otimes \mathbf{W}_3)^{\mathrm{T}}\mathbf{\Pi} \\ &= [(\mathbf{C}_1 \diamond \mathbf{C}_2) \otimes (\mathbf{W}_1 \diamond \mathbf{W}_2)](\mathbf{C}_3 \otimes \mathbf{W}_3)^{\mathrm{T}}, \end{aligned} \tag{A.1}$$

where $\mathbf{\Pi}$ is some permutation matrix. Note that if $\mathbf{Z}_P^{(1)}$ is orthogonal, then $\mathbf{Z}^{(1)}$ would be also orthogonal, since a permutation matrix is orthogonal. Defining as $\overline{\mathbf{C}} = \mathbf{C}_2 \diamond \mathbf{C}_1 \in \mathbb{C}^{M_S R \times F_1}$ and $\overline{\mathbf{W}} = \mathbf{W}_2 \diamond \mathbf{W}_1 \in \mathbb{C}^{M_{S_1} M_{R_1} \times F_2}$, and replacing in equation (A.1), multiplying by its Hermitian at the right-hand side, yields

$$\mathbf{Z}_P^{(1)}\mathbf{Z}_P^{(1)\mathrm{H}} = (\overline{\mathbf{C}} \otimes \overline{\mathbf{W}})\mathbf{G}_3^{\mathrm{T}}\mathbf{G}_3^{*}(\overline{\mathbf{C}} \otimes \overline{\mathbf{W}})^{\mathrm{H}} \tag{A.2}$$

For the term $\mathbf{G}_3^{\mathrm{T}}\mathbf{G}_3^{*}$ by choosing $\mathbf{C}_3$ and $\mathbf{W}_3$ as DFT matrices (assuming that $P = F_1$ and $J = F_2$), the product its orthogonal.

$$\begin{aligned}\mathbf{G}_3^{\mathrm{T}}\mathbf{G}_3^{*} &= \frac{1}{JP}(\mathbf{C}_3 \otimes \mathbf{W}_3)^{\mathrm{T}}(\mathbf{C}_3 \otimes \mathbf{W}_3)^{*} \\ &= \frac{1}{JP}(\mathbf{C}_3^{\mathrm{T}}\mathbf{C}_3^{*} \otimes \mathbf{W}_3^{\mathrm{T}}\mathbf{W}_3^{*}) \\ &= \mathbf{I}_{F_2 F_1}, \end{aligned} \tag{A.3}$$

where $\frac{1}{\sqrt{JP}}$ is the normalization factor for the DFTs matrices. In the case of $P > F_1$ and $J > F_2$, we design the matrices $\mathbf{C}_3$ and $\mathbf{W}_3$ as truncated DFT.

The same approach is done for the left term as

$$\begin{aligned}(\overline{\mathbf{C}} \otimes \overline{\mathbf{W}})(\overline{\mathbf{C}} \otimes \overline{\mathbf{W}})^{\mathrm{H}} &= \frac{1}{F_2 F_1}(\overline{\mathbf{C}}\overline{\mathbf{C}}^{\mathrm{H}}) \otimes (\overline{\mathbf{W}}\overline{\mathbf{W}}^{\mathrm{H}}) \\ &= \mathbf{I}_{R M_S M_{R_1} M_{S_1}} \end{aligned} \tag{A.4}$$

Then, since each column of a DFT matrix $(\overline{\mathbf{C}}, \overline{\mathbf{W}})$ can be factorized into Kronecker between two or more vectors, the DFT matrix $\overline{\mathbf{C}}$ can be factorized into the Khatri-Rao of two or more

matrices. For this, suppose that the matrix $\overline{\mathbf{C}}$ is a DFT of size $F_1 \times F_1$ and $F_1 = RM_S$ as

$$\overline{\mathbf{C}} = \frac{1}{\sqrt{F_1}} \begin{bmatrix} 1 & 1 & 1 & \cdots & 1 \\ 1 & \omega & \omega^2 & \cdots & \omega^{F_1-1} \\ 1 & \omega^2 & \omega^4 & \cdots & \omega^{2(F_1-1)} \\ \vdots & \vdots & \vdots & \cdots & \vdots \\ 1 & \omega^{F_1-1} & \omega^{2(F_1-1)} & \ldots & \omega^{(F_1-1)(F_1-1)} \end{bmatrix} \tag{A.5}$$

We factorize each column of $\overline{\mathbf{C}}$ as $\overline{\mathbf{c}}^{f_1} = \mathbf{c}_2^{f_1} \otimes \mathbf{c}_1^{f_1}$, where $\overline{\mathbf{c}}^{f_1}$ is the vector at the f_1 column of $\overline{\mathbf{C}}$. For the first columns its straightforward. For the (f_1+1)-*th* column we have the following:

$$\overline{\mathbf{c}}^{f_1} = \begin{bmatrix} 1 \\ \omega \\ \omega^2 \\ \vdots \\ \omega^{f_1(R-1)} \end{bmatrix}^{(M_S)} \otimes \begin{bmatrix} 1 \\ \omega \\ \omega^2 \\ \vdots \\ \omega^{f_1(M_S-1)} \end{bmatrix} \tag{A.6}$$

We conclude that, after factorizing all columns of $\overline{\mathbf{C}}$, the matrix $\overline{\mathbf{C}} = \mathbf{C}_2 \diamond \mathbf{C}_1$. The same approach is applied to the matrix $\overline{\mathbf{W}}$. The permutation in (A.1) was performed to change the Khatri-Rao and Kronecker product position, since we cannot performer a Kronecker factorization in a DFT matrix, but the Khatri-Rao is possible.

APPENDIX B – UNIQUENESS CONDITION

As mentioned in Section 4.1.5, the matrices $\mathbf{Z}^{(1)}$, $\mathbf{Z}^{(2)}$, $\mathbf{Z}_J$ and $\mathbf{Z}_K$ must be full row-rank. The following Properties will be used to derive the conditions:

- $\text{rank}(\mathbf{A} \otimes \mathbf{B}) = \text{rank}(\mathbf{A})\text{rank}(\mathbf{B})$
- $\text{rank}(\mathbf{AB}) = \text{rank}(\mathbf{A})$ if $\mathbf{B}$ is a full rank matrix.

The rank of $\mathbf{Z}^{(1)}$ its equal to the rank of $\mathbf{Z}_P^{(1)}$, and is given by

$$\text{rank}(\mathbf{Z}_P^{(1)}) = \text{rank}([\overline{\mathbf{C}} \otimes \overline{\mathbf{W}}]\mathbf{G}_3^{\text{T}}). \tag{B.1}$$

The rank of $\mathbf{G}_3^{\text{T}}$ is expressed as

$$\begin{aligned} \text{rank}(\mathbf{G}_3^{\text{T}}) &= \text{rank}(\mathbf{C}_3^{\text{T}} \otimes \mathbf{W}_3^{\text{T}}) \\ &= \text{rank}(\mathbf{C}_3^{\text{T}})\text{rank}(\mathbf{W}_3^{\text{T}}). \end{aligned} \tag{B.2}$$

Since $\mathbf{C}_3$ is of size $P \times F_1$ and $\mathbf{W}_3$ of size $J \times F_2$, for $\mathbf{G}_3^{\text{T}} \in \mathbb{C}^{F_2F_1 \times JP}$ being a full row-rank matrix we have $\text{rank}(\mathbf{C}_3) = F_1$ and $\text{rank}(\mathbf{W}_3) = F_2$, following that $P \geq F_1$ and $J \geq F_2$. Since the matrix $\mathbf{G}_3^{\text{T}}$ is full row-rank, the rank of $\mathbf{Z}_P^{(1)}$ is given by

$$\begin{aligned} \text{rank}(\mathbf{Z}_P^{(1)}) &= \text{rank}(\overline{\mathbf{C}} \otimes \overline{\mathbf{W}}) \\ &= \text{rank}(\overline{\mathbf{C}})\text{rank}(\overline{\mathbf{W}}) \\ &= \text{rank}([\mathbf{C}_2 \diamond \mathbf{C}_1])\text{rank}([\mathbf{W}_2 \diamond \mathbf{W}_1]). \end{aligned} \tag{B.3}$$

For $\mathbf{Z}_P^{(1)}$ being a full row-rank, then $\overline{\mathbf{C}} \in \mathbb{C}^{RM_S \times F_1}$ and $\overline{\mathbf{W}} \in \mathbb{C}^{M_{S_1}M_{R_1} \times F_2}$ also must be a full row-rank, and we have $F_1 \geq RM_S$ and $F_2 \geq M_{S_1}M_{R_1}$. At the end, for $\mathbf{Z}^{(1)}$ and $\mathbf{Z}^{(2)}$ we have the final conditions in (4.38) to (4.40).